GEOSCIENCE CANADA
JOURNAL OF THE GEOLOGICAL ASSOCIATION OF CANADA
JOURNAL DE L'ASSOCIATION GÉOLOGIQUE DU CANADA

Hadean Planets: Early Earth Versus Modern Venus

BC Pinolite: Magnificent Metasomatic Magnesite

Engaging the Elementary: Geology Outreach in Saskatchewan

Gerry Middleton: Our Founder and First Editor

Review: Future Courses of Earthly Rivers

2021 VOLUME 48

Publisher/Éditeur
Geological Association of Canada
Alexander Murray Bld., Rm ER4063
Memorial University of Newfoundland
St. John's, NL, Canada, A1B 3X5
Tel: (709) 864-7660
Fax: (709) 864-2532
gac@mun.ca
www.gac.ca

Print Edition: ISSN 0315-0941
Online Edition: ISSN 1911-4850

Volume 48

A journal published quarterly by the Geological Association of Canada, incorporating the Proceedings.
Une revue trimestrielle publiée par l'Association géologique du Canada et qui en diffuse les actes.

Subscriptions: Receiving four issues of Geoscience Canada per year for $50 is one of the benefits of being a GAC member. To obtain institutional subscriptions, please contact Érudit: www.erudit.org

Abonnement: Recevoir quatre numéros par année pour 50,00 $ du magazine Geoscience est l'un des avantages réservés aux membres de l'AGC. Pour les abonnements institutionnels, s'il vous plaît contacter Érudit: www.erudit.org

Those wishing to submit material for publication in Geoscience Canada should refer to the Instructions to Authors on the journal's website, www.geosciencecanada.ca

AUTHORS PLEASE NOTE:
Please use the web address http://journals.hil.unb.ca/index.php/GC/index for submissions; please do not submit articles directly to the editor.

The Mission of the Geological Association of Canada is to facilitate the scientific well-being and professional development of its members, the learned discussion of geoscience in Canada, and the advancement, dissemination and wise use of geosciences in public, professional and academic life. Articles in Geoscience Canada are freely available one year after their publication date, unless authors have arranged for immediate open access. Opinions expressed and interpretations presented are those of the authors and do not necessarily reflect those of the editors, publishers and other contributors. Your comments are welcome.

Cover Image: A rare rock called pinolite was used to sculpt this beautiful 35 cm tall bird from stone quarried at Quartz Creek, British Columbia. The word 'pinolite' comes from the pinecone-like texture formed by coarse-grained magnesite crystals. The sculpture was created by Deborah Wilson from Vernon, BC, (http://www.deborahwilson.bc.ca/contact.htm). The photograph taken by the artist and supplied with permission by Ian Burak.

SERIES

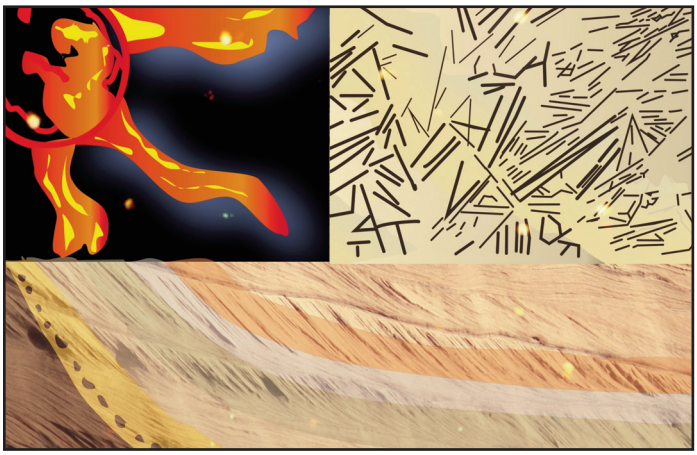

Igneous Rock Associations 28. Construction of a Venusian Greenstone Belt: A Petrological Perspective

J. Gregory Shellnutt

Department of Earth Sciences, National Taiwan Normal University
88 Tingzhou Road Section 4, Taipei 11677, Taiwan
E-mail: jgshelln@ntnu.edu.tw

"Imagination is more important than knowledge. Knowledge is limited. Imagination encircles the world" - Albert Einstein
"Every sentence I utter must be understood not as an affirmation, but as a question." - Niels Bohr

SUMMARY
The crustal evolution of Venus appears to be principally driven by intraplate processes that may be related to mantle upwelling as there is no physiographic (i.e. mid-ocean ridge, volcanic arc) evidence of Earth-like plate tectonics. Rocks with basaltic composition were identified at the Venera 9, 10, 13, and 14, and Vega 1 and 2 landing sites whereas the rock encountered at the Venera 8 landing site may be silicic. The Venera 14 rock is chemically indistinguishable from terrestrial olivine tholeiite but bears a strong resemblance to basalt from terrestrial Archean greenstone belts. Forward petrological modeling (i.e. fractional crystallization and partial melting) and primary melt composition calculations using the rock compositions of Venus can yield results indistinguishable from many volcanic (ultramafic, intermediate, silicic) and plutonic (tonalite, trondhjemite, granodiorite, anorthosite) rocks that typify Archean greenstone belts. Evidence of chemically precipitated (carbonate, evaporite, chert, banded-iron formation) and clastic (sandstone, shale) sedimentary rocks is scarce to absent, but their existence is dependent upon an ancient Venusian hydrosphere. Nevertheless, it appears that the volcanic–volcaniclastic–plutonic portion of terrestrial greenstone belts can be constructed from the known surface compositions of Venusian rocks and suggests that it is possible that Venus and Early Earth had parallel evolutionary tracks in the growth of proto-continental crust.

RÉSUMÉ
L'évolution de la croûte de Vénus semble être principalement déterminée par des processus intraplaques qui peuvent être liés à des remontées mantelliques, car il n'y a aucune preuve physiographique d'une tectonique des plaques semblable à la Terre (c.-à-d. dorsale médio-océanique, arc volcanique). Des roches de composition basaltique ont été identifiées sur les sites d'atterrissage de Venera 9, 10, 13 et 14 et Vega 1 et 2 tandis que la roche rencontrée sur le site d'atterrissage de Venera 8 peut être silicique. La roche du site de Venera 14 est indiscernable de la tholéiite à olivine terrestre de par ses propriétés chimiques, mais ressemble fortement au basalte des ceintures de roches vertes archéennes terrestres. La modélisation pétrologique prospective (c.-à-d. cristallisation fractionnaire et fusion partielle) et les calculs de la composition de fusion primaire à partir des compositions des roches de Vénus peuvent donner des résultats indiscernables de nombreuses roches volcaniques (ultramafiques, intermédiaires, siliciques) et plutoniques (tonalite, trondhjemite, granodiorite, anorthosite) qui caractérisent les ceintures de roches vertes archéennes. Les preuves de roches sédimentaires précipitées chimiquement (carbonate, évaporite, chert, formation de fer rubané) et clastiques (grès, schiste) sont rares ou absentes, mais leur existence dépend d'une ancienne hydrosphère vénusienne. Néanmoins, il semble que la partie volcanique-volcanoclastique-plutonique des ceintures de roches vertes puisse être construite à partir des compositions de surface connues des roches vénusiennes et suggère qu'il est possible que Vénus et la Terre primitive aient eu des trajectoires évolutives parallèles de croissance de la croûte proto-continentale.

Traduit par la Traductrice

Geoscience Canada, v. 48, https://doi.org/10.12789/geocanj.2021.48.176 pages 97–116

INTRODUCTION

Venus and Earth are often considered to be sister planets as they are similar in size, bulk composition, density, crater retention, and they have significant, albeit compositionally distinct, atmospheres (Table 1; Hansen 2018; Taylor et al. 2018). The modern exploration of Venus began in the 1960s and it was the first planet to be visited by a spacecraft (Mariner 2), have a probe soft-land on the surface (Venera 7), and to have surface pictures taken and sent back to Earth (Venera 9). Exploration of Venus continues to this day although the number of projects has waned since the successful Venera, Magellan, and Venus Express programs of the 1960s–1980s, 1990s, and 2000s (Basilevsky and Head 2003). Consequently, new discoveries have lagged behind that of other celestial bodies such as Mercury, Mars, Ceres, Titan, and Pluto. In spite of the lesser number of missions, new ideas and concepts on the evolution of Venus have been proposed in the past decade that could change the perception of Venus as an inhospitable hellscape. The new observations have led to suggestions that the crust of Venus may be differentiated (Hashimoto et al. 2008; Gilmore et al. 2015), that Venus may have sustained vast oceans until the middle Neoproterozoic (Way et al. 2016; Way and Del Genio 2020), that there was a climatic transition from relatively cool and wet that permitted deposition and erosion to hot and dry (Khawja et al. 2020; Byrne et al. 2021), that the surface age (~130 Ma) may be very young (Bottke et al. 2015), and that the conditions to support life may exist in the atmosphere (Seager et al. 2021).

The geology of Venus remains enigmatic as the physiographic features are known, but there is a dearth of detailed information on just about all other aspects (e.g. thermal regime, surface composition, sediment deposition) of crustal evolution (Basilevsky and Head 1988, 2003; Nimmo and McKenzie 1998; Ivanov and Head 2011). The surface of Venus is dominated (~ 80%) by relatively featureless volcanic plains that lie within ± 1 km of the mean planetary radius (mpr), whereas the remainder of the surface is composed of mesolands and highlands (Fig. 1; Basilevksy and Head 2003; Fegley Jr. 2014). The mesolands are moderately elevated, 1 km to 2 km above the mpr, and are known for their coronae (large oval volcanic domains) and chasmata (troughs) features. The highland regions represent ~ 8% of the surface and consist of tesserae terranes, large volcanic edifices, compression-related mountain belts, and may be compositionally different from the lowlands (Ansan and Vergely 1995; Basilevksy and Head 2003; Hashimoto et al. 2008; Gilmore et al. 2015). From the geomorphology of the crust, it is clear that Venus does not have Earth-like plate tectonics due to the absence of globe-encircling mid-ocean ridges and volcanic arc subduction zones (Nimmo and McKenzie 1998). However, the formation of the highlands is perplexing as it is not precisely known how or why thickened and compositionally differentiated crust can be voluminous in the absence of plate tectonics.

Different tectonic models have been proposed to explain the compressional, extensional, and deformational features and the higher elevations (> 3 km) of the highland terranes (tesserae). Models of highland formation are primarily focused on whether mantle upwelling or downwelling is the controlling factor in their development and maintenance (Bindschadler 1995; Jull and Arkani-Hamed 1995; Phillips and Hansen 1998; Hansen and Willis 1998; Hansen et al. 1999). The two largest highland terranes, Ishtar Terra and Aphrodite Terra, bear a striking resemblance to continental crust on Earth as they are elevated with respect to the volcanic plains and they appear to be older and at least partially deformed (Bindschadler and Head 1991; Ivanov 2001; Hashimoto et al. 2008; Romeo and Turcotte 2008; Gilmore et al. 2015). The apparent lack of plate tectonics and the existence of highland terranes on Venus has led to suggestions that Venus may be analogous to the pre-plate tectonics Archean Earth or possibly a post-plate tectonics setting (Hamilton 2007; Hansen 2007a, 2018; Harris and Bédard 2014). In fact, the vertical tectonic (mantle upwelling) model for the development of Venusian highland terranes is somewhat comparable to the 'unstable stagnant lid' model proposed for some granite–greenstone belts of Archean cratons (Harris and Bédard 2015; Bédard 2018). However, a major uncertainty with all geological analogues between Venus and Earth is whether the two planets have similar mantle compositions and structures, supracrustal rock types (komatiite, kimberlite, sedimentary rocks), or operated under similar tectonic regimes (plate tectonics).

Table 1. Physical properties of Venus and Earth.

Property	Venus	Earth
Radius	6052 km	6378 km
Mass	4.87×10^{24} kg	5.97×10^{24} kg
Bulk density	5.24 (g/cm^3)	5.51 (g/cm^3)
Albedo	59%	39%
Surface gravity acceleration	8.87 m/s	9.80 m/s
Average surface temperature	460°C	15°C
Atmosphere composition	N_2 (3.5%) O_2 (0-20 ppm) CO_2 (96.5%) H_2O (30 ± 15 ppm)	N_2 (78.1%) O_2 (20.9%) CO_2 (420 ppm) H_2O (4% to 40 ppm)

Values from Faure and Messing (2007).

The surface composition of Venus was measured at seven different locations between 20°S and 30°N across the volcanic plain and mesoland regions (Fig. 2; Kargel et al. 1993). The Venera 13, Venera 14, and Vega 2 landers analyzed, with the exception of Na_2O, the major elements, Cl, and SO_3 by X-ray fluorescence spectrometry (Table 2); whereas the Venera 8, Venera 9, Venera 10, Vega 1, and Vega 2 landers measured Th, U, and K by γ-ray spectrometry (Table 3; Vinogradov et al. 1973; Surkov 1977; Surkov et al. 1984, 1986, 1987). The rocks at the Venera 13 and Venera 14 sites are compositionally basaltic, but have distinct concentrations of CaO and K_2O. The compositional differences indicate the Venera 13 rock is alkaline (olivine leucitite or phonotephrite) whereas the Venera

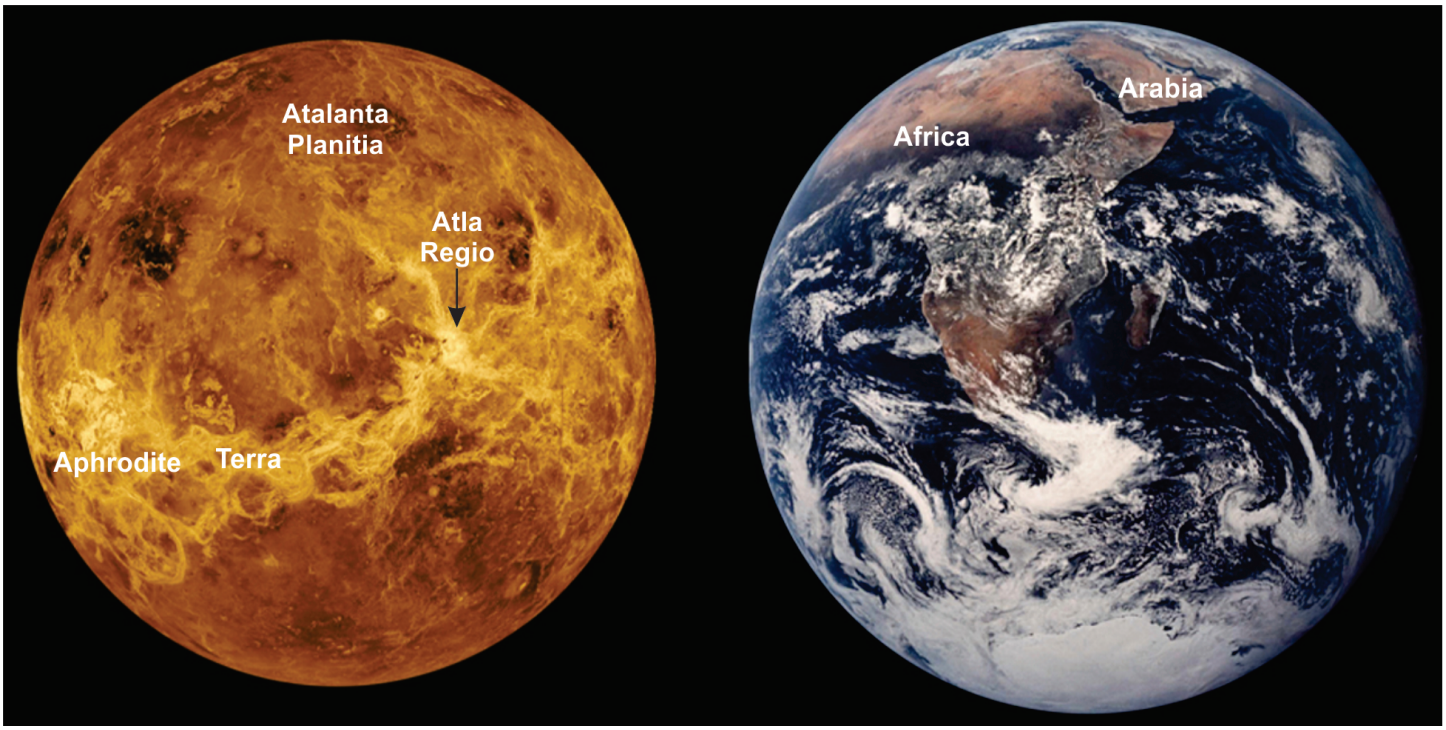

Figure 1. Size comparison of Venus and Earth. The Venus surface image is radar-based and false colour. Earth image from NASA/Apollo 17 crew.

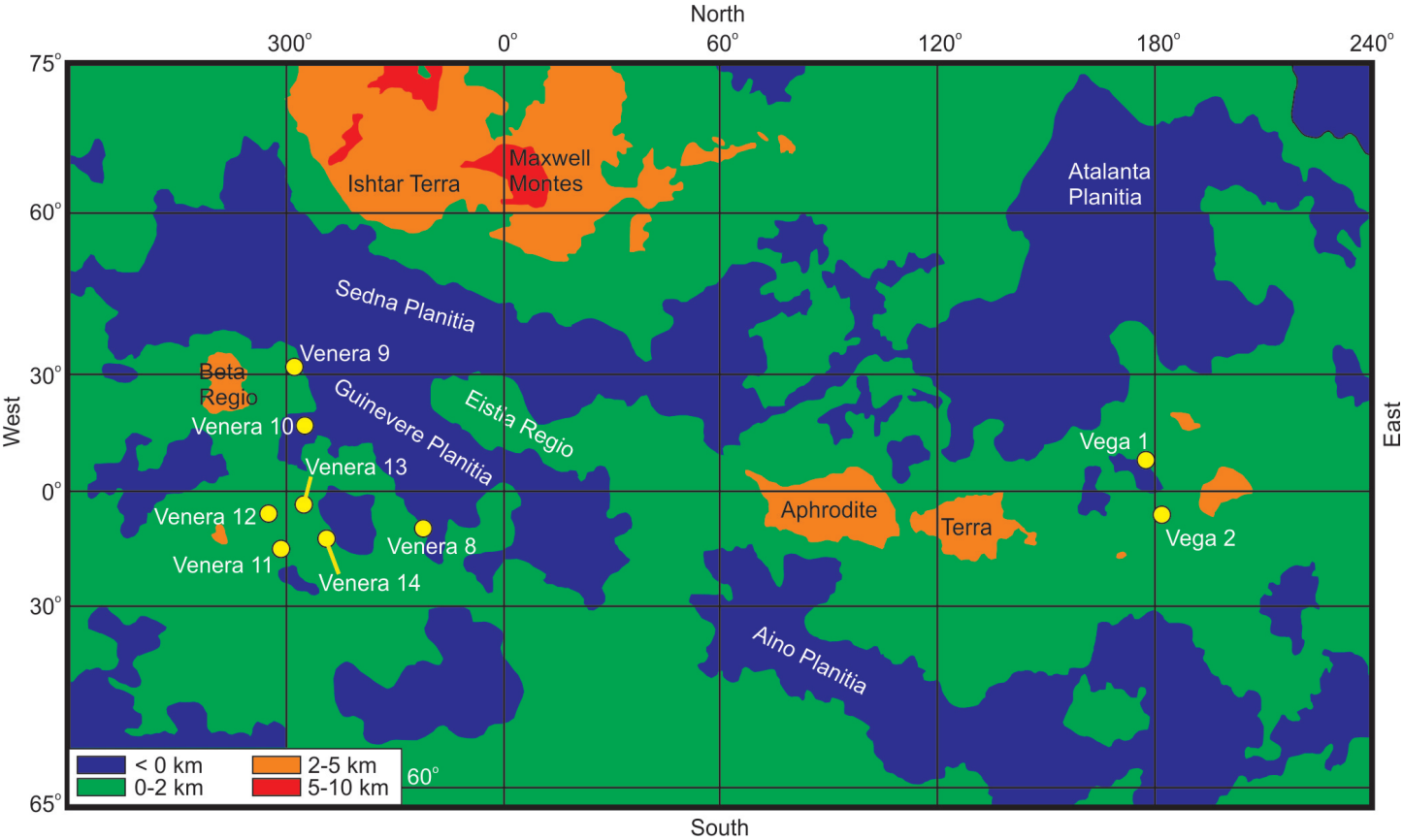

Figure 2. Mercator projection map of Venus showing the relative mean planetary radius crustal elevation and the locations of the Venera and Vega landers (modified from Faure and Messing 2007).

https://doi.org/10.12789/geocanj.2021.48.176

Table 2. Major element compositions of basalt from Venus, mid-ocean ridges, Archean greenstone belts, and the estimated composition of the Venera 8 rock.

Sample	Venera 13	Venera 14	Vega 2	Venera 8 (estimated)	N-MORB (mean)	E-MORB (mean)	Archean (DAT)	Archean (EAT)
SiO_2 (wt.%)	45.1 ± 3.0	48.7 ± 3.6	45.6 ± 3.2	58.3-65.6	50.42 ± 0.08	50.58 ± 0.33	50.90	50.91
TiO_2	1.6 ± 0.45	1.25 ± 0.41	0.20 ± 0.1	0.5-1.5	1.53 ± 0.04	1.53 ± 0.11	0.95	1.53
Al_2O_3	15.8 ± 3.0	17.9 ± 2.6	16.0 ± 1.8	13.4-16.2	15.13 ± 0.12	14.94 ± 0.38	15.72	15.63
FeO	9.3 ± 2.2	8.8 ± 1.8	7.7 ± 1.1	3.2-6.8	9.81 ± 0.15	9.64 ± 0.48	10.30	12.02
MnO	0.2 ± 0.1	0.16 ± 0.08	0.14 ± 0.12	0.1-0.2	0.17 ± 0.004	0.16 ± 0.013	0.22	0.19
MgO	11.4 ± 6.2	8.1 ± 3.3	11.5 ± 3.7	1.6-4.1	7.76 ± 0.09	7.37 ± 0.27	7.64	7.01
CaO	7.1 ± 1.0	10.3 ± 1.2	7.5 ± 0.7	2.8-6.4	11.35 ± 0.08	11.18 ± 0.27	11.76	9.04
Na_2O	2.0 ± 0.5*	2.4 ± 0.4*	2.0 ± 0.5*	2.5-4.4	2.83 ± 0.05	2.72 ± 0.18	2.18	2.78
K_2O	4.0 ± 0.6	0.2 ± 0.07	0.1 ± 0.08	3.4-4.9	0.14 ± 0.11	0.39 ± 0.075	0.22	0.71
P_2O_5				0.2-0.70	0.16 ± 0.004	0.24 ± 0.051	0.10	0.17
SO_3	1.6 ± 1.0	0.88 ± 0.77	4.7 ± 1.5					
Cl	< 0.3	< 0.4	< 0.3					
H_2O								
Th (ppm)			2.0 ± 1.0	6.4-6.7	0.25 ± 0.029	1.4 ± 0.23		
U (ppm)			0.68 ± 0.38	1.6-2.7	0.08 ± 0.008	0.39 ± 0.06		
Total	98.1	98.7	95.4					

All Venus basalt data reported at 1σ uncertainty. *The Na_2O content is calculated for the Venera 13, 14 and Vega 2 data (Surkov et al. 1984, 1986). The calculated Venera 8 composition is from Nikolayeva (1990). The mean (2σ) N-MORB (normal mid-ocean ridge basalt) and E-MORB (enriched mid-ocean ridge basalt) compositions are from Gale et al. (2013). Average Archean tholeiitic compositions from Condie (1981). DAT = depleted Archean tholeiite; EAT = enriched Archean tholeiite.

Table 3. Measured K_2O, Th and U contents from the surface rocks of Venus by g-ray spectrometry.

Sample	Vega 1	Vega 2	Venera 8	Venera 9	Venera 10
K_2O (wt.%)	0.45 ± 0.22	0.40 ± 0.20	4.0 ± 1.2	0.47 ± 0.08	0.30 ± 0.16
Th (ppm)	1.5 ± 1.2	2.0 ± 1.0	6.5 ± 2.2	3.65 ± 0.42	0.70 ± 0.34
U (ppm)	0.64 ± 0.47	0.68 ± 0.38	2.2 ± 0.7	0.60 ± 0.16	0.46 ± 0.26

The results reported by Surkov et al. (1987).

14 rock is sub-alkaline and similar to tholeiite from Archean greenstone belts and terrestrial within-plate settings (Fig. 3; Condie 1981; Filiberto 2014). The material measured at the Vega 2 landing site is unusual and may be representative of a soil–rock mixture as the reported SO_3 (4.7 ± 1.5 wt.%) content is very high. The remaining rocks are considered to be tholeiitic basalt or gabbro based on their Th–U–K contents (Fig. 4; Vinogradov et al. 1973; Surkov et al. 1986; Kargel et al. 1993; Treiman 2007).

There is significant uncertainty regarding the nature of the rock measured at the Venera 8 landing site as the Th (6.5 ± 2.2 ppm) and U (2.2 ± 0.7 ppm) concentrations are anomalously high and within the range of intermediate to silicic (granodiorite or dacite) igneous rocks (Nikolayeva 1990; Basilevsky et al. 1992). Nikolayeva (1990) suggested that the Venera 8 rock could be evidence of differentiated (continental?) crust but the K_2O (K_2O = 4.0 ± 1.2 wt.%) content of Venera 8 is indistinguishable from the value reported at the Venera 13 (K_2O = 4.0 ± 0.6 wt.%) landing site (Kargel et al. 1993; Treiman 2007). Subsequently, Basilevsky et al. (1992), due to the data uncertainty, concluded that the Venera 8 rock could be either an alkali basaltic rock (leucitite, minette, lamprophyre) or an evolved intermediate rock (diorite, granodiorite, syenite). The predominance of basaltic rocks encountered on the surface of Venus suggests that the planet may have retained its primary crust or that it is dominated by flood basalt of large igneous provinces or possibly the supracrustal successions of terrestrial Archean granite–greenstone belts (Harris and Bédard 2014; Hamilton 2015; MacLellan et al. 2021).

This contribution is a review of petrological modeling (fractional crystallization modeling, equilibrium partial melting, primary melt composition) that used the surface compositions measured at the Venera 13, Venera 14, and Vega 2 landing sites (Surkov et al. 1984, 1986, 1987). The modeling results are contextualized from within the framework of terrestrial geology and the formation mechanism of Archean supracrustal rocks as deduced from greenstone belts that typify the oldest cratons of Earth. The purpose of this manuscript is to demonstrate that the volcanic and sedimentary lithologies of terrestrial greenstone belts can be generated from rock compositions that are known to exist on the surface of Venus. Although the uncertainty in the data and the limited geological

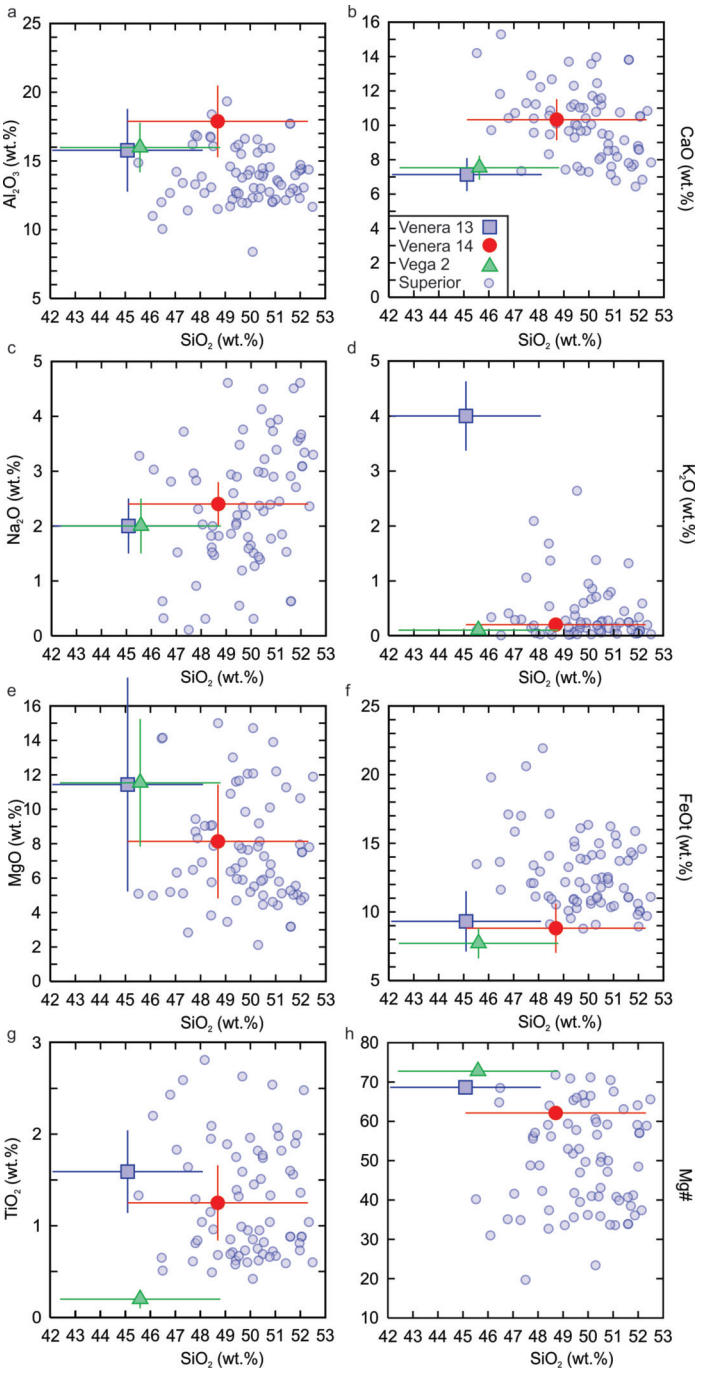

Figure 3. Major elemental comparison of Venusian basalt to tholeiitic basalt from Superior Province greenstone belts. All Superior Province data are from the GEOROC database (http://georoc.mpch-mainz.gwdg.de/georoc/). The Superior Province basalt data were selected if the sum total was > 97 wt.% and < 101 wt.% without loss on ignition and MgO < 15 wt.%. Total iron was recalculated to FeOt (Fe_2O_3 wt.% = 0.8998 ´ FeO wt.%).

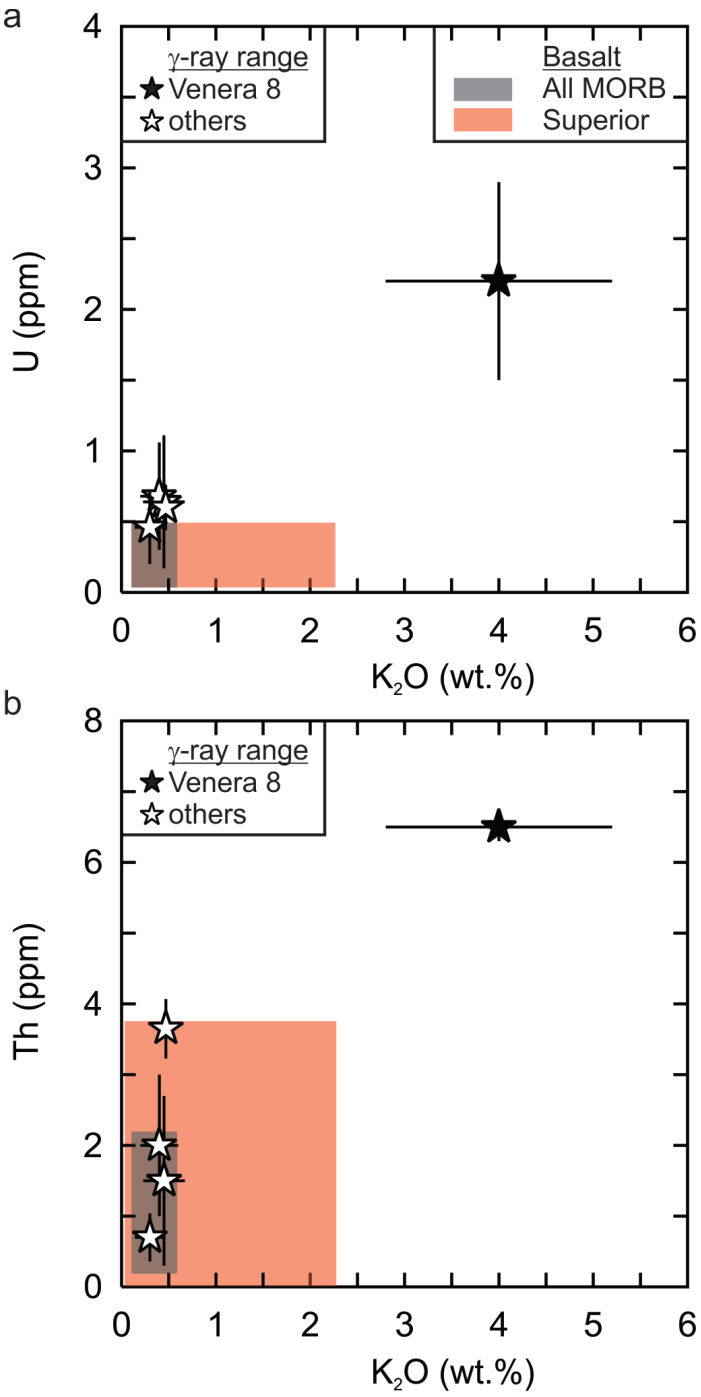

Figure 4. Trace elemental comparison of the Venusian basalts to all MORB and greenstone belt basalts from the Superior Province. All MORB values from Gale et al. (2013) and the Superior Province data is from the GEOROC database (http://georoc.mpch-mainz.gwdg.de/georoc/).

knowledge of Venus prevents a firm conclusion, the findings indicate that the existence of greenstone belt-like crust on Venus cannot currently be dismissed. Therefore, I offer a hypothesis that is eminently testable for future missions to Venus.

SUMMARY OF MODELING PARAMETERS

Fractional crystallization and equilibrium partial melting modeling of the Venusian rocks were conducted using the petrological software MELTS (Shellnutt 2013) and Rhyolite-MELTS (Shellnutt 2018, 2019; Shellnutt and Manu Prasanth 2021). The magma conditions (initial temperature, relative oxidation state,

Table 4. Summary of MELTS and Rhyolite-MELTS modeling conditions.

Model	Pressure (GPa)	Relative oxidation state (fO_2)	Water content (wt.%)	Venera 13	Venera 14	Vega 2	Primitive Venera 14	Software version
2013								
FC	0.01, 0.1, 1.0	ΔFMQ 0	0, 0.2	✓	✓			M
PM	0.01, 0.1, 1.0	ΔFMQ 0	0, 0.2	✓	✓			M
2018								
FC	0.01, 0.1, 0.5	ΔFMQ 0, -1	0, 0.5			✓		R
PM	0.01, 0.1, 0.5	ΔFMQ 0, -1	0, 0.5			✓		R
2019								
FC	0.1, 0.5	ΔFMQ +0.7	0.4		✓			R
2021								
FC	0.1, 0.5, 1.0	ΔFMQ -1, 0, +1	0, 0.20, 0.5	✓	✓	✓	✓	R

FC = fractional crystallization; PM = equilibrium partial melting. M = MELTS (Smith and Asimow 2005); R = Rhyolite-MELTS (Gualda et al. 2012). FMQ = fayalite-magnetite-quartz buffer.
All models are isobaric conditions but the models of 2018, 2019, and 2021 include polybaric conditions. Primitive Venera 14 compositions were calculated by Shellnutt (2016).

water contents) used in the models encompass a wide range due to the uncertainties of the redox state, ambient temperature, and water content of the Venusian mantle (Table 4). However, conditions similar to terrestrial within-plate tectonic settings rather than subduction zone or mid-ocean ridge settings were used as a guide.

Pressure (1.0 GPa = ~ 35 km) is the least uncertain parameter and the model conditions range from surface to near surface (0.01 GPa), upper crust (0.1 GPa), middle crust (0.5 GPa), and lower crust (1.0 GPa). Most models presented here assume isobaric conditions, however polybaric models were also modeled (Shellnutt 2018, 2019; Shellnutt and Manu Prasanth 2021). The relative oxidation states of the models are within one log unit of the fayalite–magnetite–quartz buffer (ΔFMQ ± 1) as the FeO/MnO ratios of Venusian basalt (Venus basalt ≈ 52; bulk silicate Earth ≈ 60) are similar to bulk silicate Earth. Therefore, it is likely that the redox conditions of the Venusian mantle that produced the basalt is within two log units of the fayalite–magnetite–quartz (ΔFMQ ± 2) buffer, but could be slightly less oxidizing (Haggerty 1978; Schaefer and Fegley Jr. 2017).

The water content of the Venusian mantle is the most uncertain parameter. Evidence suggests Venus lost significant quantities of surface water and that the low but stable concentration of atmospheric water is maintained by atmosphere–mantle coupling (Donahue et al. 1997; Fegley Jr. 2014; Filiberto 2014; Gillmann and Tackley 2014; Airey et al. 2015; Way et al. 2016; Filiberto et al. 2020). Due to the uncertainty of the water concentration of the Venusian mantle, anhydrous (H_2O = 0 wt.%) and hydrous conditions were used in the hope that the conditions on Venus could be deduced indirectly from these models. For the basaltic models, 0.2, 0.4, and 0.5 wt.% water were used as these values are common for terrestrial basalt at within-plate settings (Hauri 2002). For the primary melt compositions, water was set to 0.2 wt.% as this is typical of primitive mafic and ultramafic volcanic rocks (Berry et al. 2008; Husen et al. 2013; Sobolev et al. 2016).

The primary melt composition and mantle potential temperature (T_p) estimates are calculated for Venera 14 using PRIMELT3 (Herzberg and Asimow 2015; Shellnutt 2016). The important parameters for the calculations are FeOt and MgO because they are the constituent components of olivine. The CaO content is also important because it indicates whether clinopyroxene and/or plagioclase were removed from the starting composition (i.e. Venera 14 composition). Consequently, the CaO content must be adjusted to prevent a clinopyroxene fractionation warning. The maximum and minimum permitted values of MgO, FeOt and CaO (± 1σ error) were used so that the T_P range can be constrained. The remaining elements (TiO_2, Al_2O_3, MnO, CaO, Na_2O and K_2O) are not major components of olivine and thus their variability will not significantly influence the estimates. The calculated primary melt compositions were then used for the Rhyolite-MELTS fractional crystallization modeling to investigate how the primary melts evolved after separation from the mantle (Table 5).

WHAT IS A GREENSTONE BELT?

A signature feature of all Archean cratons is the occurrence of granite–greenstone belts. Simply put, granite–greenstone belts are well preserved linear to curvilinear rock suites that are typically 10–25 km wide, 100–300 km long, 5 km−30 km thick and have a characteristic stratigraphy of volcanic rocks followed by volcaniclastic and sedimentary rocks that represent the final stages of maturation (Condie 1981; Bleeker 2002; Hawkesworth and Kemp 2006; Anhaeusser 2014; Thurston 2015). All greenstone belts are metamorphosed to some extent and intruded by granitic rocks (e.g. tonalite–trondhjemite–gra-

Table 5. Calculated primitive composition of the Venera 14 basalt and mantle potential temperature estimates.

Sample	Venera 14 (model 1)	Batch Melt	AFM	Venera 14 (model 2)	Batch Melt	AFM	AFM	Venera 14 (model 3)	Batch Melt	AFM
SiO_2 (wt.%)	48.7	49.11	49.13	48.7	46.41	46.47	46.66	48.7	48.06	48.13
TiO_2	1.25	1.26	1.26	1.25	1.07	1.08	1.12	1.25	1.19	1.20
Al_2O_3	17.9	17.97	18.01	17.9	15.26	15.44	15.99	17.9	17.05	17.22
Fe_2O_3		0.63	0.63		0.53	0.54	1.12		0.60	0.60
FeO		6.62	6.61		9.0	9.0	8.44		7.57	7.56
FeOt	7.1			9.7				8.1		
MnO	0.16	0.16	0.16	0.16	0.15	0.15	0.16	0.16	0.16	0.16
MgO	9.9	10.21	10.11	11.3	15.56	15.14	13.91	11.1	12.61	12.24
CaO	11.4	11.44	11.47	11.5	9.82	9.94	10.29	10.8	10.29	10.39
Na_2O	2.4	2.41	2.42	2.4	2.04	2.07	2.14	2.4	2.29	2.31
K_2O	0.2	0.20	0.20	0.20	0.17	0.17	0.18	0.20	0.19	0.19
SO_3										
Cl										
Total	99.01	100	100	103.11	100	100	100	100.61	100	100
Pressure (bars)		100	100		100	100	100		100	100
FeO (source)		8.02	8.02		8.02	8.02	8.02		8.02	8.02
MgO (source)		38.12	38.12		38.12	38.12	38.12		38.12	38.12
Fe_2O_3/TiO_2		0.5	0.5		0.5	0.5	1.0		0.5	0.5
Mole Fraction Fe^{2+}/Fe^*		0.92	0.92		0.94	0.94	0.88		0.93	0.93
% ol addition		0.6	0.3		13.0	11.8	8.2		4.3	3.3
F (%)		0.06	0.06		0.11	0.11	0.09		0.11	0.11
Temperature (°C)		1240	1240		1360	1350	1330		1300	1290
T_P (°C)		1310	1310		1450	1440	1410		1370	1360

AFM = accumulated fractional melt. F (%) = melt fraction. The model compositions above are entered into PRIMELT3 (Herzberg and Asimow 2015). The software automatically normalizes the data to 100% for the calculation. T_P (°C) = mantle potential temperature.

nodiorite) with many hosting significant deposits of base and precious metals (e.g. Au, Zn, Pb, Ni, Cu).

The terrestrial Archean volcanic sequences are typically composed of mafic subaqueous volcanic and volcaniclastic rocks with felsic intercalations and almost no sedimentary rocks. In comparison, the upper unit is primarily composed of sedimentary caprocks with few subaerial K-rich volcanic rocks (Fig. 5; Anhaeusser 2014; Thurston 2015). The lower portion of the volcanic unit consists of subaqueous ultramafic (komatiite) to mafic (tholeiite, boninite) volcanic rocks with minor felsic tuff layers. The upper portions of the lower unit consist of a bimodal sequence of tholeiitic flows and calc-alkaline mafic and silicic (andesitic to rhyolitic) volcanic rocks (Condie 1981; Anhaeusser 2014; Thurston 2015). In some cases the mafic–ultramafic sequences are separated by thin layers of calc-alkaline rocks at intervals ranging from 3 million years to 30 million years (Harris and Bédard 2014). Deposited on top of the volcanic series are sedimentary rocks, but the lithology of each greenstone belt is unique and can be composed of volcanogenic sandstone and mud-rocks, chemically precipitated carbonate rocks, sulphate chemically precipitated rocks (e.g. gypsum, barite), and banded iron formations, chert, jaspillitic sequences, conglomerate–quartz arenite–carbonate sequences, conglomerate–wacke–pelite, and tidal sand-wave deposits (Anhaeusser 2014). Furthermore, sedimentary depositional gaps also exist between volcanic episodes that range in duration from 2 to 27 million years (Thurston et al. 2008). The total duration of magmatism of a given greenstone belt is variable and can range from ~ 50 to ~ 300 million years (Percival and Card 1986; Corfu and Andrews 1987; Byerly et al. 1996; Anhaeusser 2014; Thurston 2015).

The intrusive complexes of greenstone belts include layered mafic intrusions (LMI), sill complexes, anorthosite plutons, and granitic suites (Bédard et al. 2009; Anhaeusser 2014; Ashwal and Bybee 2017). The layered intrusions are considered to be representative of magma chambers in which komatiitic and/or basaltic magma differentiated. Furthermore, anorthosite, and associated leucogabbro and gabbro, is a minor component of some greenstone belts (e.g. Abitibi, Fiskenæsset, Barberton). Anorthosite is principally formed by crystallization and accumulation of plagioclase from a mafic or ultramafic parental magma and occurs either as layers within LMI or as megacrystic lavas or sills (Ashwal and Bybee 2017). Among the granitic rocks that intrude greenstone belts are the tonalite–trondhjemite–granodiorite (TTG) suites that are considered to be generated by partial melting of hydrous mafic lower crust or possibly derived from subduction-related magmatic processes (Moyen 2011; Anhaeusser 2014).

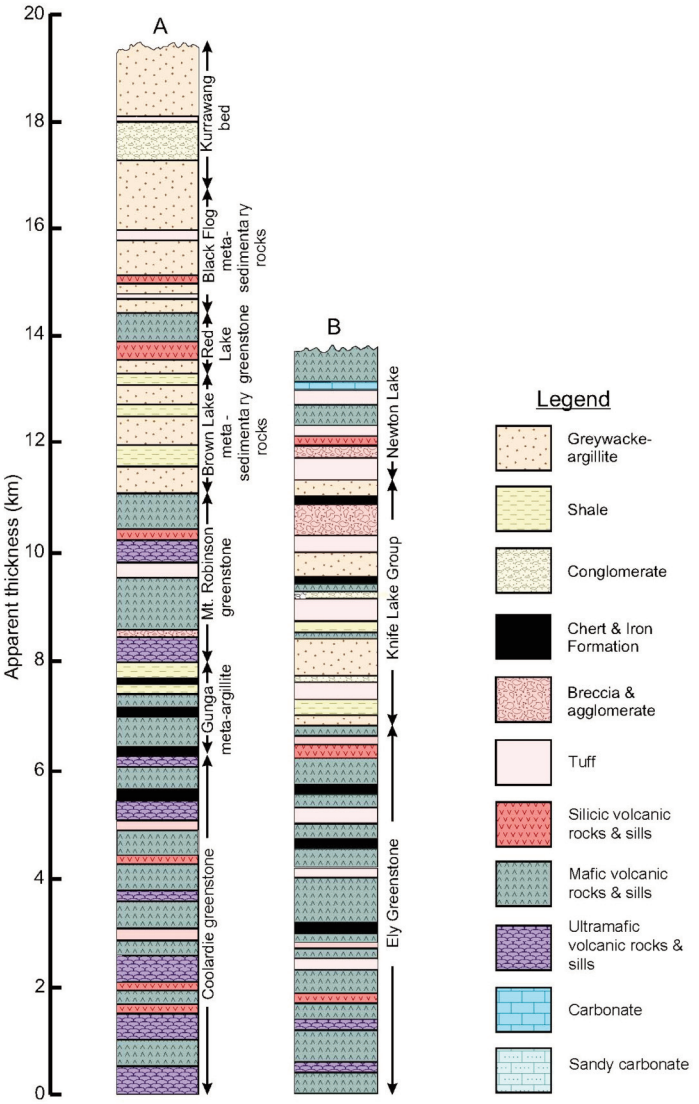

Figure 5. Greenstone belt stratigraphy of the Coolgardie–Kurrawang succession of Western Australia (A) and the Vermilion succession (B) of Minnesota (modified from Condie 1981).

The formation and origin (plate tectonic origin versus mantle-controlled) of greenstone belts has yet to be resolved as they are thought to be analogous to modern oceanic plateaus, volcanic arcs, ophiolites, or flood basalt suites that, at some level, may involve a mantle plume particularly with respect to the eruption of the lower mafic–ultramafic volcanic series (de Wit and Ashwal 1995; Bédard et al. 2003, 2013; Smithies et al. 2005a; Bédard 2006; Condie and Benn 2006; Anhaeusser 2014; Thurston 2015). The calc-alkaline nature of the silicic rocks in greenstone belts is, in some cases, considered to be evidence in favour of a volcanic arc-like origin for at least the silicic portion of the bimodal sequence (Scott et al. 2002; Wyman et al. 2002; Smithies et al. 2005b). It is likely that greenstone belts represent a glimpse into the development of primitive terrestrial crust or proto-continental crust (Smithies et al. 2005a; Thurston 2015; Bédard 2018).

TECTONOTHERMAL REGIME OF VENUS

The surface of Venus is dominated by low-lying volcanic plains that have a low crater density and an estimated crustal thickness of 10–15 km (Strom et al. 1994; Nimmo and McKenzie 1998; Byrnes and Crown 2002; James et al. 2013). Constraints on the interior processes, in particular the upper mantle, of Venus can be deduced from rock surface morphologies and compositions, large-scale physiographic features (rifts, folds, faults), and atmospheric composition (McKenzie et al. 1992a; Lee et al. 2009; Armann and Tackley 2012; Gillmann and Tackley 2014; O'Rourke and Korenaga 2015). The identification of large volcanic rises (e.g. Beta Regio), pancake domes (flat-top and steep-sided), coronae and novae (e.g. Mokos, Selu, Zemire), shield volcanoes (e.g. Maat Mons, Sapa Mons), and anastomosing lava channels indicate that Venusian lava flows have different viscosities and different compositions and/or represent different thermal regimes (Head et al. 1992; McKenzie et al. 1992b; Pavri et al. 1992; Kargel et al. 1993; Sakimoto and Zuber 1993; Lancaster et al. 1995; Nimmo and McKenzie 1998; Byrnes and Crown 2002; Buchan and Ernst 2021; MacLellan et al. 2021). The low crater density of Venus suggests volcanism was probably the main process of resurfacing and the maintenance of a young surface age, although the role of weathering and fluvial erosion in the denudation of surface features is possible, but not well established (Hauck et al. 1998; Smrekar et al. 2007; Kreslavsky et al. 2015; Way et al. 2016; Khawja et al. 2020). Hamilton (2005, 2015) offered an alternative explanation and suggested that Venus became geologically inert by 3.8 Ga due to less radiogenic heat, but this view is not widely adopted.

The absence of Earth-like subduction zones and mid-ocean ridges suggests that the interior cooling of Venus is probably facilitated primarily by advective heat transport either by mantle plumes or hotspots (Nimmo and McKenzie 1998; Phillips and Hansen 1998; Smrekar et al. 2007, 2010; Gillmannn and Tackely 2014; Gülcher et al. 2020; MacLellan et al. 2021). Conduction and rifting and mantle decompressional melting probably play important roles in mantle cooling as well. Accretion and differentiation models of Venus-like planets yielded bulk mantle compositions similar to Earth (FeO = 8.14 ± 0.90 wt.%), in particular the bulk FeO (4.52 to 8.25 wt.%) content (Herzberg and O'Hara 2002; Rubie et al. 2015). Consequently, mantle potential temperatures and primary melt compositions can be calculated from the Mg# of the Venusian basalt and offer estimates on the possible thermal regimes that operate on Venus as well as initial eruptive temperatures (Nimmo 2002; Lee et al. 2009; Filiberto 2014). A number of mantle potential temperature (T_P) estimates were calculated for Venus with temperatures of Venera 13 (T_P = 1459 ± 73°C) and Venera 14 (T_P = 1330°C, 1370 ± 70°C, 1459 ± 101°C) within the range of ambient conditions of modern Earth (i.e. T_P = 1350 ± 50°C); whereas estimates of Vega 2 (T_P = 1778 ± 167°C) are significantly higher and could be within the range of ambient Archean mantle, but the rock at Vega 2 may be representative of a soil–rock mixture (McKenzie et al. 1992a;

Lee et al. 2009; Weller and Duncan 2015; Shellnutt 2016, 2018). The initial melt composition of Venera 13 is difficult to calculate because the whole rock sum total is lower than that reported for the Venera 14 rock and it is alkaline, suggesting that was not in equilibrium with a low volatile lherzolitic mantle source (Table 5; Filiberto 2014).

The calculated thermal estimates and primary melt compositions are consistent with some of the volcanic morphologies (e.g. shield volcanoes, anastomosing lava channels) of the planitiae, although the pancake domes appear to indicate low viscosity lavas that may or may not be silicic (McKenzie et al. 1992b; Fink et al. 1993; Sakimoto and Zuber 1993). Nevertheless, as the range of model T_p similar to Earth have been calculated, the thermal regime and bulk composition of the Venusian mantle can be considered similar to the Earth, as it is consistent with known data. The possible thermal regime differences suggest that Venus may have had regions characterized by rapid eruption flux of mafic and ultramafic lavas (cf. Basilevsky and Head 2007; Hansen 2007b) and those of slower eruption rates expected for passive rifting (Basilevsky and Head 2002; Ivanov and Head 2015; Shellnutt 2016).

CONSTRUCTING A VENUSIAN GREENSTONE BELT

Lower Volcanic Sequence

When one builds a house it is wise to start with the foundation. The lower volcanic sequence of greenstone belts is commonly composed of spinifex-textured komatiite and primitive tholeiitic basalt with volcaniclastic rocks (Condie 1981; Anhaeusser 2014; Thurston 2015). The basalt measured at the Venera 14 landing site is compositionally similar to typical tholeiitic basalt of Archean greenstone belts and, more broadly, mafic volcanic rocks from continental flood basalt provinces or oceanic plateaus (Figs. 3 and 4). It is probably the only rock type from the Venus data set that can be identified with any degree of certainty and even then, the uncertainty of the measurement of Venera 14 is large.

The primary melt composition of Venera 14 was calculated using PRIMELT3 software and reported by Shellnutt (2016) and summarized in Table 5. Given the data uncertainty and the mantle redox conditions of the Venusian mantle, four primary melt compositions were calculated by accumulated fractional melting (AFM) whereas three were calculated using batch melting (Table 5). The AFM compositions, probably more representative of actual melt accumulation, show that the Venera 14 rock was either very close to a primitive basaltic melt or possibly a picritic melt as it has mantle potential temperature estimates ranging from 1310°C to 1440°C, and eruption temperatures of 1240°C to 1350°C. Although the picritic composition is ultramafic (MgO = 15.1 wt.%), it is not similar to a komatiite and the maximum mantle potential temperature estimate (1440°C) obtained is much lower than that expected for the terrestrial Archean (1500–1600°C) mantle (Herzberg et al. 2010). However, it does suggest that both mafic and ultramafic lavas can erupt on Venus. In this regard, it is expected that interlayering of mafic–ultramafic lavas and sills occurred and that would resemble the lower volcanic sequences of a greenstone belt. Whether komatiite-like lavas erupted on Venus or if subaqueous eruptions occurred is speculative at best, but considering the Venusian mantle was compositionally suitable to generate a rock similar terrestrial to olivine tholeiite, then it would be expected that they would exist at higher mantle potential temperatures.

Bimodal Volcanic Sequence

Overlying the lower mafic–ultramafic volcanic sequence of some greenstone belts is a bimodal volcanic sequence. The bimodal volcanic sequence consists of mafic tholeiitic (basalt, basaltic andesite) flows and intermediate (andesite, boninite) to silicic (dacite and rhyolite) calc-alkaline flows (Condie 1981; Anhaeusser 2014; Thurston 2015). The calc-alkaline nature of the intermediate to silicic rocks is considered to be evidence of an active margin (island arc or continental arc) origin for these rocks by some (Kohler and Anhaeusser 2002; Polat et al. 2002; Smithies et al. 2005b), but it is debated (Pearce 2008; Bédard et al. 2013; Barnes and Van Kranedonk 2014; Bédard 2018).

Intermediate and silicic igneous rocks have not conclusively been identified on the surface of Venus. The rock encountered at the Venera 8 landing site is currently the only hard evidence for the existence of an evolved igneous rock on Venus as it has high Th and U contents (Fig. 4). However, as discussed above, there are contrasting interpretations on the nature of the Venera 8 rock (Nikolayeva 1990; Basilevsky et al. 1992; Kargel et al. 1993). Ghail and Wilson (2015) identified large-scale, welded and possibly volatile-rich pyroclastic flow deposits, but there is little evidence at this moment to support or refute a silicic composition. Furthermore, pancake dome volcanic structures indicate that high viscosity lava flows erupted, but it does not confirm an intermediate or silicic composition (Fink et al. 1993).

Fractional crystallization modeling using the Venera 13, Venera 14, Vega 2, and the calculated Venera 14 primitive liquid compositions as the parental magmas yield intermediate to silicic compositions over a range of pressure, redox conditions, and water contents (Shellnutt 2013, 2018, 2019; Shellnutt and Manu Prasanth 2021). The modeled compositions include andesitic, trachytic, dacitic, rhyolitic, and phonolitic liquids. In other words, with the exception of foidite, many intermediate and silicic rocks described on the total alkalis versus silica diagram of Le Bas et al. (1986) can be generated by fractional crystallization of a spectrum of Venusian basalt. The Venera 13 alkaline basalt can generate the highly alkaline rocks (phonolite) after ~ 60% or more crystallization, whereas the subalkaline Venera 14 and Vega 2 compositions can yield the basaltic andesite–andesite–dacite–rhyolite series (Shellnutt 2013). The Vega 2 tholeiitic basalt can produce the trachytic liquid series under specific (e.g. hydrous, polybaric) conditions (cf. Shellnutt 2018).

Of particular interest is the Venera 8 rock because the Th–U–K contents indicate that it could be silicic. Using the Th–U–K contents of the Venera 8 rock, Nikolayeva (1990) calculated a likely bulk composition by comparing it to the distribution of the same elements in terrestrial rocks and concluded that it could be similar to granodiorite or dacite (Table 2).

https://doi.org/10.12789/geocanj.2021.48.176

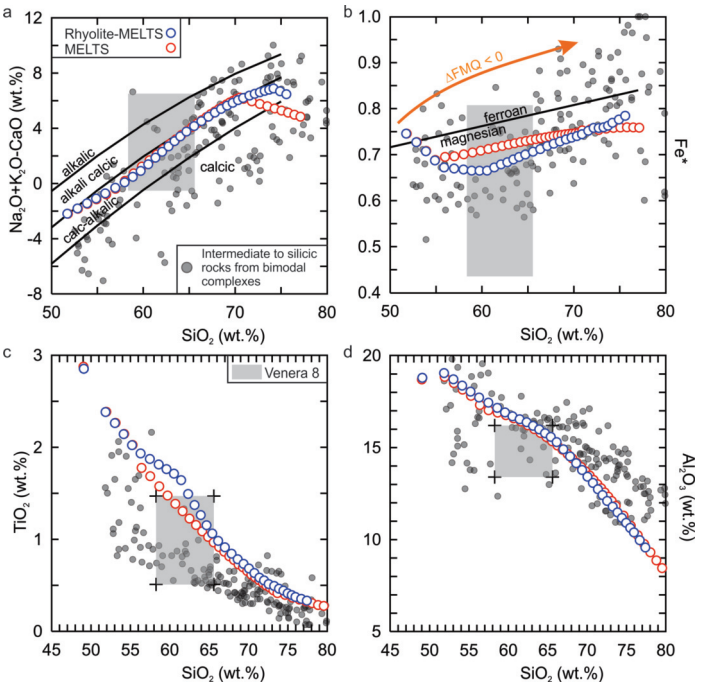

Figure 6. The results of the low pressure (0.1 GPa) MELTS and Rhyolite-MELTS models from Shellnutt (2019) compared to the silicic rocks of greenstone belts and Haida Gwaii using (a) the modified alkali–lime (Na_2O+K_2O–CaO) index (Frost et al. 2001), (b) Fe* [(FeOt/(FeOt+MgO))] value (Frost et al. 2001), (c) TiO_2 vs. SiO_2 and (d) Al_2O_3 vs. SiO_2. The calculated Venera 8 composition of Nikolayeva (1990) is shown in grey. Silicic rocks from greenstone belts (Uchi-Confederation, Wawa, Wutaishan, Gadwal, Central Bundelkhand) and the bimodal Masset Formation of Haida Gwaii. Data from Thurston and Fryer (1983), Sage et al. (1996), Polat et al. (2005), Manikyamba et al. (2007), Singh and Slabunov (2015) and Dostal et al. (2017).

Shellnutt (2019) demonstrated that fractional crystallization of a parental magma similar to Venera 14 subalkaline basalt could yield a residual silicic liquid within the range that Nikolayeva (1990) calculated. The modeling conditions that yielded the calculated Venera 8 composition were hydrous (H_2O = 0.4 wt.%), relatively oxidizing (ΔFMQ + 0.7), and polybaric crystallization. Moreover, not only did the Venera 14 subalkaline basalt fractional crystallization model yield compositions similar to the calculated Verena 8 composition, but the results also generated liquids that are similar to intermediate to silicic volcanic rocks from terrestrial Archean bimodal complexes (Fig. 6).

The formation of a bimodal volcanic sequence on Venus is plausible, more so with water and other volatile (Cl, F, CO_2) elements, and does not require unusual or special circumstances. The identification of pyroclastic deposits by Ghail and Wilson (2015) provides support for the possibility that both mafic and silicic volcaniclastic rocks would be present as well. The identification of rocks with basaltic composition is confirmed on Venus and it is expected that a mafic magma will yield a residual silicic liquid by fractional crystallization. Thus, bimodal volcanic complexes generated by fractional crystallization should exist on Venus. However, the formation of bimodal sequences of terrestrial greenstone belts is more complex than just fractional crystallization and involves assimilation–fractional crystallization (AFC) processes and the volcanism is likely cyclic (Leclerc et al. 2011). Assimilation–fractional crystallization (AFC) within Venusian volcanic and plutonic systems is expected, but there are no constraints on the composition of possible source rock (e.g. sedimentary rock, volcaniclastic rock) of the contaminant beyond the melt compositions that are generated by the fractional crystallization models.

Upper Sedimentary Sequence

The upper unit of greenstone belts is largely composed of sedimentary rocks with subordinate amounts of volcanic and volcaniclastic rocks (Condie 1981; Anhaeusser 2014; Thurston 2015). In many cases, the sedimentary sequences consist of lower chemically precipitated sedimentary rocks (carbonate rocks, banded-iron formation, and chert) and upper clastic sedimentary rocks (wacke, conglomerate, pelite). The changing nature of the sedimentary rock formations indicates terrestrial, shallow marine, marginal marine, and tidal zone depositional environments are possible (Anhaeusser 2014).

Key to the discussion on the existence of Venusian sedimentary rocks is the presence of a paleohydrosphere. At the moment, the atmosphere of Venus contains a stable amount (30 ± 15 ppm) of water vapour which is thought to be maintained by volcanic degassing (Grinspoon 1993; Zolotov et al. 1997; Fegley Jr. 2014; Filiberto et al. 2020). Furthermore, the high deuterium-to-hydrogen ratio (150 ± 30 times that of terrestrial water) indicates that Venus may have had a significant amount of surface water that was at least 4 m deep and possibly up to 530 m deep (Donahue et al. 1982, 1997). Atmospheric and planetary modeling indicates that Venus may have been able to sustain a hydrosphere until ~ 750 million years ago (Way et al. 2016; Way and Del Genio 2020).

Unconsolidated sediment was observed directly from the Venera 9, 10, 13, and 14 landers indicating that the Venusian surface experiences weathering and erosion (Florensky et al. 1983; Warner 1983). The sediments observed by the landers suggest that they were either deposited recently or that compaction has not occurred since their formation. At the moment, the evidence for lithified or chemically precipitated sedimentary rocks on Venus is limited, although Florensky et al. (1977) and Basilevsky et al. (1985) opined that a sedimentary origin of the rocks encountered at the Venera 9, 10, 13, and 14 landing sites is one of at least six possible interpretations. However, given their major and trace elemental compositions and assuming a sedimentary origin, then they would most likely be mafic volcaniclastic rocks. The rock compositions at the Venera 13, Venera 14, and Vega 2 landing sites reported relatively high SO_3 and Cl contents. Specifically, the Vega 2 (SO_3 = 4.7 ± 1.5 wt.%; Cl < 0.3 wt.%) site has high SO_3 content and it appears that the sample was likely a mixture of basaltic rock and regolith (Surkov et al. 1984, 1986). Although the data cannot distinguish between sulphide (S^{2-}) and sulphate (SO_4^{2-}), it is possible that the high sulphur content is due to the breakdown of evaporites, oxidation of sulphide minerals (gypsum, anhydrite, kieserite, langbeinite, polyhalite, kainite, barite, celestine, anglesite), or fumarolic activity. The whole-rock data certainly raise the possibility, although by no means definitive, that water

existed on the surface and that chemically precipitated sedimentary rocks were deposited. If this was the case then it is conceivable that other chemically precipitated (chert, banded iron formation, carbonate) sedimentary rocks may have existed and that the rock units typical of the upper sedimentary sequences of greenstone belts could be present. Moreover, a Venusian hydrosphere would have accentuated deposition of clastic sedimentary rocks via weathering and erosion. There is evidence of channel erosion and possible folding of strata but the features may be of volcanic origin rather than sedimentary (Khawja et al. 2020; Byrne et al. 2021).

On Venus the formation of lithified epiclastic sedimentary rocks or chemically precipitated sedimentary rocks is uncertain and would be dependent on the existence of a paleohydrosphere. At the moment there is evidence for volcaniclastic deposits and erosional channels, and indications that sedimentary layering may exist in the highland terranes, but unequivocal identification of lithified or chemically precipitated sedimentary rocks is needed. Consequently, the development of an upper sedimentary sequence within a Venusian greenstone belt is the least constrained feature.

Anorthosite and Layered Mafic Intrusions

The oldest anorthosite bodies (≥ 2.4 Ga) on Earth are spatially and temporally associated with Archean greenstone belts. Archean anorthosite is also distinguished by its megacrystic, equidimensional plagioclase with anorthite contents (An% = $[Ca^{2+}/Ca^{2+}+Na^{+}+K^{+}]*100$) of An_{91} to An_{61} and have an average value of An_{80} (Ashwal and Bybee 2017). The megacrysts are commonly spherical, ~ 0.5 cm to > 30 cm in diameter, and are surrounded by a finer grained matrix of mafic silicate minerals (olivine, pyroxene) or a gabbroic groundmass (Ashwal 1993; Ashwal and Bybee 2017). Most Archean anorthosite intrusions are small (< 500 km^2) and likely developed within shallow crustal magma chambers (Phinney et al. 1988; Ashwal 1993; Polat et al. 2009; Ashwal and Bybee 2017). The initial melt composition that produced the anorthosite is thought to be primitive (komatiite, picrite, basalt) and may have experienced early high pressure crystal fractionation of olivine and/or orthopyroxene. Subsequent to high pressure fractionation, the less dense, hydrous, high Ca/Na and Al/Si tholeiitic melt migrates to a magma chamber within the shallow crust (0.1 GPa to 0.2 GPa) and crystallizes mafic silicate minerals and accumulates megacrystic plagioclase. It is possible that the plagioclase megacryst-rich magma is purged by new pulses of mafic melt into the magma chamber (Phinney et al. 1988). Of particular interest is the Venera 14 basalt (Mg# = 60 ± 15; Al_2O_3 = 17.9 ± 2.6 wt.%; CaO = 10.3 ± 1.2 wt.%) because it is similar to tholeiitic basalt of terrestrial Archean greenstone belts and the compositional range (i.e. Mg# = 35–60; Al_2O_3 = 14–18 wt.%; CaO = 9–15 wt.%) of the parental magmas that are thought to generate Archean megacrystic anorthosite (Ashwal and Bybee 2017).

Shellnutt and Manu Prasanth (2021) presented a comprehensive evaluation of the range of modeled plagioclase compositions from all known Venusian basalt that are expected to crystallize at low pressure (0.1 GPa), under variable redox states (ΔFMQ ± 1), and hydrous to anhydrous conditions. Plagioclase crystallizes relatively early (1230–1190°C) within all melt compositions (Venera 13, Venera 14, Vega 2) and is typically > 70 vol.% of the total mineral assemblage with the remaining ~ 30 vol.% being olivine (1370–1190°C). With such a high proportion of plagioclase crystallizing early and the density contrast with olivine (olivine ρ = 3.2–3.3 g/cm^3; plagioclase ρ = 2.6–2.7 g/cm^3), plagioclase could accumulate either by density stratification or convection redistribution to the point where it forms an anorthosite mush. The highest anorthite values from each low pressure model ranges from An_{85} to An_{77} (Table 6) and within the range of many Archean anorthosite examples (Fig. 7). The compositions of plagioclase after 50% of the total plagioclase crystallized range from An_{76} to An_{48}. The Venera 13 alkaline basalt models are the reason for the lowest anorthite contents ($An_{68–48}$) whereas the Venera 14- and Vega 2 subalkaline basalt models are more calcic ($An_{76–70}$). However, Archean anorthosite plutons are unlikely to be generated from alkaline magma (Ashwal and Bybee 2017).

As Venus has similar gravitational force (~ 91% of Earth) and similar basalt composition with similar temperature and phase relations, then it is likely that magma chambers would also exist. Layered mafic intrusions (LMI) are expected within the crust of Venus as the petrological processes of differentiation (e.g. fractionation) and crystal layering can occur. The estimated parental magma compositions of some terrestrial LMIs are broadly similar to the Venera 14 rock composition and would have similar liquidus phases (Table 7). Cumulus mafic minerals could generate layered mafic or ultramafic intrusions in the crust of Venus similar to those on Earth (e.g. Bushveld, Kiglapait, Muskox). From a crystallization point of view and assuming no crystal redistribution, an unlikely prospect, all models can yield cumulate rocks following the liquid line of descent of the modeling conditions (i.e. redox, pressure, water). Dunite (≥ 90 vol.% olivine) can be generated in the low (0.1 GPa) and medium (0.5 GPa) pressure models and some high (1.0 GPa) pressure models settings, as olivine is typically the liquidus mineral and is followed by plagioclase (troctolite) and then clinopyroxene (gabbro). The high pressure models can yield pyroxene-rich cumulate rocks (websterite, clinopyroxenite, orthopyroxenite). Some cumulate rock types could only be produced by specific parental compositions. For example, norite (opx + pl) was produced in the medium and low pressure Vega 2 models whereas harzburgite can be produced by the primitive Venera 14 compositions and wehrlite can be produced in Venera 13 models.

Venusian basaltic magma can produce LMIs in the crust and there is no reason why they could not develop cumulate monomineralic (anorthosite, dunite) layers or polyphase (gabbro, norite, troctolite, pyroxenite, websterite, wehrlite) layers (Pavri et al. 1992; Shellnutt 2013, 2018; Smith and Maier 2021). The principal uncertainties regarding the existence of LMI on Venus are their abundance, size, and thickness.

Tonalite–Trondhjemite–Granodiorite Suites

Tonalite–trondhjemite–granodiorite (TTG) suites are a common intrusive rock type within Archean cratons (Jahn et al.

Table 6. Summary of modeled plagioclase anorthite content (An%) compositions.

Model	Total An range			Initial An content			An content at 50% crystallization
P (GPa)	0.1	0.5	1.0	0.1	0.5	1.0	0.1
Anhydrous							
Vega 2a	79-23	78-13	75-16	79-77	78-77	75-71	74-72
Vega 2b	77-30	75-36	74-28	77-75	75-73	74-72	72-70
Venera 13	84-20	66-22	38-17	84-78	66-59	38-33	68-48
Venera 14	79-20	74-19	72-24	79-77	74-73	72-71	71-70
V14P1	80-13	78-15	73-17	80-79	78-76	73-71	76-72
V14P2	82-10	78-14	62-12	82-81	78-75	62-58	75-74
V14P3	80-11	79-14	73-17	80-79	79-73	73-70	73-72
Hydrous							
Vega 2a	82-30	82-11	78-5	82-81	82-81	78-76	76-75
Vega 2b	80-26	80-24	77-14	80-79	80-79	77-75	75-74
Venera 13	85-32	62-24	34-21	85-80	62-60	34-32	66-59
Venera 14	81-26	78-18	74-8	81-80	78-77	74-70	75-74
V14P1	82-16	78-13	74-8	82-81	78-76	74-71	75-72
V14P2	82-14	80-11	57-8	82-81	80-76	57-50	76-74
V14P3	82-16	79-12	73-8	82-80	79-75	73-66	75-74

Anorthite content (An%) = [(Ca^{2+}/(Ca^{2+}+Na^{+}+K^{+}))*100]. Anorthite contents are rounded to whole numbers across all redox conditions relative to the fayalite-magnetite-quartz buffer (ΔFMQ +1, 0, -1). Anorthite content at 50% crystallization is the compositional range of plagioclase when ~50% of all plagioclase in the system crystallized in the low pressure model. P = pressure in gigapascal.

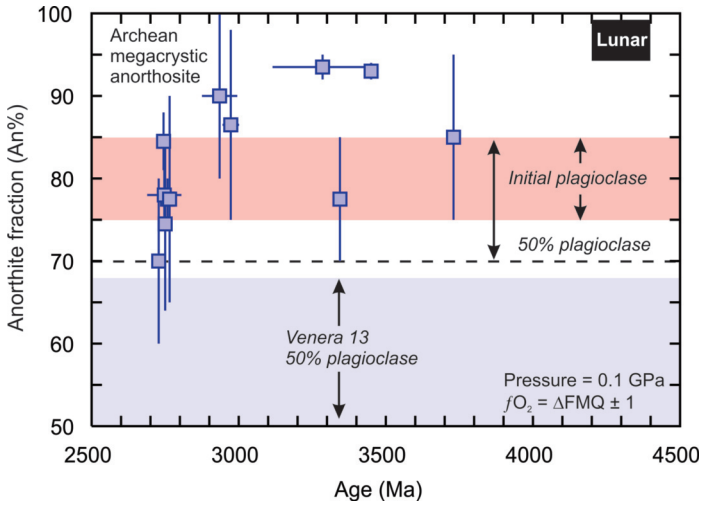

Figure 7. A comparison of modeled plagioclase compositions to those from Archean (≥ 2.5 Ga) megacrystic anorthosite (anorthosite data from Ashwal 1993). The range of initial plagioclase compositions from all models at shallow pressure (0.1 GPa) is shown in pink. The range of anorthite content at ~ 50% plagioclase crystallization for all models except Venera 13 is extended to the dashed line. The Venera 13 anorthite content at ~ 50% plagioclase crystallization is shown in light purple.

1981; Martin 1994; Martin and Moyen 2002; Moyen 2011; Moyen and Martin 2012). The TTG series is silicic (SiO_2 > 64 wt.%), sodic (Na_2O = 3.0 wt.% to 7.0 wt.%), and leucocratic (TiO_2+Fe_2O_3t+MnO+MgO ≈ 5.0 wt.%) with generally high alumina (Al_2O_3 > 15 wt.%) content at high SiO_2 (> 70 wt.%) content, depleted heavy rare earth element (HREE) signatures, and Mg numbers (~ 10 to ~ 70) that cover a wide range (Drummond and Defant 1990; Moyen 2011; Martin and Moyen 2012). It is thought that the TTG suites are derived primarily by partial melting of metamafic rocks extending from low to high pressure (< 1.0 GPa to > 2.5 GPa) conditions across a range of proposed geodynamic settings that include orogenic/subduction and anorogenic (Moyen 2011; Bédard et al. 2013; Johnson et al. 2017).

Although Venus does not appear to have Earth-like plate tectonics, there are compressional features (e.g. Ishtar Terra) and possibly structures related to subduction or underthrusting-like structures (e.g. Artemis corona) that suggest horizontal and vertical thickening both occurred (Suppe and Connors 1992; Davaille et al. 2017). Moreover, crustal thickness estimates suggest that some regions of the highland terranes may exceed 30 km and up to 65 km (Head 1990; James et al. 2013; Harris and Bédard 2015). Therefore, it is possible that partial melting of tectonically thickened Venusian mafic crust could yield magmas that fall within the range of the TTG series. In fact, the Venera 14 composition is somewhat similar to the 3.5 Ga Coucal Formation basalt of the lower Pilbara Supergroup of Western Australia. Johnson et al. (2017) demonstrated by phase equilibria modeling that the Coucal basalt can yield TTG magmas after 20–30% partial melting along a high geothermal gradient (700°C/GPa).

Shellnutt (2013) showed that hydrous (0.2 wt.%) equilibrium partial melting of the Venera 14 sub-alkaline basalt at 1 GPa under moderately oxidizing conditions (ΔFMQ 0) will yield liquid compositions at 1040°C to 950°C that are very

Table 7. Major elemental compositions of the Venera 14 basalt and proposed parental magma compositions of layered mafic intrusions.

Sample	Venera 14	Skaergaard	Kiglapait	Stillwater	Bushveld Critical Zone	Bushveld Upper Zone
SiO_2 (wt.%)	48.7 ± 3.6	48.1	47.97	49.41	48.50	49.32
TiO_2	1.25 ± 0.41	1.17	1.24	1.20	0.75	0.81
Al_2O_3	17.9 ± 2.6	17.2	18.95	15.79	16.49	15.67
FeO	8.8 ± 1.8	9.6	11.67	12.14	12.41	12.77
MnO	0.16 ± 0.08	0.16	0.14	0.20	0.19	0.19
MgO	8.1 ± 3.3	8.6	7.67	7.36	7.57	6.08
CaO	10.3 ± 1.2	11.4	8.60	10.88	11.15	10.83
Na_2O	2.4 ± 0.4*	2.34	3.21	2.19	2.17	2.94
K_2O	0.2 ± 0.07	0.25	0.40	0.16	0.14	0.25
P_2O_5		0.10	0.13	0.11	0.18	0.07
SO_3	0.88 ± 0.77					
Cl	< 0.4					

Uncertainty of Venera 14 data is at 1σ level. *The Na_2O content is calculated for the Venera 14 rock (Surkov et al. 1984). Proposed parental magma compositions of the Skaergaard intrusion (McBirney 1996), Kiglapait intrusion (Morse 2015), Stillwater Complex (McCallum 1996), and the Critical Zone and Upper Zone of the Bushveld Complex (Eales and Cawthorn 1996).

similar to TTG suites after 6–8% melting (Fig. 8). The estimated tectonothermal conditions of Venus are sufficient to melt mafic crust at the modeled primary liquid temperatures and the modeling pressure is within the range of crustal thickness estimates (> 30 km) of Ishtar Terra and Ovda Regio regions (James et al. 2013; Harris and Bédard 2015). Therefore, it is conceivable that TTG-like magmas could form within the highland regions of Venus provided that the base of the crust was broadly similar to olivine tholeiite and moderately hydrous. The models using the Venera 13 and Vega 2 compositions could not yield TTG-like compositions by equilibrium partial melting because they are either too alkaline or deficient in silica.

Summary

The modeling results indicate that the principal lithologies of terrestrial Archean granite–greenstone belts can be formed from the known rock compositions of Venus. There is significant uncertainty in the generation of the chemically precipitated sedimentary sequences, but unlithified sediments do exist on Venus and it is possible that lithified clastic sedimentary rocks also exist. Therefore, it is possible that Venus and Earth may have evolved along similar paths from the Hadean to the Neoarchean. The implication is that Venus may provide evidence for the development of proto-continental crust of Earth prior to the initiation of plate tectonics.

WAS EARLY VENUS ANALOGOUS TO ARCHEAN EARTH?

One of the most important first order geological features of Venus is the dichotomy between the low crater density of the crust and the apparent absence of modern Earth-like plate tectonics. The estimated crater retention surface age of Venus is fairly young (≤ 1 Ga) in comparison to Mars or the Moon (Turcotte 1993; Strom et al. 1994; Basilevsky and Head 2002; Herrick and Rumpf 2011; Bottke et al. 2015; Fasset 2016) although Hamilton (2007) suggested that the surface of Venus could be closer to ~ 3.8 Ga. The absence of a planet-wide geodynamic mechanism responsible for maintaining a low crater density and generating morphologically and tectonically distinct terranes is perplexing. Given the absence of plate tectonics, the most likely explanation for the young surface features of Venus is advective transport of mantle material via hotspots or mantle plumes that may periodically and/or catastrophically erupt (Phillips and Hansen 1998; Ernst and Desnoyers 2004; Hansen 2007b; Romeo and Turcotte 2010; Smrekar et al. 2010; Smrekar and Sotin 2012; O'Rourke et al. 2014; Ghail 2015; Ivanov and Head 2015; Kreslavsky et al. 2015; Gülcher et al. 2020; Uppalapati et al. 2020). It is from this perspective that Venus is frequently considered as an analogue for Archean Earth as it is thought that modern plate tectonics did not commence until ~ 2.5 billion years or later and that the tectonic regime was mostly driven by a vertical process, that is, mantle plume-initiated rifting and collision (Smithies et al. 2005a; Condie et al. 2016; Bédard 2018; Brown et al. 2020; Dewey et al. 2021).

Compared to the Phanerozoic (~ 540 Ma to present) or even the Proterozoic (~ 2.5 Ga to ~ 0.54 Ga), less is known about the tectonic regime and development of the Archean (~ 4.0 Ga to ~ 2.5 Ga) Earth due to the progressive degradation of the geological record (Brown et al. 2020; Hawkesworth et al. 2020). Moreover, there is debate on the timing of plate tectonics initiation (Condie and Kröner 2008; Stern 2008; Hamilton 2011, 2019; Dewey et al. 2021). However, most agree that the thermal regime under which Archean crust developed was 300°C to 500°C higher than ambient conditions of today (T_p = 1350 ± 50°C). There is virtually no rock record of the Hadean (~ 4.5 Ga to ~ 4.0 Ga) as most of the information is inferred from the Acasta Gneiss, detrital zircon, or isotopic

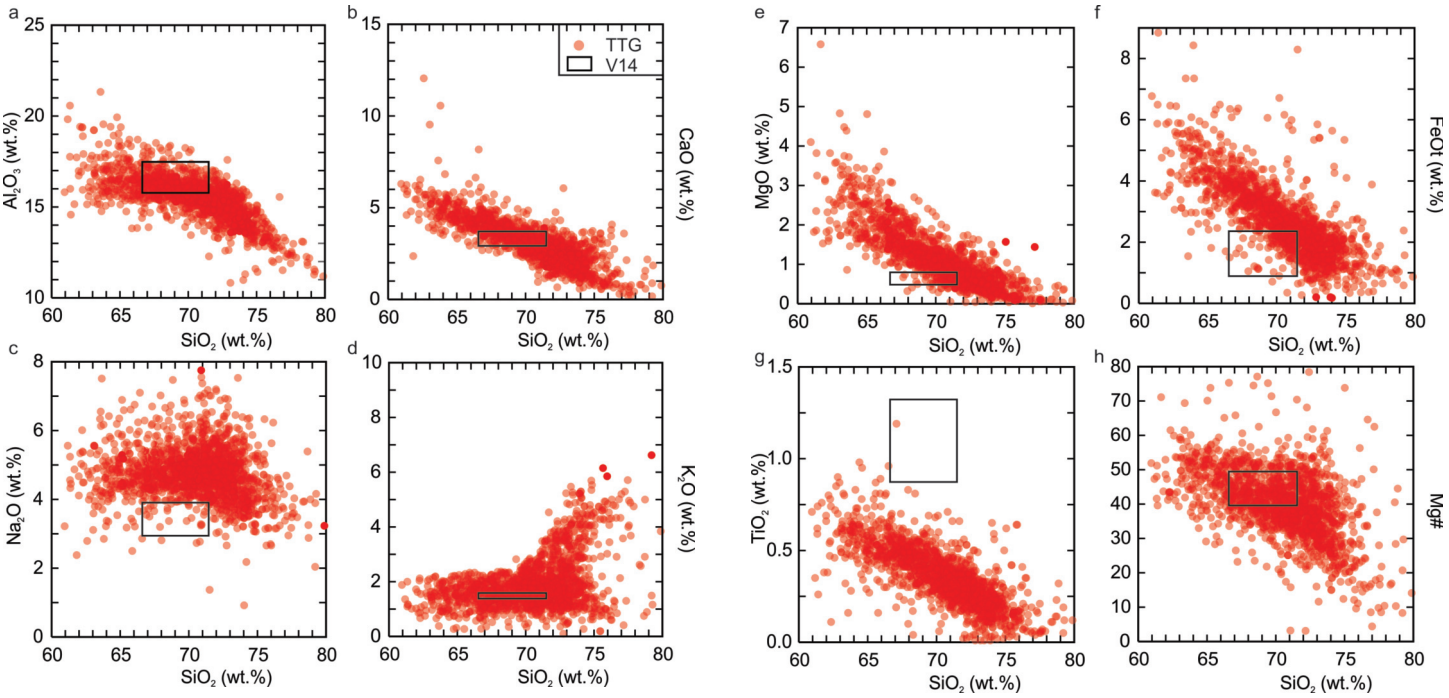

Figure 8. Major elemental comparison of the high pressure (GPa = 1.0) partial melts of the Venera 14 rock (in outlined box) to tonalite–trondhjemite–granodiorite (TTG) rocks. TTG data from the GEOROC database (http://georoc.mpch-mainz.gwdg.de/georoc/) and all data are recalculated to 100% on an anhydrous basis.

model ages (Harrison 2009; O'Neil et al. 2012; Roth et al. 2014; O'Neil and Carlson 2017; Reimink et al. 2020). It is likely that granite–greenstone and granulite–gneiss belts of Archean cratons represent a glimpse into the formation of primitive terrestrial crust or proto-continental crust (Smithies et al. 2005a; Van Kranendonk 2010; Thurston 2015; Bédard 2018). Of the two belts, the granite–greenstone belts are probably more widely known as they are a major source of gold and record supracrustal rock sequences whereas the granulite–gneiss belts record middle to lower crust metamorphic conditions, but may have protoliths of rock sequences from the upper to middle crust (Condie 1981).

The surface of Venus is broadly divided into low-lying (~ 90%) volcanic plains (planitia) and that are dominated by volcanic features (e.g. shield volcanoes, pyroclastic flows, lava channels) and highland (> 2 km) regions of older and deformed tesserae terrain and mountain belts (Lancaster et al. 1995; Nimmo and McKenzie 1998; Herrick et al. 2005; Smrekar et al. 2010; Airey et al. 2015; Ghail and Wilson 2015; Gilmore and Head 2018; Gülcher et al. 2020). At first glance the topography of Venus resembles the continental and oceanic crust dichotomy of Earth where the tesserae represent 'continental' or sialic crust and the planitiae represent 'oceanic' or simatic crust (Fig. 2). Crustal thickness estimates indicate that the planitiae could be 10–20 km thick whereas the tesserae may be up to ~ 65 km thick, although there are a number of different estimates (Head 1990; Anderson and Smrekar 2006; James et al. 2013; Harris and Bédard 2015). Near-infrared mapping spectrometer data suggest the plains (low SiO_2, high MgO, high FeOt) and tesserae (high SiO_2, low MgO, low FeOt) are compositionally different (Hashimoto et al. 2008; Basilevsky et al. 2012). The crustal thickness estimates of Venus are within the range of granite–greenstone belts (10–20 km) and granulite–gneiss belts (~ 40 km) and the surface chemical mapping is consistent with the compositional differences between terrestrial continental and oceanic crust. The major elemental composition of basalt measured at the Venera 14 landing site is similar to olivine tholeiite of Archean greenstone belts and the estimated composition of the rock at the Venera 8 landing site is granodiorite or dacite and is geochemically similar to the Archean calc-alkaline silicic rocks from greenstone belts (Nikolayeva 1990; Shellnutt 2019). Moreover, visible and infrared thermal imaging spectrometry (VIRTIS) of Alpha Regio (tesserae) indicates the presence of low-Fe rocks suggesting either anorthositic cumulate rocks or plagioclase-rich tonalite can satisfy the emissivity signature (Gilmore et al. 2015). Furthermore, modeling suggests it is possible that surface water may have been present on Venus during the Archean and only disappeared within the last billion years or when the extreme CO_2 greenhouse developed (Way et al. 2016; Khawja et al. 2020). Therefore, it is entirely possible that sedimentary rocks were precipitated and deposited and hydrothermal metamorphism and mineralization occurred previously. Coupled with the compressional mountain features of Ishtar Terra and large volcanic rise of Beta Regio, it would appear that Venus, in the absence of plate tectonics, may be a near perfect analogue of pre-plate tectonics Earth (Harris and Bédard 2014; Hansen 2018; Wyman 2018).

In spite of the possible similarities from a macro perspective, there is significant debate on the exact composition of the tesserae, depositional processes, role of a hydrosphere, origin of coronae, the mantle thermal regime, and the tectonic regimes that were operating on ancient Earth and Venus. Recent investigations suggest that the tesserae could be com-

posed of mafic volcanic–sedimentary sequences rather than intermediate to silicic rocks (Wroblewski et al. 2019; Byrne et al. 2021). Silicic rocks and anorthosite have not been positively identified and an argument can be made that the high U (2.2 ± 0.7 ppm), Th (6.5 ± 2.2 ppm), and K_2O (4.0 ± 1.2 wt.%) contents reported at the Venera 8 landing site could be lamprophyric (alkali basalt) rather than silicic (Basilevsky et al. 1992). It is possible that Venus had a hydrosphere during the Archean, but lithified sedimentary rocks (or their metamorphic equivalents) derived by mechanical weathering (sandstone, shale, greywacke, conglomerate) and chemical precipitation (limestone, evaporites, banded iron formation) have not been positively identified. The only possible evidence for the existence of S-rich evaporite rocks or material (gypsum, anhydrite, kieserite) is the high SO_3 (4.7 ± 1.5 wt.%) content measured at the Vega 2 landing site but whether the sulphur is from a sulphide (S^{2-}) or sulphate (SO_4^{2-}) is unknown. Given the possibility of an ocean, it would be expected that volcanogenic massive sulphide deposits would exist as shallow basaltic intrusions provide the heat engine to drive the circulation of hydrothermal cells that can transport metals. Corona structures, a common volcanic feature of Venus, do not appear to have a terrestrial analogue, although there are suggestions that a similar volcanic feature may exist (Lopez et al. 1997; Buchan and Ernst 2021). It is entirely possible that coronae existed on Earth and were a feature of Archean oceanic crust but were subducted prior to or during the Paleoproterozoic. The T_P estimates and the K/U and K/Th ratios indicate conditions, mantle compositions, and temperatures of cyclicity and decay similar to modern Earth (Taylor and McLennan 1986; Lee et al. 2009; Gillmannn and Tackley 2014; Ogawa and Yanagisawa 2014; Rubie et al. 2015; Weller and Duncan 2015; Shellnutt 2016; Walzer and Hendel 2017). However, the identification of volcanic features indicative of mantle plumes, plume swarms, and hotspot regimes appears to suggest that, of all the uncertainties, this could be the most similar to Archean Earth or a non-plate tectonic regime (Herrick et al. 2005; Basilevksy and Head 2007; Smrekar et al. 2010; Gülcher et al. 2020). Therefore, the tectonic regimes of Venus and Earth may have been similar during the earliest Archean, but diverged after the initiation of plate tectonics.

The initiation of modern (Phanerozoic) terrestrial plate tectonics is vociferously debated and there are advocates that suggest it may have always operated or that it began at ~ 3.2 Ga, ~ 2.5 Ga, ~ 1.0 Ga, or ~ 0.8 Ga (Condie and Kröner 2008; Stern 2008; Hamilton 2011, 2019; Dewey et al. 2021; Windley et al. 2021). This is a key argument for the comparison of Earth and Venus as it is clear that the two most recognizable physiographical features (mid-ocean ridge, subduction zones) attributed to plate tectonics are not present on Venus. The precise origin of granite–greenstone and granulite–gneiss belts is still debated and there are compelling arguments for and against the operation of plate tectonic-related processes in their development (de Wit and Ashwal 1995; Anhaeusser 2014; Thurston 2015). Nevertheless, it is clear that the generation of highly differentiated continental crust appears to have been absent, very slow, or stunted on Venus.

The continental crust represents ~ 41% of the Earth's surface area and ~ 0.7% of its volume. It has taken ~ 4.5 billion years to create the volume of continental crust but the rate of crustal growth across geological time is uncertain (Hawkesworth et al. 2019, 2020). The end-member models of crustal growth are rapid development followed by steady state, continuous growth, and continuous but episodic growth. The different models are illustrated in Figure 9. There are a number of uncertainties in the models but perhaps the most significant uncertainty is the timing of modern plate tectonics (Condie 2018; Windley et al. 2021). Assuming Venus was a perfect analogue to Earth and everything is proportionate (i.e. thermal structure, tectonic regimes) to the size difference of the planets then its surface should have a similar but lower absolute area and volume of continental crust as the Earth today. Clearly this is not the case as the tesserae, assuming they are similar to continental crust, represent ~ 7.3% of the surface area and 0.1% of the volume (Ivanov and Head 2011; James et al. 2013). If the surface areas of tesserae and continental crust are compared, then Venus developed only 17% of its total expected crust. If the volumes are compared then, depending on the thickness of the smaller tesserae, the amount reaches up to 20% of the expected crust. According to different terrestrial crustal growth models, the proportion of continental crust equaling 17% to 20% corresponds to three different potential age ranges (Fig. 9). The oldest age range is Hadean to Eoarchean (4.4 Ga to 3.9 Ga), the middle age range is Mesoarchean to Neoarchean (3.1 Ga to 2.7 Ga), and the youngest range is Paleoproterozoic (2.4 Ga to 2.1 Ga). Thus, it would seem that the geological processes of crustal evolution on Venus either operate at a significantly slower pace than Earth or they functionally stopped, possibly on or before the Paleoproterozoic (i.e. ≥ 2.1 Ga).

Is Venus analogous to Archean Earth? The answer appears to be maybe as there are some large scale motions and magma fluxes capable of resurfacing the planet with lava and moving small continental blocks that could be indicative of pre-plate tectonics Earth. However, the level of understanding of the crustal evolution of Venus is in its infancy and there is only a limited understanding of a possible Venusian hydrosphere. New geological observations and geochemical and isotopic surface measurements are needed to robustly evaluate the possibility that Venus and Earth evolved along similar paths during the Archean. Although it is possible that Venus and Early Earth may bear some resemblance there are too many uncertainties at the moment to provide a firm conclusion.

CONCLUSIONS

The basalt identified at the Venera 14 landing site is compositionally similar to tholeiitic basalt of terrestrial Archean greenstone belts. Primitive melt reconstruction (ultramafic) and petrological modeling of Venusian basalt shows that most of the tholeiitic and calc-alkaline volcanic (mafic, intermediate, silicic) and plutonic (granite, anorthosite, cumulate-layered mafic intrusions) rocks of a greenstone belt can be generated by conventional physio-chemical processes acting on these basaltic melts, such as low to medium (0.1 to 0.5 GPa) pressure

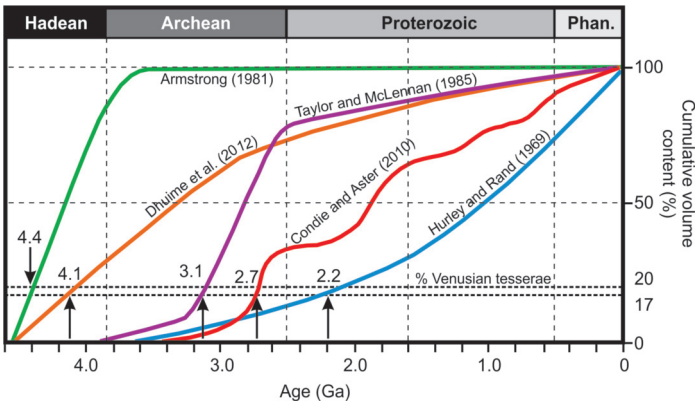

Figure 9. Crustal growth curves showing the models that constrain the volume of crust in the past independent of present day age distributions (Hurley and Rand 1969; Armstrong 1981; Taylor and McLennan 1985; Condie and Aster 2010; Dhuime et al. 2012).

fractional crystallization (intermediate, silicic), mineral accumulation (layered mafic intrusions, anorthosite), or high pressure (≥ 0.5 GPa) partial melting (tonalite–trondhjemite–granodiorite). The formation of clastic sedimentary rocks and chemically precipitated sedimentary rocks on Venus is uncertain and dependent on the existence of a paleohydrosphere. Consequently, it is possible that the crust of Venus could have produced the submarine igneous rock suites that typify terrestrial Archean greenstone belts. Although the present-day tectonic regimes of Venus and Earth are vastly different, it is possible that they were very similar until the moment that modern plate tectonics began on Earth or ended on Venus.

ACKNOWLEDGEMENTS

I thank Andrew Kerr and Jaroslav Dostal for their editorial handling and Richard Ernst and Jean Bédard for their constructive comments that helped to improve this manuscript. The project was supported by the Ministry of Science and Technology (Taiwan) through grant 110-2116-M-003-003.

REFERENCES

Airey, M.W., Mather, T.A., Pyle, D.M., Glaze, L.S., Ghail, R.C., and Wilson, C.F., 2015, Explosive volcanic activity on Venus: the roles of volatile contribution, degassing, and external environment: Planetary and Space Science, v. 113–114, p. 33–48, https://doi.org/10.1016/j.pss.2015.01.009.

Anderson, F.S., and Smrekar, S.E., 2006, Global mapping of crustal and lithospheric thickness on Venus: Journal of Geophysical Research, v. 111, E08006, https://doi.org/10.1029/2004JE002395.

Anhaeusser, C.R., 2014, Archaean greenstone belts and associated granitic rocks – A review: Journal of African Earth Sciences, v. 100, p. 684–732, https://doi.org/10.1016/j.jafrearsci.2014.07.019.

Ansan, V., and Vergely, P., 1995, Evidence of vertical and horizontal motions on Venus: Maxwell Montes: Earth, Moon, and Planets, v. 69, p. 285–310, https://doi.org/10.1007/BF00643789.

Armann, N., and Tackley, P.J., 2012, Simulating the thermomechanical magmatic and tectonic evolution of Venus's mantle and lithosphere: two-dimensional models: Journal of Geophysical Research, v. 117, E12003, https://doi.org/10.1029/2012JE004231.

Armstrong, R.L., 1981, Radiogenic isotopes: the case for crustal recycling on a near-steady-state no-continental-growth Earth: Philosophical Transactions of the Royal Society of London Series A, v. 301, p. 443–472, https://doi.org/10.1098/rsta.1981.0122.

Ashwal, L.D., 1993, Anorthosites: Springer-Verlag, Heidelberg, 422 p.

Ashwal, L.D., and Bybee, G.M., 2017, Crustal evolution and the temporality of anorthosites: Earth-Science Reviews, v. 173, p. 307–330, https://doi.org/10.1016/j.earscirev.2017.09.002.

Barnes, S.J., and Van Kranendonk, M.J., 2014, Archean andesites in the east Yilgarn craton, Australia: products of plume-crust interaction?: Lithosphere, v. 6, p. 80–92, https://doi.org/10.1130/L356.1.

Basilevsky, A.T., and Head III, J.W., 1988, The geology of Venus: Annual Reviews of Earth and Planetary Sciences, v. 16, p. 295–317, https://doi.org/10.1146/annurev.ea.a6.050188.001455.

Basilevsky, A.T., and Head, J.W., 2002, Venus: timing and rates of geologic activity: Geology, v. 30, p. 1015–1018, https://doi.org/10.1130/0091-7613(2002)030<1015:VTAROG>2.0.CO;2.

Basilevsky, A.T., and Head, J.W., 2003, The surface of Venus: Reports on Progress in Physics, v. 66, p. 1699–1734, https://doi.org/10.1088/0034-4885/66/10/R04.

Basilevsky, A.T., and Head, J.W., 2007, Beta Regio, Venus: evidence for uplift, rifting, and volcanism due to a mantle plume: Icarus, v. 192, p. 167–186, https://doi.org/10.1016/j.icarus.2007.07.007.

Basilevsky, A.T., Kuzmin, R.O., Nikolaeva, O.V., Pronin, A.A., Ronca, L.B., Avduevsky, V.S., Uspensky, G.R., Cheremukhina, Z.P., Semenchenko, V.V., and Ladygin, V.M., 1985, The surface of Venus as revealed by the Venera landings: Part II: Geological Society of America Bulletin, v. 96, p. 137–144, https://doi.org/10.1130/0016-7606(1985)96<137:TSOVAR>2.0.CO;2.

Basilevsky, A.T., Nikolaeva, O.V., and Weitz, C.M., 1992, Geology of the Venera 8 landing site region from Magellan data: morphological and geochemical considerations: Journal of Geophysical Research, v. 97, p. 16315–16335, https://doi.org/10.1029/92JE01557.

Basilevsky, A.T., Shalygin, E.V., Titov, D.V., Markiewicz, W.J., Scholten, F., Roatsch, Th., Kreslavsky, M.A., Moroz, L.V., Ignatiev, N.I., Fiethe, B., Osterloh, B., and Michalik, H., 2012, Geologic interpretation of the near-infrared images of the surface taken by the Venus Monitoring Camera, Venus Express: Icarus, v. 217, p. 434–450, https://doi.org/10.1016/j.icarus.2011.11.003.

Bédard, J.H., 2006, A catalytic delamination-driven model for coupled genesis of Archaean crust and sub-continental lithospheric mantle: Geochimica et Cosmochimica Acta, v. 70, p. 1188–1214, https://doi.org/10.1016/j.gca.2005.11.008.

Bédard, J.H., 2018, Stagnant lids and mantle overturns: implications for Archaean tectonics, magmagenesis, crustal growth, mantle evolution, and the start of plate tectonics: Geoscience Frontiers, v. 9, p. 19–49, https://doi.org/10.1016/j.gsf.2017.01.005.

Bédard, J.H., Brouillette, P., Madore, L., and Berclaz, A., 2003, Archaean cratonization and deformation in the northern Superior Province, Canada: an evaluation of plate tectonic versus vertical tectonic models: Precambrian Research, v. 127, p. 61–87, https://doi.org/10.1016/S0301-9268(03)00181-5.

Bédard, J.H., Leclerc, F., Harris, L.B., and Goulet, N., 2009, Intra-sill magmatic evolution in the Cummings Complex, Abitibi greenstone belt: tholeiitic to calc-alkaline magmatism recorded in an Archaean subvolcanic conduit system: Lithos, v. 111, p. 47–71, https://doi.org/10.1016/j.lithos.2009.03.013.

Bédard, J.H., Harris, L.B., and Thurston, P.C., 2013, The hunting of the snArc: Precambrian Research, v. 229, p. 20–48, https://doi.org/10.1016/j.precamres.2012.04.001.

Berry, A.J., Danyushevsky, L.V., O'Neill, H.StC., Newville, M., and Sutton, S.R., 2008, Oxidation state of iron in komatiitic melt inclusions indicates hot Archaean mantle: Nature, v. 455, p. 960–963, https://doi.org/10.1038/nature07377.

Bindschadler, D.L., 1995, Magellan: a new view of Venus' geology and geophysics: Reviews of Geophysics, v. 33, p. 459–467, https://doi.org/10.1029/95RG00281.

Bindschadler, D.L., and Head, J.W., 1991, Tessera Terrain, Venus: characterization and models for origin and evolution: Journal of Geophysical Research, v. 96, p. 5889–5907, https://doi.org/10.1029/90JB02742.

Bleeker, W., 2002, Archaean tectonics: a review, with illustrations from the Slave craton, *in* Fowler, C.M.R, Ebinger, C.J., and Hawkesworth, C.J., *eds.*, The Early Earth: Physical, Chemical and Biological Development: Geological Society, London, Special Publications, v. 199, p. 151–181, https://doi.org/10.1144/GSL.SP.2002.199.01.09.

Bottke, W., Ghent, R., Mazrouri, S., Robbins, S., and Vokrouhlicky, D., 2015, Asteroid impacts, crater scaling laws, and a proposed younger age for Venus's surface (Abstract): AAS DSP Meeting, 2015 Abstracts, v. 47, p. 20107.

Brown, M., Johnson, T., and Gardiner, N.J., 2020, Plate tectonics and the Archean Earth: Annual Review of Earth and Planetary Sciences, v. 48, p. 291–320, https://doi.org/10.1146/annurev-earth-081619-052705.

Buchan, K.L., and Ernst, R.E., 2021, Plumbing systems of large igneous provinces (LIPs) on Earth and Venus: investigating the role of giant circumferential and radiating dyke swarms, coronae and novae, and mid-crustal intrusive complexes: Gondwana Research, v. 100, p. 25–43, https://doi.org/10.1016/j.gr.2021.02.014.

Byerly, G.R., Kröner, A., Lowe, D.R., Todt, W., and Walsh, M.M., 1996, Prolonged magmatism and time constraints for sediment deposition in the early Archean Barberton greenstone belt: evidence from the Upper Onverwacht and Fig Tree groups: Precambrian Research, v. 78, p. 125–138.

Byrne, P.K., Ghail, R.C., Gilmore, M.S., Şengör, A.M.C., Klimczak, C., Senske, D.A., Whitten, J.L., Khawja, S., Ernst, R.E., and Solomon, S.C., 2021, Venus tesserae feature layered, folded, and eroded rocks: Geology, v. 49, p. 81–85, https://doi.org/10.1130/G47940.1.

Byrnes, J.M., and Crown, D.A., 2002, Morphology, stratigraphy, and surface roughness properties of Venusian lava flow fields: Journal of Geophysical Research, v. 107, p. 9-1–9-22, https://doi.org/10.1029/2001JE001828.

Condie, K.C., 1981, Greenstone belt stratigraphy, *in* Condie, K.C., *ed.*, Developments in Precambrian Geology, v. 3, p. 45–66, https://doi.org/10.1016/S0166-2635(08)70075-6.

Condie, K.C., 2018, A planet in transition: the onset of plate tectonics on Earth between 3 and 2 Ga?: Geoscience Frontiers, v. 9, p. 51–60, https://doi.org/10.1016/j.gsf.2016.09.001.

Condie, K.C., and Aster, R.C., 2010, Episodic zircon age spectra of orogenic granitoids: the supercontinent connection and continental growth: Precambrian Research, v. 180, p. 227–236, https://doi.org/10.1016/j.precamres.2010.03.008.

Condie, K.C., and Benn, K., 2006, Archean geodynamics: similar to or different from modern geodynamics?, *in* Benn, K., Mareschal, J.-C., and Condie, K.C., *eds.*, Archean Geodynamics and Environments Planet: American Geophysical Union, Geophysical Monograph Series, v. 164, p. 47–59, https://doi.org/10.1029/164GM05.

Condie, K.C., and Kröner, A., 2008, When did plate tectonics begin? Evidence from the geologic record, *in* Condie, K.C., and Pease, V., *eds.*, When Did Plate Tectonics Begin on Planet Earth?: Geological Society of America Special Papers, v. 440, p. 281–294, https://doi.org/10.1130/2008.2440(14).

Condie, K.C., Aster, R.C., and van Hunen, J., 2016, A great thermal divergence in the mantle beginning 2.5 Ga: geochemical constraints from greenstone basalts and komatiites: Geoscience Frontiers, v. 7, p. 543–553, https://doi.org/10.1016/j.gsf.2016.01.006.

Corfu, F., and Andrews, A.J., 1987, Geochronological constraints on the timing of magmatism, deformation, and gold mineralization in the Red Lake greenstone belt, northwestern Ontario: Canadian Journal of Earth Sciences, v. 24, p. 1302–1320, https://doi.org/10.1139/e87-126.

Davaille, A., Smrekar, S.E., and Tomlinson, S., 2017, Experimental and observational evidence for plume-induced subduction on Venus: Nature Geoscience, v. 10, p. 349–355, https://doi.org/10.1038/ngeo2928.

de Wit, M.J., and Ashwal, L.D., 1995, Greenstone belts: what are they?: South African Journal of Geology, v. 98, p. 505–520, https://doi.org/10520/EJC-943d19ff8.

Dewey, J.F., Kiseeva, E.S., Pearce, J.A., and Robb, L.J., 2021, Precambrian tectonic evolution of Earth: an outline: South African Journal of Geology, v. 124, p. 141–162, https://doi.org/10.25131/sajg.124.0019.

Dhuime, B., Hawkesworth, C.J., Cawood, P.A., and Storey, C.D., 2012, A change in the geodynamics of continental growth 3 billion years ago: Science, v. 335, p. 1334–1336, https://doi.org/10.1126/science.1216066.

Donahue, T.M., Hoffman, J.H., Hodges Jr., R.R., and Watson, A.J., 1982, Venus was wet: a measurement of the ratio of deuterium to hydrogen: Science, v. 216, p. 630–633, https://doi.org/10.1126/science.216.4546.630.

Donahue, T.M., Grinspoon, D.H., Hartle, R.E., and Hodges, R.R., 1997, Ion/neutral escape of hydrogen and deuterium: evolution of water, *in* Bougher, S.W., Hunten, D.M., and Phillips, R.J., *eds.*, Venus II: Geology Geophysics, Atmosphere, and Solar Wind Environment: University of Arizona Press, Tucson, p. 385–414.

Dostal, J., Hamilton, T.S., and Shellnutt, J.G., 2017, Generation of felsic rocks of bimodal volcanic suites from thinned and rifted continental margins: geochemical and Nd, Sr, Pb-isotopic evidence from Haida Gwaii, British Columbia, Canada: Lithos, v. 292–293, p. 146–160, https://doi.org/10.1016/j.lithos.2017.09.005.

Drummond, M.S., and Defant, M.J., 1990, A model for trondhjemite-tonalite-dacite genesis and crustal growth via slab melting: Archean to modern comparison: Journal of Geophysical Research, v. 95, p. 21503–21521, https://doi.org/10.1029/JB095iB13p21503.

Eales, H.V., and Cawthorn, R.G., 1996, The Bushveld Complex, *in* Cawthorn, R.G., *ed.*, Layered Intrusions: Developments in Petrology, v. 15, p. 181–229, https://doi.org/10.1016/S0167-2894(96)80008-X.

Ernst, R.E., and Desnoyers, D.W., 2004, Lessons from Venus for understanding mantle plumes on Earth, *in* Maruyama, S., Kennett, B.L.N., Yuen, D.A., and Windley, B.F., *eds.,* Plumes and Superplumes: Physics of Earth and Planetary Interiors, v. 146, p. 195–229, https://doi.org/10.1016/j.pepi.2003.10.012.

Fassett, C.I., 2016, Analysis of impact crater populations and the geochronology of planetary surfaces in the inner solar system: Journal of Geophysical Research, v. 121, p. 1900–1926, https://doi.org/10.1002/2016JE005094.

Faure, G., and Messing, T.M., 2007, Introduction to Planetary Science: The Geological Perspective: Springer, Dordrecht, 526 p., https://doi.org/10.1007/978-1-4020-5544-7.

Fegley Jr., B., 2014, Venus, *in* Holland, H.D., Turekian, K.K., *eds.*, Treatise on Geochemistry, Planets, Asteroids, Comets and The Solar System: Elsevier, v. 2, p. 127–147.

Filiberto, J., 2014, Magmatic diversity on Venus: constraints from terrestrial analog crystallization experiments: Icarus, v. 231, p. 131–136, https://doi.org/10.1016/J.ICARUS.2013.12.003.

Filiberto, J., Trang, D., Treiman, A.H., and Gilmore, M.S., 2020, Present-day volcanism on Venus as evidenced from weathering rates of olivine: Science Advances, v. 6, eaax7455, https://doi.org/10.1126/sciadv.aax7445.

Fink, J.H., Bridges, N.T., and Grimm, R.E., 1993, Shapes of Venusian "pancake" domes imply episodic emplacement and silicic composition: Geophysical Research Letters, v. 20, p. 261–264, https://doi.org/10.1029/92GL03010.

Florensky, C.P., Ronca, L.B., Basilevsky, A.T., Burba, G.A., Nikolaeva, O.V., Pronin, A.A., Trakhtman, A.M., Volkov, V.P., and Zazetsky, V.V., 1977, The surface of Venus as revealed by Soviet Venera 9 and 10: Geological Society of America Bulletin, v. 88, p. 1537–1545, https://doi.org/10.1130/0016-7606(1977)88<1537:TSOVAR>2.0.CO;2.

Florensky, C.P., Basilevsky, A.T., Kryuchkov, V.P., Kusmin, R.O., Nikolaeva, O.V., Pronin, A.A., Chernaya, I.M., Tyuflin, YU.S., Selivanov, A.S., Naraeva, M.K., and Ronca, L.B., 1983, Venera 13 and Venera 14: sedimentary rocks on Venus?: Science, v. 221, p. 57–59, https://doi.org/10.1126/science.221.4605.57.

Frost, B.R., Barnes, C.G., Collins, W.J., Arculus, R.J., Ellis, D.J., and Frost, C.D., 2001, A geochemical classification for granitic rocks: Journal of Petrology, v. 42, p. 2033–2048, https://doi.org/10.1093/petrology/42.11.2033.

Gale, A., Dalton, C.A., Langmuir, C.H., Su, Y., and Schilling, J.-G., 2013, The mean composition of oceanic ridge basalts: Geochemistry, Geophysics, Geosystems, v. 14, p. 489–518, https://doi.org/10.1029/2012gc004334.

Ghail, R.., 2015, Rheological and petrological implications for a stagnant lid regime on Venus: Planetary and Space Science, v. 113–114, p. 2–9, https://doi.org/10.1016/j.pss.2015.02.005.

Ghail, R.C., and Wilson, L., 2015, A pyroclastic flow deposit on Venus, *in* Plattz, T., Massironi, M., Byrne, P.K., and Hiesinger, H., *eds.*, Volcanism and Tectonism Across the Inner Solar System: Geological Society, London, Special Publications, v. 401, p. 97–106, https://doi.org/10.1144/SP401.1.

Gillmann, C., and Tackley, P., 2014, Atmosphere/mantle coupling and feedbacks on Venus: Journal of Geophysical Research, v. 119, p. 1189–1217, https://doi.org/10.1002/2013JE004505.

Gilmore, M.S., and Head, J.W., 2018, Morphology and deformational history of Tellus Regio, Venus: evidence for assembly and collision: Planetary and Space Science, v. 154, p. 5–20, https://doi.org/10.1016/j.pss.2018.02.001.

Gilmore, M.S., Mueller, N., and Helbert, J., 2015, VIRTIS emissivity of Alpha Regio, Venus, with implications for tessera composition: Icarus, v. 254, p. 350–361, https:///doi.org/10.1016/j.icarus.2015.04.008.

Grinspoon, D.H., 1993, Implications of the high D/H ratio for the sources of water in Venus' atmosphere: Nature, v. 363, p. 428–431, https://doi.org/10.1038/363428a0.

Gualda, G.A.R., Ghiorso, M.S., Lemons, R.V., and Carley, T.L., 2012, Rhyolite-MELTS: a modified calibration of MELTS optimized for silica-rich, fluid-bearing magmatic systems: Journal of Petrology, v. 53, p. 875–890, https://doi.org/10.1093/petrology/egr080.

Gülcher, A.J.P., Gerya, T.V., Montési, L.G.J., and Munch, J., 2020, Corona structures driven by plume-lithosphere interactions and evidence for ongoing plume activity on Venus: Nature Geoscience, v. 13, p. 547–554, https://www.nature.com/articles/s41561-020-0606-1.

Haggerty, S.E., 1978, The redox state of planetary basalts: Geophysical Research Letters, v. 5, p. 443–446, https://doi.org/10.1029/GL005i006p00443.

Hamilton, W.B., 2005, Plumeless Venus preserves an ancient impact-accretionary surface, *in* Foulger, G.R., Natland, J.H., Presnall, D.C., and Anderson, D.L., *eds.*, Plate, Plumes, and Paradigms: Geological Society of America Special Papers, v. 388, p. 781–814, https://doi.org/10.1130/0-8137-2388-4.781.

Hamilton, W.B., 2007, An alternative Venus, *in* Foulger, G.R., and Jurdy, D.M., *eds.*, Plate, Plumes, and Planetary processes: Geological Society of America Special Papers, v. 430, p. 879–911, https://doi.org/10.1130/2007.2430(41).

Hamilton, W.B., 2011, Plate tectonics began in Neoproterozoic time, and plumes from deep mantle have never operated: Lithos, v. 123, p. 1–20, https://doi.org/10.1016/j.lithos.2010.12.007.

Hamilton, W.B., 2015, Terrestrial planets fractionated synchronously with accretion,

but Earth progressed through subsequent internally dynamic stages whereas Venus and Mars have been inert for more than 4 billion years, *in* Foulger, G.R., Lustrino, M., and King, S.D., *eds*., The Interdisciplinary Earth: A Volume in Honor of Don L. Anderson: Geological Society of America Special Papers, v. 514, https://doi.org/10.1130/2015.2514(09).

Hamilton, W.B., 2019, Toward a myth-free geodynamic history of Earth and its neighbors: Earth-Science Reviews, v. 198, 102905, https://doi.org/10.1016/j.earscirev.2019.102905.

Hansen, V.L., 2007a, Venus: a thin-lithosphere analog for early Earth?, *in* van Kranendonk, M.J., Smithies, R.H., and Bennett, V.C., *eds*., Earth's Oldest Rocks: Developments in Precambrian Geology, v. 15, p. 987–1012, https://doi.org/10.1016/S0166-2635(07)15081-7.

Hansen, V.L., 2007b., LIPs on Venus: Chemical Geology, v. 241, p. 354–374, https://doi.org/10.1016/J.CHEMGEO.2007.01.020.

Hansen, V.L., 2018, Global tectonic evolution of Venus, from exogenic to endogenic over time, and implications for early Earth processes: Philosophical Transactions of the Royal Society A, v. 376, 20170412, https://doi.org/10.1098/rsta.2017.0412.

Hansen, V.L., and Willis, J.J., 1998, Ribbon terrain formation, southwestern Fortuna Tessera, Venus: implications for lithosphere evolution: Icarus, v. 132, p. 321–343, https://doi.org/10.1006/icar.1998.5897.

Hansen, V.L., Banks, B.K., and Ghent, R.R., 1999, Tessera terrain and crustal plateaus, Venus: Geology, v. 27, p. 1071–1074, https://doi.org/10.1130/0091-7613(1999)027<1071:TTACPV>2.3.CO;2.

Harris, L.B., and Bédard, J.H., 2014, Crustal evolution and deformation in a non-plate-tectonic Archaean Earth: comparisons with Venus, *in* Dilek, Y., and Furnes, H., *eds*., Evolution of Archean Crust and Early Life: Modern Approaches in Solid Earth Sciences: Springer, Dordrecht, p. 215–291, https://doi.org/10.1007/978-94-007-7615-9_9.

Harris, L.B., and Bédard, J.H., 2015, Interactions between continent-like 'drift' rifting and mantle flow on Venus: gravity interpretations and Earth analogues, *in* Plattz, T., Massironi, M., Byrne, P.K., and Hiesinger, H., *eds*., Volcanism and Tectonism Across the Inner Solar System: Geological Society, London, Special Publications, v. 401, p. 327–356, https://doi.org/10.1144/SP401.9.

Harrison, T.M., 2009, The Hadean crust: evidence from > 4 Ga zircons: Annual Review in Earth and Planetary Sciences, v. 37, p. 479–505, https://doi.org/10.1146/annurev.earth.031208.100151.

Hashimoto, G.L., Roos-Serote, M., Sugita, S., Gilmore, M.S., Kamp, L.W., Carlson, R.W., and Baines, K.H., 2008, Felsic highland crust on Venus suggested by Galileo Near-Infrared Mapping Spectrometer data: Journal of Geophysical Research, v. 113, E00B24, https://doi.org/10.1029/2008JE003134.

Hauck II, S.A., Phillips, R.J., and Price, M.H., 1998, Venus: crater distribution and plains resurfacing models: Journal of Geophysical Research, v. 103, p. 13635–13642, https://doi.org/10.1029/98JE00400.

Hauri, E., 2002, SIMS analysis of volatiles in silicate glasses, 2: isotopes and abundances in Hawaiian melt inclusions: Chemical Geology, v. 183, p. 115–141, https://doi.org/10.1016/S0009-2541(01)00374-6.

Hawkesworth, C.J., and Kemp, A.I.S., 2006, Evolution of continental crust: Nature, v. 443, p. 811–817, https://doi.org/10.1038/nature05191.

Hawkesworth, C.J., Cawood, P.A., and Dhuime, B., 2019, Rates of generation and growth of the continental crust: Geoscience Frontiers, v. 10, p. 165–173, https://doi.org/10.1016/j.gsf.2018.02.004.

Hawkesworth, C.J., Cawood, P.A., and Dhuime, B., 2020, The evolution of the continental crust and the onset of plate tectonics: Frontiers in Earth Science, v. 8, 326, https://doi.org/10.3389/feart.2020.00326.

Head, J.W., 1990, Processes of crustal formation and evolution on Venus: an analysis of topography, hypsometry, and crustal thickness variations: Earth, Moon, and Planets, v. 50, p. 25–55, https://doi.org/10.1007/BF00142388.

Head, J.W., Crumpler, L.S., Aubele, J.C., Guest, J.E., and Saunders, R.S., 1992, Venus volcanism: classification of volcanic features and structures, associations, and global distribution from Magellan data: Journal of Geophysical Research, v. 97, p. 13153–13197, https://doi.org/10.1029/92JE01273.

Herrick, R.R., and Rumpf, M.E., 2011, Postimpact modification by volcanic or tectonic processes as the rule, not the exception, for Venusian craters: Journal of Geophysical Research, v. 116, E02004, https://doi.org/10.1029/2010JE003722.

Herrick, R.R., Dufek, J., and McGovern, P.J., 2005, Evolution of large shield volcanoes on Venus: Journal of Geophysical Research, v. 110, E01002, https://doi.org/10.1029/2004JE002283.

Herzberg, C., and Asimow, P.D., 2015, PRIMELT3 MEGA.XLSM software for primary magma calculation: peridotite primary magma MgO contents from the liquidus to the solidus: Geochemistry, Geophysics, Geosystems, v. 16, p. 563–578, https://doi.org/10.1002/2014GC005631.

Herzberg, C., and O'Hara, M.J., 2002, Plume-associated ultramafic magmas of Phanerozoic age: Journal of Petrology, v. 43, p. 1857–1883, https://doi.org/10.1093/petrology/43.10.1857.

Herzberg, C., Condie, K., and Korenaga, J., 2010, Thermal history of the Earth and its petrological expression: Earth and Planetary Science Letters, v. 292, p. 79–88, https://doi.org/10.1016/j.epsl.2010.01.022.

Hurley, P.M., and Rand, J.R., 1969, Pre-drift continental nuclei: Two ancient nuclei appear to have had a peripheral growth and no pre-drift fragmentation and dispersal: Science, v. 164, p. 1229–1242, https://doi.org/10.1126/SCIENCE.164.3885.1229.

Husen, A., Almeev, R.R., Holtz, F., Koepke, J., Sano, T., and Mengel, K., 2013, Geothermobarometry of basaltic glasses from the Tamu Massif, Shatsky Rise oceanic plateau: Geochemistry, Geophysics, Geosystems, v. 14, p. 3908–3928, https://doi.org/10.1002/ggge.20231.

Ivanov, M.A., 2001, Morphology of the tessera terrain on Venus: implications for the composition of tessera material: Solar System Research, v. 35, p. 1–17, https://doi.org/10.1023/A:1005289305927.

Ivanov, M.A., and Head, J.W., 2011, Global geological map of Venus: Planetary and Space Science, v. 59, p. 1559–1600, https://doi.org/10.1016/j.pss.2011.07.008.

Ivanov, M.A., and Head, J.W., 2015, Volcanically embayed craters on Venus: testing the catastrophic and equilibrium resurfacing models: Planetary and Space Science, v. 106, p. 116–121, https://doi.org/10.1016/J.PSS.2014.12.004.

Jahn, B.-M., Glikson, A.Y., Peucat, J.J., and Hickman, A.H., 1981, REE geochemistry and isotopic data of Archean silicic volcanics and granitoids from the Pilbara Block, Western Australia: implications for the early crustal evolution: Geochimica et Cosmochimica Acta, v. 45, p. 1633–1652, https://doi.org/10.1016/S0016-7037(81)80002-6.

James, P.B., Zuber, M.T., and Phillips, R.J., 2013, Crustal thickness and support of topography on Venus: Journal of Geophysical Research, v. 118, p. 859–875, https://doi.org/10.1029/2012JE004237.

Johnson, T.E., Brown, M., Gardiner, N.J., Kirkland, C.L., and Smithies, R.H., 2017, Earth's first stable continents did not form by subduction: Nature, v. 543, p. 239–242, https://doi.org/10.1038/nature21383.

Jull, M.G., and Arkani-Hamed, J., 1995, The implications of basalt in the formation and evolution on mountains on Venus: Physics of the Earth and Planetary Interiors, v. 89, p. 163–175, https://doi.org/10.1016/0031-9201(95)03015-O.

Kargel, J.S., Komatsu, G., Baker, V.R., and Strom, R.G., 1993, The volcanology of Venera and VEGA landing sites and the geochemistry of Venus: Icarus, v. 103, p. 253–275, https://doi.org/10.1006/ICAR.1993.1069.

Khawja, S., Ernst, R.E., Samson, C., Byrne, P.K., Ghail, R.C., and MacLellan, L.M., 2020, Tesserae on Venus may preserve evidence of fluvial erosion: Nature Communications, v. 11, 5789, https://doi.org/10.1038/s41467-020-19336-1.

Kohler, E.A., and Anhaeusser, C.R., 2002, Geology and geodynamic setting of Archaean silicic metavolcaniclastic rocks of the Bien Venue Formation, Fig Tree group, northeastern Barberton greenstone belt, South Africa: Precambrian Research, v. 116, p. 199–235, https://doi.org/10.1016/S0301-9268(02)00021-9.

Kreslavsky, M.A., Ivanov, M.A., and Head, J.W., 2015, The resurfacing history of Venus: constraints from buffered crater densities: Icarus, v. 250, p. 438–450, https://doi.org/10.1016/j.icarus.2014.12.024.

Lancaster, M.G., Guest, J.E., and Magee, K.P., 1995, Great lava flow fields on Venus: Icarus, v. 118, p. 69–86, https://doi.org/10.1006/ICAR.1995.1178.

Le Bas, M.J., Le Maitre, R.W., Streckeisen, A., and Zanettin, B., 1986, A chemical classification of volcanic rocks based on the total alkali-silica diagram: Journal of Petrology, v. 27, p. 745–750, https://doi.org/10.1093/petrology/27.3.745.

Leclerc, F., Bédard, J.H., Harris, L.B., McNicoll, V.J., Goulet, N., Roy, P., and Houle, P., 2011, Tholeiitic to calc-alkaline cyclic volcanism in the Roy Group, Chibougamau area, Abitibi greenstone belt – revised stratigraphy and implications for VHMS exploration: Canadian Journal of Earth Sciences, v. 48, p. 661–694, https://doi.org/10.1139/E10-088.

Lee, C.-T.A., Luffi, P., Plank, T., Dalton, H., and Leeman, W.P., 2009, Constraints on the depths and temperatures of basaltic magma generation on Earth and other terrestrial planets using new thermobarometers for mafic magmas: Earth and Planetary Science Letters, v. 279, p. 20–33, https://doi.org/10.1016/j.epsl.2008.12.020.

Lopez, I., Marquez, A., and Oyarzun, R., 1997, Are coronae restricted to Venus?: corona-like tectonovolcanic structures on Earth: Earth, Moon, and Planets, v. 77, p. 125–137, https://doi.org/10.1023/A:1006227431552.

MacLellan, L., Ernst, R., El Bilali, H., Ghail, R., and Bethell, E., 2021, Volcanic history of the Derceto large igneous province, Astkhik Planum, Venus: Earth-Science Reviews, v. 220, 103619, https://doi.org/10.1016/j.earscirev.2021.103619.

Manikyamba, C., Kerrich, R., Khanna, T.C., and Subba Rao, D.V., 2007, Geochemistry of adakites and rhyolites from the Neoarchaean Gadwal greenstone belt, eastern Dharwar craton, India: implications for sources and geodynamic setting:

Canadian Journal of Earth Science, v. 44, p. 1517–1535, https://doi.org/10.1139/E07-034.

Martin, H., 1994, The Archean grey gneisses and the genesis of continental crust, *in* Condie, K.C., *ed*., Archean Crustal Evolution: Developments in Precambrian Geology, v. 11, p. 205–259, https://doi.org/10.1016/S0166-2635(08)70224-X.

Martin, H., and Moyen, J.-F., 2002, Secular changes in tonalite-trondhjemite-granodiorite composition as markers of the progressive cooling of the Earth: Geology, v. 30, p. 319–322, https://doi.org/10.1130/0091-7613(2002)030<0319:SCITTG>2.0.CO;2.

McBirney, A.R., 1996, The Skaergaard Intrusion, *in* Cawthorn, R.G., *ed*., Layered Intrusions: Developments in Petrology, v. 15, p. 147–180, https://doi.org/10.1016/S0167-2894(96)80007-8.

McCallum, I.S., 1996, The Stillwater Complex, *in* Cawthorn, R.G., *ed*., Layered Intrusions: Developments in Petrology, v. 15, p. 441–483, https://doi.org/10.1016/S0167-2894(96)80015-7.

McKenzie, D., Ford, P.G., Johnson, C., Parsons, B., Sandwell, D., Saunders, S., and Solomon, S.C., 1992a, Features on Venus generated by plate boundary processes: Journal of Geophysical Research, v. 97, p. 13533–13544, https://doi.org/10.1029/92JE01350.

McKenzie, D., Ford, P.G., Liu, F., and Pettengill, G.H., 1992b, Pancakelike domes on Venus: Journal of Geophysical Research, v. 97, p. 15967–15976, https://doi.org/10.1029/92JE01349.

Morse, S., 2015, Kiglapait intrusion, Labrador, *in* Charlier, B., Namur, O., Latypov, R., and Tegner, C., *eds*., Layered Intrusions: Springer, Dordrecht, p. 589–648, https://doi.org/10.1007/978-94-017-9652-1_13.

Moyen, J.-F., 2011, The composite Archaean grey gneisses: petrological significance, and evidence for a non-unique tectonic setting for Archaean crustal growth: Lithos, v. 123, p. 21–36, https://doi.org/10.1016/j.lithos.2010.09.015.

Moyen, J.-F., and Martin, H., 2012, Forty years of TTG research: Lithos, v. 148, p. 312–336, https://doi.org/10.1016/j.lithos.2012.06.010.

Nikolayeva, O.V., 1990, Geochemistry of the Venera 8 material demonstrates the presence of continental crust on Venus: Earth, Moon, and Planets, v. 50, p. 329–341, https://doi.org/10.1007/BF00142398.

Nimmo, F., 2002, Why does Venus lack a magnetic field?: Geology, v. 30, p. 987–990, https://doi.org/10.1130/0091-7613(2002)030<0987:WDVLAM>2.0.CO;2.

Nimmo, F., and McKenzie, D., 1998, Volcanism and tectonics on Venus: Annual Review of Earth and Planetary Sciences, v. 26, p. 23–51, https://doi.org/10.1146/annurev.earth.26.1.23.

Ogawa, M., and Yanagisawa, T., 2014, Mantle evolution in Venus due to magmatism and phase transitions: from punctuated layered convection to whole-mantle convection: Journal of Geophysical Research, v. 119, p. 867–883, https://doi.org/10.1002/2013JE004593.

O'Neil, J., and Carlson, R.W., 2017, Building Archean cratons from Hadean mafic crust: Science, v. 355, p. 1199–1202, https://doi.org/10.1126/science.aah3823.

O'Neil, J., Carlson, R.W., Paquette, J.-L., and Francis, D., 2012, Formation age and metamorphic history of the Nuvvuagittuq greenstone belt: Precambrian Research, v. 220–221, p. 23–44, https://doi.org/10.1016/j.precamres.2012.07.009.

O'Rourke, J.G., and Korenaga, J., 2015, Thermal evolution of Venus with argon degassing: Icarus, v. 260, p. 128–140, https://doi.org/10.1016/j.icarus.2015.07.009.

O'Rourke, J.G., Wolf, A.S., and Ehlmann, B.L., 2014, Venus: interpreting the spatial distribution of volcanically modified craters: Geophysical Research Letters, v. 41, p. 8252–8260, https://doi.org/10.1002/2014GL062121.

Pavri, B., Head III, J.W., Klose, K.B., and Wilson, L., 1992, Steep-sided domes on Venus: characteristics, geologic setting, and eruption conditions from Magellan data: Journal of Geophysical Research, v. 97, p. 13445–13478, https://doi.org/10.1029/92JE01162.

Pearce, J.A., 2008, Geochemical fingerprinting of oceanic basalts with applications to ophiolite classification and the search for Archean oceanic crust: Lithos, v. 100, p. 14–48, https://doi.org/10.1016/j.lithos.2007.06.016.

Percival, J.A., and Card, K.D., 1986, Greenstone belts: their boundaries, surrounding rock terrains, and interrelationships, *in* de Wit, M.J., and Ashwal, L.D., *eds*., Workshop on Tectonic Evolution of Greenstone Belts: Lunar and Planetary Institute Technical Report 86-10, p. 170–173.

Phillips, R.J., and Hansen, V.L., 1998, Geological evolution of Venus: rises, plains, plumes, and plateaus: Science, v. 279, p. 1492–1497, https://doi.org/10.1126/science.279.5356.1492.

Phinney, W.C., Morrison, D.A., and Maczuga, D.E., 1988, Anorthosites and related megacrystic units in the evolution of Archean crust: Journal of Petrology, v. 29, p. 1283–1323, https://doi.org/10.1093/petrology/29.6.1283.

Polat, A., Hofmann, A.W., and Rosing, M.T., 2002, Boninite-like volcanic rocks in the 3.7–3.8 Ga Isua greentone belt, West Greenland: geochemical evidence for intra-oceanic subduction zone processes in the early Earth: Chemical Geology, v. 184, p. 231–254, https://doi.org/10.1016/S0009-2541(01)00363-1.

Polat, A., Kusky, T., Li, J., Fryer, B., Kerrich, R., and Patrick, K., 2005, Geochemistry of Neoarchean (ca. 2.55–2.50 Ga) volcanic and ophiolitic rocks in the Wutaishan greenstone belt, central orogenic belt, North China craton: implications for geodynamic setting and continental growth: Geological Society of America Bulletin, v. 117, p. 1387–1399, https://doi.org/10.1130/B25724.1.

Polat, A., Appel, P.W.U., Fryer, B., Windley, B., Frei, R., Samson, I.M., and Huang, H., 2009, Trace element systematics of the Neoarchean Fiskenæsset anorthosite complex and associated meta-volcanic rocks, SW Greenland: evidence for a magmatic arc origin: Precambrian Research, v. 175, p. 87–115, https://doi.org/10.1016/j.precamres.2009.09.002.

Reimink, J.R., Davies, J.H.F.L., Bauer, A.M., and Chacko, T., 2020, A comparison between zircons from the Acasta gneiss complex and the Jack Hills region: Earth and Planetary Science Letters, v. 531, 115975, https://doi.org/10.1016/j.epsl.2019.115975.

Romeo, I., and Turcotte, D.L., 2008, Pulsating continents on Venus: an explanation for crustal plateaus and tessera terrains: Earth and Planetary Science Letters, v. 276, p. 85–97, https://doi.org/10.1016/j.epsl.2008.09.009.

Romeo, I., and Turcotte, D.L., 2010, Resurfacing on Venus: Planetary and Space Science, v. 58, p. 1374–1380, https://doi.org/10.1016/j.pss.2010.05.022.

Roth, A.S.G., Bourdon, B., Mojzsis, S.J, Rudge, J.F., Guitreau, M., and Blichert-Toft, J., 2014, Combined ^{147,146}Sm–^{143,142}Nd constraints on the longevity and residence time of early terrestrial crust: Geochemistry, Geophysics, Geosystems, v. 15, p. 2329–2345, https://doi.org/10.1002/2014GC005313.

Rubie, D.C., Jacobson, S.A., Morbidelli, A., O'Brien, D.P., Young, E.D., de Vries, J., Nimmo, F., Palme, H., and Frost, D.J., 2015, Accretion and differentiation of the terrestrial planets with implications for the compositions of early-formed Solar System bodies and accretion of water: Icarus, v. 248, p. 89–108, https://doi.org/10.1016/j.icarus.2014.10.015.

Sage, R.P., Lightfoot, P.C., and Doherty, W., 1996, Bimodal cyclical Archean basalts and rhyolites from the Michipicoten (Wawa) greenstone belt, Ontario: geochemical evidence for magma contributions from the asthenospheric mantle and ancient continental lithosphere near the southern margin of the Superior Province: Precambrian Research, v. 76, p. 119–153, https://doi.org/10.1016/0301-9268(95)00020-8.

Sakimoto, S.E.H., and Zuber, M.T., 1993, Venus pancake dome formation: morphologic effects of a cooling-induced variable viscosity during emplacement (Conference Paper): Proceedings of the Twenty-fourth Lunar and Planetary Sciences Conference, v. 24, p. 1233–1234.

Schaefer, L., and Fegley Jr., B., 2017, Redox states of initial atmosphere outgassed on rocky planets and planetesimals: The Astrophysical Journal, v. 843, 120, https://doi.org/10.3847/1538-4357/aa784f.

Scott, C.R., Mueller, W.U., and Pilote, P., 2002, Physical volcanology, stratigraphy, and lithogeochemistry of an Archean volcanic arc: evolution from plume-related volcanism to arc rifting of SE Abitibi greenstone belt, Val d'Or, Canada: Precambrian Research, v. 115, p. 223–260, https://doi.org/10.1016/S0301-9268(02)00011-6.

Seager, S., Petkowski, J.J., Gao, P., Bains, W., Bryan, N.C., Ranjan, S., and Greaves, J., 2021, The Venusian lower atmosphere haze as a depot for desiccated microbial life: a proposed life cycle for persistence of the Venusian aerial biosphere: Astrobiology, v. 21, p. 1206–1223, https://doi.org/10.1089/ast.2020.2244.

Shellnutt, J.G., 2013, Petrological modeling of basaltic rocks from Venus: a case for the presence of silicic rocks: Journal of Geophysical Research, v. 118, p. 1350–1364, https://doi.org/10.1002/JGRE.20094.

Shellnutt, J.G., 2016, Mantle potential temperature estimates of basalt from the surface of Venus: Icarus, v. 277, p. 98–102, https://doi.org/10.1016/j.icarus.2016.05.014.

Shellnutt, J.G., 2018, Derivation of intermediate to silicic magma from the basalt analyzed at the Vega 2 landing site, Venus: PLoS ONE, v. 13, e019415, https://doi.org/10.1371/journal.pone.0194155.

Shellnutt, J.G., 2019, The curious case of the rock at Venera 8: Icarus, v. 321, p. 50–61, https://doi.org/10.1016/j.icarus.2018.11.001.

Shellnutt, J.G., and Manu Prasanth, M.P., 2021, Modeling results for the composition and typology of non-primary venusian anorthosite: Icarus, v. 366, 114531, https://doi.org/10.1016/j.icarus.2021.114531.

Singh, V.K., and Slabunov, A., 2015, The central Bundelkhand Archaean greenstone complex, Bundelkhand craton, central India: geology, composition, and geochronology of supracrustal rocks: International Geology Review, v. 57, p. 1349–1364, https://doi.org/10.1080/00206814.2014.919613.

Smith, P.M., and Asimow, P.D., 2005, Adiabat_1ph: a new public front-end to the MELTS, pMELTS, and pHMELTS models: Geochemistry, Geophysics, Geosystems, v. 6, Q02004, https://doi.org/10.1029/2004GC000816.

Smith, W.D., and Maier, W.D., 2021, The geotectonic setting, age and mineral deposit inventory of global layered intrusions: Earth-Science Reviews, v. 220, 103736, https://doi.org/10.1016/j.earscirev.2021.103736.

Smithies, R.H., Van Kranendonk, M.J., and Champion, D.C., 2005a, It started with a plume – early Archaean basaltic proto-continental crust: Earth and Planetary Science Letters, v. 238, p. 284–297, https://doi.org/10.1016/j.epsl.2005.07.023.

Smithies, R.H., Champion, D.C., Van Kranendonk, M.J., Howard, H.M., and Hickman, A.H., 2005b, Modern-style subduction processes in the Mesoarchaean: geochemical evidence from the 3.12 Ga Whundo intra-oceanic arc: Earth and Planetary Science Letters, v. 231, p. 221–237, https://doi.org/10.1016/j.epsl.2004.12.026.

Smrekar, S.E., and Sotin, C., 2012, Constraints on mantle plumes on Venus: implications for volatile history: Icarus, v. 217, p. 510–523, https://doi.org/10.1016/j.icarus.2011.09.011.

Smrekar, S.E., Elkins-Tanton, L., Leitner, J.J., Lenardic, A., Mackwell, S., Moresi, L., Sotin, C., and Stofan, E.R., 2007, Tectonic and thermal evolution of Venus and the role of volatiles: implications for understanding the terrestrial planets, *in* Esposito, L.W., Stofan, E.R., and Cravens, T.E., *eds.*, Exploring Venus as a Terrestrial Planet: American Geophysical Union, Geophysical Monograph Series, v. 176, p. 45–71, https://doi.org/10.1029/176GM05.

Smrekar, S.E., Stofan, E.R., Mueller, N., Treiman, A., Elkins-Tanton, L., Helbert, J., Piccioni, G., and Drossart, P., 2010, Recent hotspot volcanism on Venus from VIRTIS emissivity data: Science, v. 328, p. 605–608, https://doi.org/10.1126/science.1186785.

Sobolev, A.V., Asafov, E.V., Gurenko, A.A., Arndt, N.T., Batanova, V.G., Portnyagin, M.V., Garbe-Schönberg, D., and Krasheninnikov, S.P., 2016, Komatiites reveal a hydrous Archaean deep-mantle reservoir: Nature, v. 531, p. 628–632, https://doi.org/10.1038/nature17152.

Stern, R.J., 2008, Modern-style plate tectonics began in Neoproterozoic time: an alternative interpretation of Earth's tectonic history, *in* Condie, K.C., and Pease, V., *eds.*, When Did Plate Tectonics Begin on Planet Earth?: Geological Society of America Special Papers, v. 440, p. 265–280, https://doi.org/10.1130/2008.2440(13).

Strom, R.G., Schaber, G.G., and Dawson, D.D., 1994, The global resurfacing of Venus: Journal of Geophysical Research, v. 99, p. 10899–10926, https://doi.org/10.1029/94JE00388.

Suppe, J., and Connors, C., 1992, Linear mountain belts and related deformation on Venus: Proceedings of the Lunar and Planetary Sciences Conference, v. 23, p. 1389–1390.

Surkov, Y.A., 1977, Geochemical studies of Venus by Venera 9 and 10 automatic interplanetary stations: Proceedings of the Lunar and Science Conference 8th, p. 2665–2689.

Surkov, Yu.A., Barsukov, V.L., Moskalyeva, L.P., Kharyukova, V.P., and Kemurdzhian, A.L., 1984, New data on the composition, structure, and properties of Venus rock obtained by Venera 13 and Venera 14: Journal of Geophysical Research, v. 89, p. B393–B402, https://doi.org/10.1029/JB089IS02P0B393.

Surkov, Yu.A., Moskalyova, L.P., Kharyukova, V.P., Dudin, A.D., Smirnov, G.G., and Zaitseva, S.Ye., 1986, Venus rock composition at the Vega 2 landing site: Journal of Geophysical Research. v. 91, p. B215–B218, https://doi.org/10.1029/JB091iB13p0E215.

Surkov, Yu.A., Kirnozov, F.F., Glazov, V.N., Dunchenko, A.G., Tatsy, L.P., and Sobornov, O.P., 1987, Uranium, thorium, and potassium in the Venusian rocks at the landing sites of Vega 1 and 2: Journal of Geophysical Research, v. 92, p. E537–E540, https://doi.org/10.1029/JB092iB04p0E537.

Taylor, S.R., and McLennan, S.M., 1985, The Continental Crust: its Composition and Evolution: Blackwell Scientific Publications, Oxford, 312 p.

Taylor, S.R., and McLennan, S.M., 1986, The chemical composition of the Archaean crust, *in* Dawson, J.B., Carswell, D.A., Hall, J., and Wedepohl, K.H., *eds.*, The Nature of the Lower Continental Crust: Geological Society, London, Special Publications, v. 24, p. 173–178, https://doi.org/10.1144/GSL.SP.1986.024.01.16.

Taylor, F.W., Svedhem, H., and Head III, J.W., 2018, Venus: the atmosphere, climate surface, interior and near-space environment of an Earth-like planet: Space Science Reviews, v. 214, 35, https://doi.org/10.1007/s11214-018-0467-8.

Thurston, P.C., 2015, Igneous Rock Associations 19. Greenstone belts and granite-greenstone terranes: constraints on the nature of the Archean world: Geoscience Canada, v. 42, p. 437–484, https://doi.org/10.12789/geocanj.2015.42.081.

Thurston, P.C., and Fryer, B.J., 1983, The geochemistry of repetitive cyclical volcanism from basalt through rhyolite in the Uchi-Confederation greenstone belt, Canada: Contributions to Mineralogy and Petrology, v. 83, p. 204–226, https://doi.org/10.1007/BF00371189.

Thurston, P.C., Ayer, J.A., Goutier, J., and Hamilton, M.A., 2008, Depositional gaps in Abitibi greenstone belt stratigraphy: a key to exploration of syngenetic mineralization: Economic Geology, v. 103, p. 1097–1134, https://doi.org/10.2113/gsecongeo.103.6.1097.

Treiman, A.H., 2007, Geochemistry of Venus' surface: current limitations as future opportunities, *in* Esposito, L.W., Stofan, E.R., and Cravens, T.E., *eds.*, Exploring Venus as a Terrestrial Planet: American Geophysical Union, Geophysical Monograph Series, v. 176, p. 7–22, https://doi.org/10.1029/176GM03.

Turcotte, D.L., 1993, An episodic hypothesis for Venusian tectonics: Journal of Geophysical Research, v. 98, p. 17061–17068, https://doi.org/10.1029/93JE01775.

Uppalapati, S., Rolf, T., Crameri, F., and Werner, S.C., 2020, Dynamics of lithospheric overturns and implications for Venus's surface: Journal of Geophysical Research, v. 125, e2019JE006258, https://doi.org/10.1029/2019JE006258.

Van Kranendonk, M.J., 2010, Two types of Archean continental crust: plume and plate tectonics on early Earth: American Journal of Science, v. 310, p. 1187–1209, https://doi.org/10.2475/10.2010.01.

Vinogradov, A.P., Surkov, Yu.A., and Kirnozov, F.F., 1973, The content of uranium, thorium, and potassium in the rocks of Venus as measured by Venera 8: Icarus, v. 20, p. 253–259, https://doi.org/10.1016/0019-1035(73)90001-8.

Walzer, U., and Hendel, R., 2017, Continental crust formation: numerical modelling of chemical evolution and geological implications: Lithos, v. 278–281, p. 215–228, https://doi.org/10.1016/J.LITHOS.2016.12.014.

Warner, J.L., 1983, Sedimentary processes and crustal cycling on Venus: Journal of Geophysical Research, v. 88, p. A495–A500, https://doi.org/10.1029/JB088iS02p0A495.

Way, M.J., and Del Genio, A.D., 2020, Venusian habitable climate scenarios: modeling Venus through time and applications to slowly rotating Venus-like exoplanets: Journal of Geophysical Research, v. 125, e2019JE006276, https://doi.org/10.1029/2019JE006276.

Way, M.J., Del Genio, A.D., Kiang, N.Y., Sohl, L.E., Grinspoon, D.H., Aleinov, I., Kelley, M., and Clune, T., 2016, Was Venus the first habitable world of our solar system: Geophysical Research Letters, v. 43, p. 8376–8383, https://doi.org/10.1002/2016GL069790.

Weller, M.B., and Duncan, M.S., 2015, Insight into terrestrial planetary evolution via mantle potential temperatures (Abstract): 46th Lunar and Planetary Sciences Conference, 2015, Abstracts, #2749.

Windley, B.F., Kusky, T., and Polat, A., 2021, Onset of plate tectonics by the Eoarchean: Precambrian Research, v. 352, 105980, https://doi.org/10.1016/j.precamres.2020.105980.

Wroblewski, F.B., Treiman, A.H., Bhiravarasu, S., and Gregg, T.K.P., 2019, Ovda Fluctus, the festoon lava flow on Ovda Region, Venus: not silica-rich: Journal of Geophysical Research, v. 124, p. 2233–2245, https://doi.org/10.1029/2019JE006039.

Wyman, D.A., 2018, Do cratons preserve evidence of stagnant lid tectonics?: Geoscience Frontiers, v. 9, p. 3–17, https://doi.org/10.1016/j.gsf.2017.02.001.

Wyman, D.A., Kerrich, R., and Polat, A., 2002, Assembly of Archean cratonic mantle lithosphere and crust: plume-arc interaction in the Abitibi-Wawa subduction-accretion complex: Precambrian Research, v. 115, p. 37–62, https://doi.org/10.1016/S0301-9268(02)00005-0.

Zolotov, M.Yu., Fegley Jr., B., and Lodders, K., 1997, Hydrous silicates and water on Venus: Icarus, v. 130, p. 475–494, https://doi.org/10.1006/icar.1997.5838.

Received July 2021
Accepted as revised November 2021

SERIES

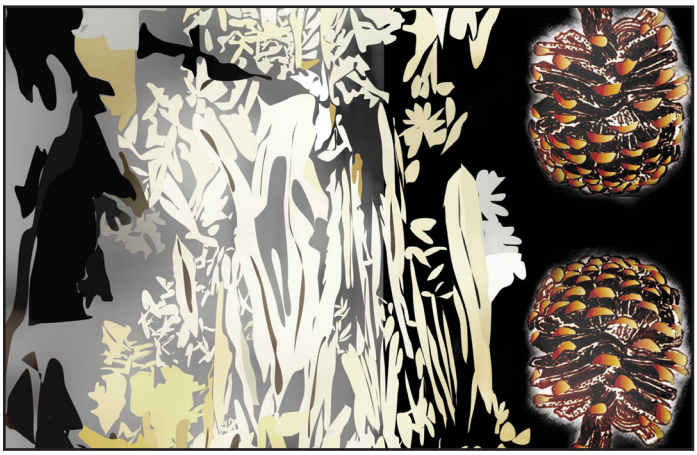

Heritage Stone 8.
Formation of Pinolitic Magnesite at Quartz Creek, British Columbia, Canada: Inferences from Preliminary Petrographic, Geochemical and Geochronological Studies

Alexandria Littlejohn-Regular, John D. Greenough and Kyle Larson

Department of Earth Environmental and Geographic Sciences
University of British Columbia Okanagan
3333 University Way, Kelowna, British Columbia
V1V 1V7, Canada
E-mail: john.greenough@ubc.ca

SUMMARY
Rocks in the Late Proterozoic Horsethief Creek Group at Quartz Creek in British Columbia display rare 'pinolitic' textures resembling those described in some sparry magnesite deposits elsewhere in the world. Elongated white magnesite crystals up to 30 cm long occur in a contrasting, dark, fine-grained matrix of dolomite, chlorite, organic material, clay minerals and pyrite. The rocks are aesthetically appealing for use in sculpture and as dimension stone. The term 'pinolite' is derived from the superficial similarities between these unusual textures and pinecones. Petrographic examination indicates that these textures formed when metasomatic fluids replaced primary sedimentary dolomite with magnesite. Fluids moved along fractures and bedding planes with repeated fracturing yielding magnesite crystals oriented in opposite directions on either side of annealed fractures, and broken magnesite crystals adjacent to later fractures. Magnesite contains dolomite microinclusions and has elevated Ca contents that are consistent with its formation by replacement of dolomite. Low concentrations of Cr, Ni, Co, Ti, Sr, and Ba in magnesite also imply formation in a metasomatic rather than a sedimentary environment. The rare earth element (REE) concentrations in the Quartz Creek magnesite are higher than those in most evaporitic magnesite and REE patterns lack the Ce and Eu anomalies that characterize carbonate rocks from sedimentary environments. Enrichment in light REE relative to heavy REE, and the similarities between dolomite, chlorite, and magnesite REE profiles, imply that metasomatic fluids modified the original sedimentary geochemical signature of the dolostones during formation of the pinolite rocks. A Late Ordovician to Early Silurian U–Pb age (433 ± 12 Ma), for titanite in the black matrix surrounding the sparry magnesite is younger than the local host rocks, and also younger than the Mesoproterozoic to Middle Cambrian stratigraphic ages of the host rocks for nearby magnesite deposits. The ca. 433 Ma titanite overlaps the ages for numerous fault-associated diatremes and volcaniclastic deposits in the area. Possibly the igneous activity furnished heat for, and/or was the source for, metasomatic fluids that produced the pinolite deposits.

RÉSUMÉ
Les roches du groupe de Horsethief Creek de la fin du Protérozoïque à Quartz Creek en Colombie-Britannique présentent des textures « pinolitiques » rares ressemblant à celles décrites dans certains dépôts de magnésite sparitique ailleurs dans le monde. Des cristaux de magnésite blancs et allongés, atteignant 30 cm de long, se trouvent dans une matrice à grains fins, sombre et contrastante, et composée de dolomie, de chlorite, de matière organique, de minéraux argileux et de pyrite. Les roches sont esthétiquement attrayantes pour un usage en sculpture et en tant que pierre de taille. Le terme « pinolite » est dérivé des similitudes superficielles entre ces textures inhabituelles et les pommes de pin. L'examen pétrographique indique que ces textures se sont formées lorsque les fluides métasomatiques ont remplacé la dolomie sédimentaire pri-

Geoscience Canada, v. 48, https://doi.org/10.12789/geocanj.2021.48.177 pages 117–132

GC Data Repository: Heritage Stone Series at https://GAC.ca/GC-data-repository

maire par de la magnésite. Les fluides se sont déplacés le long des fractures et des plans de stratification présentant des fracturations répétées, produisant des cristaux de magnésite orientés dans des directions opposées de chaque côté des fractures recuites, et des cristaux de magnésite brisés adjacents aux fractures ultérieures. La magnésite contient des micro-inclusions de dolomie et a des teneurs élevées en Ca qui sont compatibles avec sa formation par remplacement de la dolomie. De faibles concentrations de Cr, Ni, Co, Ti, Sr et Ba dans la magnésite impliquent également la formation dans un environnement métasomatique plutôt que sédimentaire. Les concentrations d'éléments des terres rares (ETR) dans la magnésite de Quartz Creek sont plus élevées que celles de la plupart des magnésites évaporitiques et les profils d'ETR ne présentent pas les anomalies en Ce et Eu qui caractérisent les roches carbonatées des environnements sédimentaires. L'enrichissement en ETR légers par rapport aux ETR lourds, et les similitudes entre les profils des ETR de la dolomie, de la chlorite et de la magnésite, impliquent que les fluides métasomatiques ont modifié la signature géochimique sédimentaire originale des dolomies lors de la formation des pinolites. Un âge U–Pb de la fin de l'Ordovicien au début du Silurien (433 ± 12 Ma), pour la titanite dans la matrice noire entourant la magnésite sparitique, est plus récent que celui des roches hôtes locales, et également plus récent que les âges stratigraphiques du Mésoprotérozoïque au Cambrien moyen des roches hôtes des dépôts de magnésite voisins. La titanite d'environ 433 Ma chevauche les âges de nombreux diatrèmes et dépôts volcanoclastiques associés à des failles dans la région. Il est possible que l'activité ignée a fourni la chaleur et/ou a été la source des fluides métasomatiques qui ont produit les dépôts de pinolites.

Traduit par la Traductrice

INTRODUCTION

Rocks exhibiting spectacular pinolitic textures were discovered in 2018 by placer gold miners working at Quartz Creek in the Northern Purcell Mountains, near Golden in southeastern British Columbia (Fig. 1). The term 'pinolite' has been used for rare, aesthetically pleasing textures resembling pinecones. These textures are found in sparry magnesite deposits that are generally hosted in metamorphosed Proterozoic and Paleozoic sedimentary rocks (Pohl 1989; Pohl 2011, p. 336). Sparry magnesite deposits are also informally referred to as Veitsch-type magnesite deposits in reference to a former mine in Austria, where magnesite forms stratiform lenses within marine platform sedimentary rocks (Redlich 1909). Pinolitic textures found in parts of these deposits typically consist of elongated white magnesite crystals in a fine-grained dark matrix consisting of chlorite, organic material, pyrite, talc and dolomite (Pohl 2011, p. 336). These textures have also been described from Russia, Spain and elsewhere in Canada, primarily in operating magnesite mines (Simandl and Hancock 1991; Lugli et al. 2000; Krupenin and Ellmies 2001; Krupenin 2005; Kilias et al. 2006; Azim Zadeh et al. 2015; Paradis and Simandl 2018).

The pinolite rocks at Quartz Creek are hosted by Neoproterozoic carbonate rocks of the Horsethief Creek Group (Fig. 1). Pinolitic textures have also been reported at Mount Brussilof Mine, a magnesite deposit located approximately 130 kilometres southeast of the study area (Fig. 1 inset). At Mount Brussilof, they are interpreted as diagenetic or metasomatic replacement textures (Simandl and Hancock 1991; Paradis and Simandl 2018). Other significant sparry magnesite occurrences in southeastern British Columbia include the Marysville, Brisco and Driftwood Creek deposits (Fig. 1; Hancock and Simandl 1992; Simandl and Hancock 1992, 1999). However, these do not necessarily contain widely developed pinolite textures.

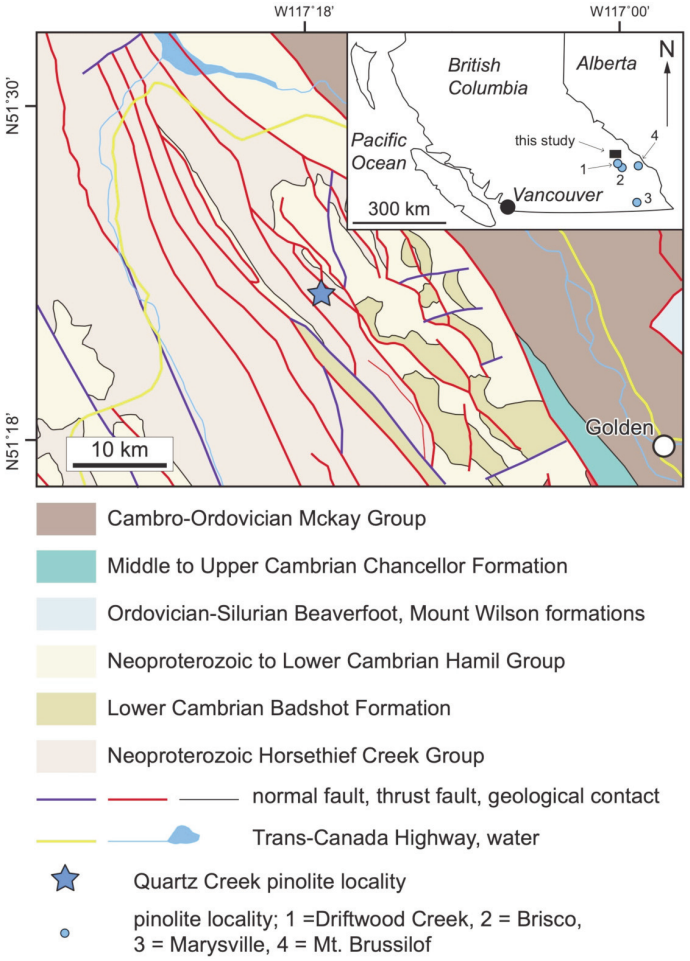

Figure 1. Geological map of the area surrounding the Quartz Creek pinolite quarry. Quarry location and the sampling site are shown. The index map shows location of the study area and selected magnesite deposits in southeastern British Columbia. Map redrafted using geological data from MapPlace [https://www2.gov.bc.ca/gov/content/industry/mineral-exploration-mining/british-columbia-geological-survey/mapplace].

The genesis of sparry magnesite deposits and pinolite has been debated at length, and the two principal hypotheses propose syngenetic and epigenetic origins, respectively (e.g. Simandl and Hancock 1999; Marshall et al. 2004). Studies in support of a syngenetic origin suggest that magnesite was deposited under evaporitic conditions or during diagenetic recrystallization of a magnesite protolith deposited as a chemical precipitate in marine or lacustrine settings (Pohl 1990). In contrast, the epigenetic hypothesis invokes hydrothermal metasomatic replacement of dolomitized, permeable carbon-

ates by magnesite. Metasomatic hydrothermal models involving Mg-rich fluids have been suggested for sparry magnesite deposits in Spain and Austria (Pohl and Siegl 1986; Nesbitt and Prochaska 1998; Kilias et al. 2006; Azim Zadeh et al. 2015) as well as in Canada (Simandl and Hancock 1991, 1992, 1999; Hancock and Simandl 1992; Simandl et al. 1992). This paper represents a contribution to the debate surrounding the origins of such textures.

The Quartz Creek pinolite rocks discussed here are of economic interest. Their exceptional and aesthetically pleasing textures (Fig. 2) make them valuable for carving and dimension stone and led to the establishment of the first pinolite quarry in North America. The Quartz Creek site is also of interest in the context of the debate concerning the origin(s) of pinolite textures and associated magnesite deposits. The research summarized in this paper was completed as part of a thesis project by the senior author, focused on optical and scanning electron microscopy and major and trace element analysis of whole-rock samples and constituent minerals. Electron microprobe (EMPA) analysis and laser ablation inductively coupled plasma mass spectrometry (LA-ICP-MS) trace element analysis were used to determine mineral compositions. We also report a U–Pb titanite age, obtained using LA-ICP-MS methods, that probably pinpoints the timing of pinolite formation. The study compares the data from Quartz Creek with results for other sparry magnesite deposits including local deposits which exhibit similar pinolite textures (Simandl and Hancock 1991). Our research is limited to a small number of analyses and a single U–Pb age; more work is required to substantiate and extend its findings. Nevertheless, the results are interesting, and provide new information about an unusual semi-precious stone that may have wider importance in British Columbia. Although the Quartz Creek pinolite quarry is not associated with a sparry magnesite deposit exploited for magnesium, understanding its origins may provide useful insight into the genesis of such deposits.

GEOLOGICAL SETTING AND SAMPLE COLLECTION

Based on geological mapping by Poulton and Simony (1980), the Quartz Creek pinolite quarry is hosted in the Neoproterozoic Horsethief Creek Group but its precise stratigraphic position within the group is unclear. The following summary of regional geology applies to Figure 1 and the surrounding area.

The Quartz Creek pinolite rocks occur in the Dogtooth Range, the most northern subrange of the Purcell Mountains, and within the Horsethief Creek Group, which is in turn a subdivision of the Neoproterozoic Windermere Supergroup. The regional geology was documented by Wheeler and Fox (1962) and Kubli (1990) and the stratigraphy and sedimentology of the Horsethief Creek Group was studied by Poulton (1973) with most emphasis on the upper unit of carbonate rocks. The Dogtooth Range appears to have a relatively simple deformation history consisting of a single, extended phase of northeastward-directed compression under low grade, greenschist facies metamorphism (Kubli 1990). The rocks of the Horsethief Creek Group are cut by several north-easterly-directed thrust faults (Poulton 1973), and the pinolite locality sits within a structural subdivision termed the Quartz Creek thrust sheet (Fig. 1). The term 'slate' is commonly used for argillitic rocks interpreted to be derived from shales, and the term 'grit' is used for coarse sandstones to fine pebble conglomerates (Poulton and Simony 1980).

Available mapping does not distinguish formal units within the Horsethief Creek Group but its overall stratigraphy is known in general terms (Kubli 1990). These sedimentary rocks transition upward over ~3000 m from beds dominated by slates (Basal Pelite), coarse sandstones and slate (Lower Grit), into a carbonate-bearing unit (Baird Brook unit, up to 140 m thick), followed by another siliciclastic unit (Upper Grit), a slate unit (Slate Division) and a thick limestone and dolostone unit (Carbonate Division, up to 390 m thick). The top of the Horsethief Creek Group section is defined by another siliciclastic unit up to 230 m thick (Kubli 1990). The stratigraphic position of the carbonate rocks that host the pinolite at Quartz Creek is uncertain; they could be part of the Baird Brook unit or the upper Carbonate Division. The Baird Brook unit is dominated by slate and limestone interpreted to have formed during sea-level rise associated with a reduction in the supply of coarse clastic detritus (Kubli 1990). There is no previous record of magnesite or pinolitic textures in the area, but a massive dolostone unit in the Carbonate Division was documented by Poulton and Simony (1980). The only clear stratigraphic or structural constraint on the timing of pinolite texture formation is given by the Neoproterozoic age of the Horsethief Creek Group, which provides an upper limit.

Rocks that display well-developed pinolitic textured rocks form weathered outcrops, and occur as relatively unweathered boulders, in steep scree slopes on the east side of Quartz Creek approximately 25 km northwest of Golden (Fig. 1). Numerous specimens were collected from the quarry site, which is located at 117°16'42.25" W and 51°23'7.43" N. Five samples, representing end-member variations in texture, were selected for detailed study. Specimens PIN 1 and 2 are from outcrop at the quarry site whereas PIN 3, 4 and 5 are locally derived boulders showing textures that are not represented in the more limited outcrop at the site.

ANALYTICAL METHODS

Full details of analytical procedures are given in Appendix A (see Geoscience Canada data repository). Polished thin sections were examined using a petrographic microscope, mineral identifications were confirmed by SEM EDS (Scanning Electron Microscope, Energy Dispersive Spectrometry) and analyses and textures were documented with back-scattered electron (BSE) images. The whole-rock samples were analyzed for major and trace elements at ACME Analytical Laboratories, Vancouver, by ICP-ES (Inductively Coupled Plasma - Emission Spectroscopy) and ICP-MS (Mass Spectrometry), respectively. All SEM work and all mineral analyses were performed at the Fipke Laboratory for Trace Element Research (FiLTER) of the University of British Columbia, Okanagan campus. Major element mineral analyses were performed by Electron

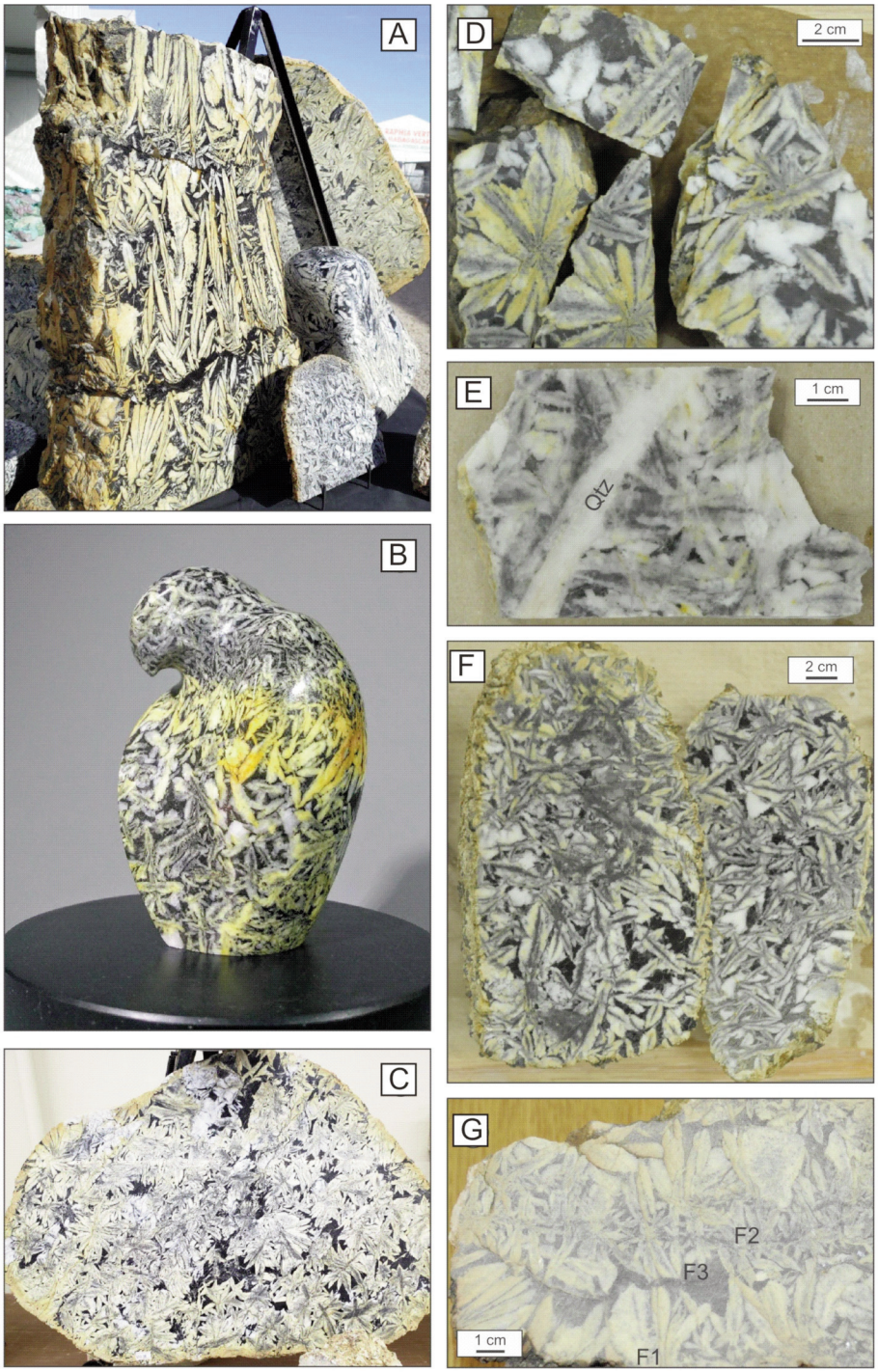

Figure 2. Photographs of pinolite from Canadian Pinolite's Quartz Creek quarry. A) large dimension-stone slab ~120 cm tall, exhibiting light-colored magnesite crystals up to ~ 30 cm long radiating toward the centre of the slab from two irregular, subhorizontal fractures in the upper and lower third of the rock. Black material in the fractures, and between magnesite crystals is interpreted as relict host rock. Photograph courtesy of Ian Burak. B) Bird sculpture (~ 35 cm tall) carved from pinolite. Yellow areas reflect oxidation due to incipient weathering. Sculpture and photograph by Deborah Wilson (Vernon, BC); photograph from Ian Burak who owns the image and the sculpture. C) Photograph showing a ~ 50 cm-wide dimension-stone slice through a pinolite rock with typical, radiating, sparry magnesite crystals surrounded by darker matrix rock. D) Assorted slices through sample PIN 1 showing magnesite with a radiating texture. The photograph also shows the colour contrast between magnesite crystals and dark matrix material. Together, the radiating texture and colour contrast create an unusual, aesthetically-pleasing rock that is in demand from sculptors and for dimension stone. E) Close-up photograph of a slice through sample PIN 2 showing a quartz vein cutting the rock. F) Pinolite sample PIN 5 showing pinolite texture. Magnesite grains are separated by a thin dark matrix. G) Pinolite sample PIN 4 showing magnesite crystals growing up (in the photograph) from a fracture (F1) along which the sample was broken in freeing it from the outcrop. In the centre of the rock and fracture system there is a faint line (F2) where crystals apparently grew both up and down and away from the poorly-defined fracture. The rock underwent another episode of fracturing (F3) that terminates crystals previously grown from F1 and F2, but the dark country rock forming the matrix in this fracture shows no preferential tendency to break at the matrix-magnesite boundaries, suggesting annealing after F3. Many of the magnesite crystals have a feather-like appearance with a line of dark inclusions parallel to the long axes of the crystals. Faint orange coloration reflects minor, incipient weathering at the outcrop surface.

Microprobe Analysis (EMPA) and mineral trace element analyses by laser-ablation (LA-ICP-MS). The U–Pb dating of titanite in sample PIN 4 used *in-situ* LA-ICP-MS.

RESULTS

Petrography and Mineralogy

Specimens PIN 1 to 5 were selected for detailed petrographic and geochemical analysis because they represent the wide range of textures present at Quartz Creek, and all exhibit typical pinolitic textures where large light-coloured crystals of magnesite occur in a dark matrix (Fig. 2). These magnesite crystals are elongate (prismatic or scalenohedral; length/width ratios of 2 to 4), typically exhibit a black band of inclusions parallel to their long axes and are generally separated from one another by thin (mm – cm) irregular patches of dark matrix. The large magnesite crystals are the dominant component of all samples examined in detail, as illustrated in Figure 2. The maximum size of magnesite crystals (long dimension) varies from about 1 cm in sample PIN 3 to 4.4 cm in sample PIN 1. All samples, excluding PIN 3, are illustrated in Figure 2 (see panels D, F and G). Locally, magnesite crystals reach lengths of 30 cm, as shown in a large display sample (Fig. 2A). Crystal sizes can also vary over short distances, as shown in the bird sculpture (Fig. 2B). Specimen PIN 1 (Fig. 2D) contains radiating rosettes of magnesite crystals but in others the crystals appear to be randomly oriented (Fig. 2F). Specimen PIN 2 contains a quartz vein ~ 1 cm wide, cutting through magnesite crystals (Fig. 2E). Some magnesite crystals appear to have nucleated on the walls of fractures and to have grown away from the fracture centre. The fractures and fracture systems are cm to tens of cm wide and underwent multiple episodes of brittle opening that broke apart the earliest-formed magnesite crystals (Fig. 2A, 2G). Black relict wall rock forms the dark material in fractures and wraps around the magnesite crystals but remains strongly adhered to them, making the material coherent for cutting and polishing. Weathering close to exposed rock surfaces produces yellow to orange and locally brown discolouration, as shown by several samples illustrated in Figure 2.

Back-scattered electron microscope images (Fig. 3) reveal that dolomite is more abundant than originally estimated from macroscopic examination. Dolomite forms cm-sized idiomorphic crystals associated with anhedral sparry magnesite (Fig. 3A) but also occurs as microinclusions (≤ 10 μm to 200 μm) within magnesite (Fig. 3B) and as larger multigrain masses included in magnesite (Fig. 3C). The dark matrix consists of

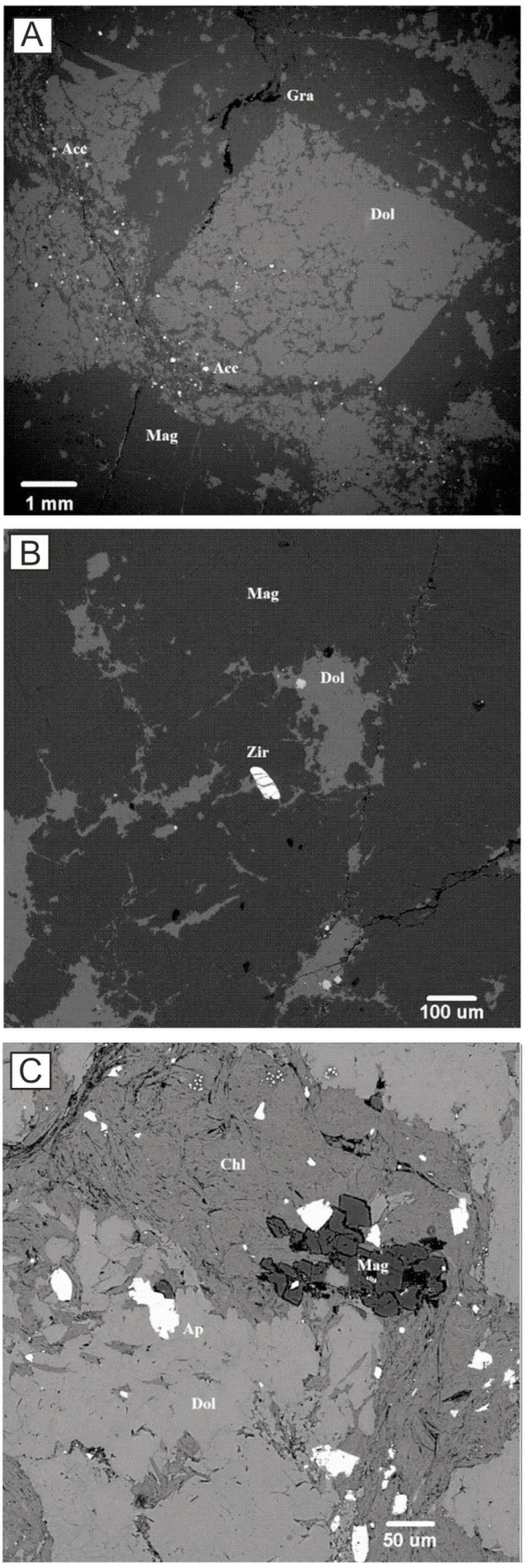

Figure 3. *(opposite)* Back-scattered electron (BSE) images showing dolomite (Dol; light grey), magnesite (Mag; dark grey) and chlorite (Chl). A, B) Images from sample PIN 4 in which accessory minerals including zircon, apatite, titanite, rutile and Fe-Ti oxides are bright white (labelled Acc) and small black patches and irregular lines are graphite (Gra). Relict dolomite patches and microinclusions occur in the magnesite, and idiomorphic (recrystallized?) dolomite is locally riddled with magnesite. A rounded (detrital?) 50 μm zircon occurs in the centre of image B. C) Back-scattered electron (BSE) image of sample PIN 5 showing chlorite (Chl) within dolomite (Dol). A magnesite (Mag) grain and apatite crystals (white grains) occur within chlorite and a large apatite grain (Ap) occurs in dolomite.

https://doi.org/10.12789/geocanj.2021.48.177

fine-grained dolomite, minor magnesite (< 10%), Mg-chlorite (< 10%), calcite, quartz, and several other accessory minerals (Fig. 3A). The Mg-chlorite was identified as clinochlore, and locally forms sinuous masses bearing various accessory minerals, idiomorphic magnesite inclusions and elongate carbonaceous inclusions oriented parallel to cleavage (Fig. 3C). The carbonaceous material also forms ≤ 0.2 mm wide stringers that wrap around magnesite and dolomite grains and also occur within grains (Fig. 3A). The carbonaceous material most likely consists of graphite considering the regional greenschist facies metamorphism reported by Kubli (1990). Non-carbonate accessory minerals make up ≤ 10% of the samples and include rutile, apatite, pyrite, zircon, titanite, micas (paragonite and muscovite), iron oxides and clay minerals. Rounded to irregular, small (≤ 60 μm) fluorapatite grains are scattered within magnesite, chlorite, and dolomite grains (Fig. 3C). These accessory minerals, including the titanite used for dating, are most abundant in the black matrix material, between larger magnesite and dolomite crystals and are typically concentrated in narrow bands that have a thin (≤ 1 mm) linear array of magnesite grains in the centre (Fig. 3A). Zircon grains in the matrix show variable sizes (30 μm – 100 μm), are very diverse in shape (angular to well-rounded) and exhibit varied internal textures (Fig. 3B).

Whole Rock and Mineral Geochemistry

Whole rock major and trace element contents of the pinolite specimens are highly variable (Table 1; Fig. 4). For example, MgO varies from 18.2 to 37.8 wt. % and Sr varies from 27 to 180 ppm. MgO shows a negative correlation with CaO and Sr, and a positive correlation with Fe_2O_3, but has no clear relationship with SiO_2, Al_2O_3 or trace elements (e.g. Zr and Y). The interpretation of geochemical patterns is hampered by the small number of samples that were analyzed and a larger dataset might reveal more coherent patterns.

Analyses of the dominant minerals (Table 2) show that chlorite and magnesite have the highest FeO contents, as would be expected. The high CaO and Sr contents of dolomite are also predictable, but this mineral also seems to have high Y and REE compared to magnesite and chlorite (Table 2). Enrichment in High Field Strength Elements (HFSE: Zr, Hf, U, Th) is seen in chlorite. A primitive-mantle-normalized spider diagram for whole rock analyses (Fig. 5A) displays strong negative Ti anomalies and positive Th and U anomalies. These profiles are compared to those of average shale, which shows higher normalized concentrations for most elements (Fig. 5A). The normalized profiles for the Quartz Creek samples are somewhat more jagged than those of average shale, with prominent positive Th, U, Sr, Sm and Eu anomalies and negative Ba, Nb, K, Zr, Hf and Ti anomalies (Fig. 5A). A similar primitive-mantle-normalized spider diagram for average mineral analyses (Fig. 5B; average of data in Table 2) shows that chlorite is depleted in most elements, but has positive Zr, Hf, Sr and U anomalies. Dolomite shows negative Ba and positive Eu, Sm and Sr anomalies. Note that both magnesite and dolomite have Ti concentrations below the detection limit, so values for this element cannot be represented. The trace element pattern for magnesite resembles that for dolomite in most respects, but magnesite tends to have lower normalized concentrations for most of the analyzed elements.

Table 1. Whole rock major and trace element compositions of pinolite samples.

Element	PIN 1	PIN 2	PIN 3	PIN 4	PIN 5	DL
SiO_2	4.55	14.52	3.30	8.68	9.39	0.01
TiO_2	0.03	0.01	0.02	0.06	0.02	0.01
Al_2O_3	0.96	0.28	0.51	1.16	0.29	0.01
Fe_2O_3	0.93	0.88	1.39	1.96	0.77	0.01
MnO	0.02	0.02	0.03	0.03	0.02	0.01
MgO	21.23	18.23	30.79	37.77	20.23	0.01
CaO	26.56	24.97	16.05	3.39	25.65	0.01
Na_2O	0.12	0.03	<DL	0.15	<DL	0.01
K_2O	0.06	0.03	<DL	0.09	0.01	0.01
P_2O_5	0.03	<DL	0.03	0.03	0.02	0.01
LOI	45.10	40.70	47.40	46.10	43.30	
Sum	99.59	99.67	99.52	99.40	99.70	
Tot C	12.76	11.59	6.80	12.96	11.90	0.02
Rb	2.80	1.20	<DL	3.35	<DL	0.10
Cs	0.10	<DL	<DL	0.20	<DL	0.10
Sr	103	166	90.0	26.6	181	0.50
Ba	4.00	4.00	4.00	5.50	3.00	1.00
Zr	10.5	19.9	5.30	69.6	12.5	0.10
Hf	0.30	0.50	0.20	1.75	0.30	0.10
Nb	0.90	1.10	0.70	2.20	0.20	0.10
Th	0.70	0.60	0.50	2.25	0.70	0.20
U	0.80	0.20	0.50	0.65	0.40	0.10
La	3.60	2.20	1.50	2.00	2.90	0.10
Ce	5.80	5.20	3.90	4.25	6.30	0.10
Pr	0.89	0.83	0.73	0.83	1.00	0.02
Nd	5.10	5.20	4.40	5.80	5.30	0.30
Sm	2.63	3.87	1.04	3.38	1.64	0.05
Eu	0.91	1.27	0.45	1.07	0.59	0.02
Gd	2.39	5.07	0.98	3.24	1.38	0.05
Tb	0.24	0.64	0.18	0.33	0.16	0.01
Dy	0.87	2.71	0.49	1.37	0.71	0.05
Ho	0.15	0.45	0.14	0.22	0.13	0.02
Er	0.34	0.91	0.22	0.53	0.37	0.03
Tm	0.04	0.10	0.09	0.07	0.05	0.01
Yb	0.26	0.57	0.18	0.45	0.25	0.05
Lu	0.04	0.07	0.07	0.07	0.04	0.01
Y	4.70	13.00	4.40	6.70	4.30	0.10
Ga	0.70	<DL	<DL	0.70	<DL	0.50
Ni	2.60	0.80	1.70	3.40	0.40	0.10
Co	3.70	0.30	2.30	2.20	<DL	0.20
Cu	3.50	0.80	2.85	1.30	1.20	0.10
Pb	1.70	0.60	0.80	0.90	0.20	0.10
As	2.70	<DL	1.40	4.50	<DL	0.50
W	40.4	1.80	0.70	3.00	1.00	0.50
Sb	0.20	<DL	0.20	<DL	<DL	0.10

Notes: Major element oxides in wt. %. Total Fe as Fe_2O_3.
Sum = Sum of oxides + LOI (Loss on Ignition).
Tot C = Total carbon in Wt. %. Trace elements in ppm.
DL= Detection Limit; <DL indicates results below Detection Limits.
PIN4 = average of 2 replicate analyses for most elements.
PIN5 = average of 2 replicate analyses for Cu, Pb, Ni, As, Sb.
For details of accuracy and precision, see analytical methods.

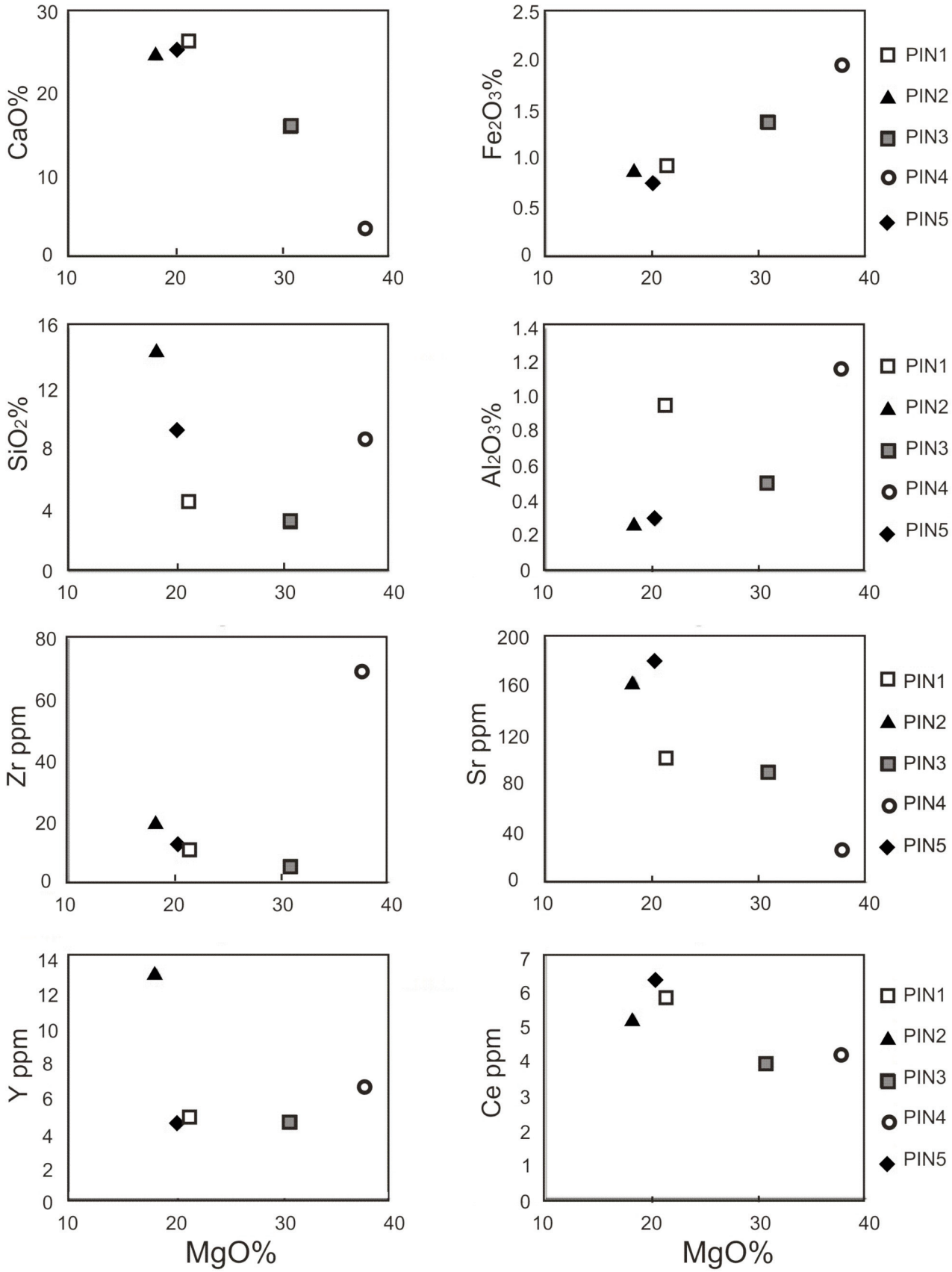

Figure 4. Relationship between MgO wt. % and major element oxides and trace elements for whole rock analyses of Quartz Creek Pinolite rocks.

https://doi.org/10.12789/geocanj.2021.48.177

Table 2. Mineral compositions for magnesite, dolomite and chlorite, determined by electron microprobe as major element oxides (wt.%) and by LA ICP-MS as trace elements (ppm).

Analysis Specimen	M-1 PIN 3	M-2 PIN 3	M-3 PIN 3	D-1 PIN 3	D-2 PIN 3	D-3 PIN 3	C-1 PIN 5	C-2 PIN 5	C-3 PIN 5	DL
SiO_2	<DL	0.01	<DL	<DL	<DL	<DL	30.49	30.6	30.28	0.01
TiO_2	<DL	<DL	<DL	<DL	<DL	<DL	0.02	0.02	0.01	0.01
Al_2O_3	<DL	<DL	<DL	<DL	<DL	<DL	21.33	20.5	20.92	0.01
FeO	1.48	2.51	1.40	0.49	0.58	0.51	1.60	1.92	1.54	0.01
MnO	<DL	0.05	0.03	0.03	0.03	0.01	<DL	0.01	0.01	0.01
MgO	48.46	50.5	49.17	24.3	24.7	25.63	35.15	34.65	32.28	0.01
CaO	0.86	0.10	0.71	32.64	33.63	33.73	0.02	0.03	0.05	0.01
Na_2O	0.01	0.02	0.02	0.02	<DL	<DL	0.06	0.05	0.07	0.01
K_2O	<DL	0.01	<DL	<DL	<DL	<DL	0.08	0.04	0.05	0.01
P_2O_5	<DL	<DL	<DL	0.03	0.03	0.01	0.03	0.03	0.05	0.01
F	<DL	<DL	<DL	<DL	<DL	<DL	0.70	0.74	0.76	0.01
Cl	<DL	<DL	<DL	<DL	<DL	<DL	0.03	0.07	0.11	0.01
Total	50.81	53.19	51.34	57.5	58.97	59.89	89.50	88.63	86.13	
Sc	1.09	0.53	0.66	1.74	1.03	0.29	0.27	0.52	1.55	0.18
V	4.03	3.48	4.05	5.74	4.21	1.6	47.4	51.8	78.7	0.05
Cr	<DL	<DL	<DL	<DL	<DL	<DL	67.2	87.7	77.7	1.71
Co	1.82	0.04	0.04	0.2	<DL	<DL	0.66	1.71	2.77	0.03
Ni	1.20	<DL	<DL	<DL	<DL	<DL	24.3	28.6	32.8	0.97
Cu	1.07	<DL	<DL	<DL	<DL	<DL	28.5	2.02	5.32	0.50
Zn	3.66	2.36	3.62	2.26	2.02	1.41	12.3	9.89	13.7	1.24
As	1.49	<DL	<DL	1.30	<DL	<DL	2.16	2.59	17.3	0.88
Rb	0.64	<DL	<DL	0.17	<DL	<DL	0.27	0.14	0.65	0.05
Sr	19.2	1.43	2.67	143	153	89.7	13.8	9.11	123	0.05
Y	3.75	3.87	4.37	19.4	17.4	2.82	2.20	2.44	7.67	0.02
Zr	4.26	1.28	0.20	0.22	<DL	<DL	38.9	119	169	0.03
Nb	0.32	<DL	<DL	0.19	<DL	<DL	5.75	0.61	5.05	0.01
Sb	0.45	<DL	<DL	0.27	<DL	<DL	<DL	0.43	4.43	0.13
Ba	1.55	0.20	0.68	0.35	0.19	0.01	1.72	20.2	36.9	1.09
La	0.86	0.62	0.77	5.11	4.65	0.50	0.52	0.22	0.62	0.04
Ce	3.66	3.59	4.2	18.2	16.7	1.94	2.26	1.1	1.46	0.05
Pr	0.94	0.73	0.8	3.5	3.06	0.37	0.36	0.13	0.27	0.04
Nd	4.00	4.71	5.13	20.8	19.0	2.50	2.35	0.92	1.73	0.50
Sm	1.83	1.52	1.67	9.29	8.65	1.25	0.95	0.40	0.75	0.07
Eu	0.92	0.69	0.72	3.61	2.85	0.40	0.27	0.11	0.21	0.03
Gd	1.27	1.19	1.06	8.96	7.72	1.20	0.78	0.43	0.59	0.04
Tb	0.38	0.09	0.10	1.03	0.71	0.11	0.06	0.03		0.03
Dy	0.83	0.53	0.55	3.74	3.20	0.60	0.37	0.39	0.89	0.03
Ho	0.44	0.09	0.11	0.79	0.55	0.09	0.09	0.06	0.19	0.03
Er	0.61	0.31	0.36	1.63	1.22	0.19	0.21	0.3	0.87	0.03
Tm	0.35	<DL	0.03	0.36	0.15	0.03	0.02	0.03	0.14	0.02
Yb	0.55	0.25	0.26	1.15	0.90	0.13	0.18	0.34	0.91	0.04
Lu	0.34	<DL	<DL	0.31	0.12	<DL	0.03	0.04	0.12	0.02
Hf	0.39	<DL	<DL	0.18	<DL	<DL	0.89	3.24	4.49	0.03
Ta	0.32	<DL	<DL	0.19	<DL	<DL	0.37	0.02	0.18	0.03
Pb	0.58	<DL	<DL	0.28	<DL	<DL	0.21	1.02	3.14	0.11
Th	0.53	0.06	0.06	0.35	0.10	0.03	2.83	6.48	6.94	0.01
U	0.70	0.08	0.03	0.26	<DL	<DL	3.45	5.78	7.29	0.01

Notes: Major element concentrations in oxide wt. % with all Fe as FeO. Trace elements in ppm.
EMPA = electron microprobe analysis; DL = Average detection limit. < DL is below Detection Limit.
For details of precision and accuracy, see analytical methods.

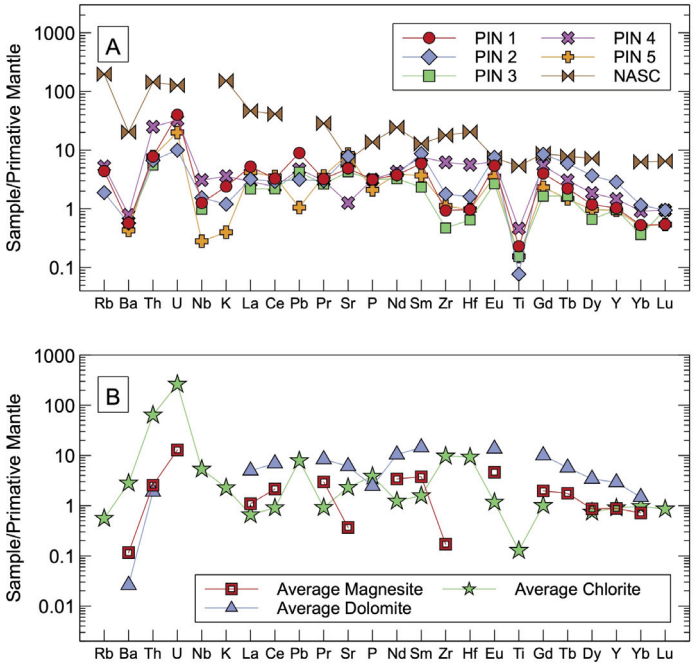

Figure 5. Primitive-mantle-normalized spider diagrams. A) Whole rock analyses (data in Table 1) and North America Shale Composite (NASC) from Gromet et al. (1984). B) average mineral analyses by LA ICP-MS (data in Table 2). Elements missing in part B patterns were below detection limit in one or more of the analyses and are not included. Primitive mantle normalizing values are from McDonough and Sun (1995).

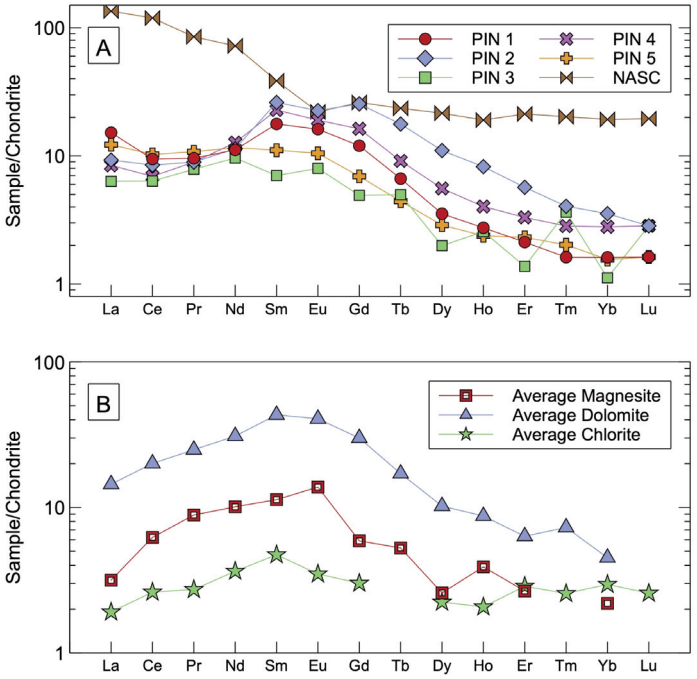

Figure 6. A) Chondrite-normalized REE patterns for whole rock pinolite analyses (Table 1) and North American Shale Composite (Gromet et al. 1984). B) Chondrite normalized REE patterns for averages of LA-ICP-MS mineral analyses in Table 2. Missing points reflect that one or more analyses were below the detection limit and the average not plotted. Chondrite normalizing values from McDonough and Sun (1995).

Rare Earth Elements

Rare Earth Element (REE) concentrations from whole rock and mineral analyses are listed in Table 1 and Table 2, respectively. Specimens are characterized by low total REE concentrations, ranging from 14 to 29 ppm in whole rock analyses. The total REE content of individual minerals tends to be higher for dolomite (9–78 ppm) than for magnesite (14–17 ppm; Table 3). Normalized to chondritic REE abundances, both whole-rock and mineral data show enrichment in light REE relative to heavy REE (Table 3). The chondrite-normalized REE patterns for whole-rock analyses and those from individual minerals (magnesite, dolomite and chlorite) show similar convex-upward patterns that have peak abundances at Sm and Eu (Fig. 6). In this respect, the REE patterns for whole-rock samples from Quartz Creek (Fig. 6A) contrast with the REE pattern for the North American Shale Composite, which is relatively enriched in light and heavy REE and depleted in the middle REE.

The shapes of average dolomite, magnesite and chlorite REE patterns are similar (Fig. 6B). The data in Table 3 and Figure 6 do not reveal any significant positive or negative anomalies for Ce or Eu. Magnesite analyses indicate a small positive Eu anomaly (Eu/Eu*) but there is no consistent pattern for Ce/Ce* values (Table 3). This is interesting because prominent Ce or Eu anomalies are commonly seen in carbonate rocks and have been used to infer the origins of some magnesite deposits (e.g. Bau and Möller 1992).

Titanite Dating

U–Pb Titanite dating was performed on sample PIN 4, using 24 spot analyses distributed across 17 individual grains; results for unknowns and standards are listed in Table 4. The analyzed titanite grains showed consistent textural features suggesting that they represent a single generation, and all are associated with magnesite. The analyses show varying degrees of common Pb incorporation in Tera-Wasserburg concordia space (Table 4; Fig. 7A). A subset of 18 analyses defines an isochron with a $^{238}U/^{206}Pb$ intercept of 433 ± 12 Ma (2SE; s = 0.63) with a $^{207}Pb/^{206}Pb$ intercept of 0.83 using the robust regression method of Powell et al. (2020). The isochron age overlaps with a ^{207}Pb-corrected $^{206}Pb/^{238}U$ weighted mean age (following Stacey and Kramers 1975) defined by 11 of the 24 analyses. This second method indicates a slightly older age of 442 ± 10 (MSWD = 3.6), shown in Figure 7B. The overlapping ages indicate that titanite formed in Late Ordovician–Early Silurian times. In the discussion that follows, we suggest that this age also represents the timing of metasomatism that resulted in the formation of pinolite textures.

DISCUSSION

Texture and Mineralogy

Pinolitic textures, such as those observed in magnesite deposits in Austria and Spain, have been interpreted as replacement features produced by Mg-rich hydrothermal fluids

Table 3. Rare earth element ratios and total REE for whole rock analyses and mineral analyses by LA-ICP-MS.

Specimen	Ce/Ce*	Eu/Eu*	Total REE	Total LREE	Total HREE	LREE/ HREE(N)
PIN 1	1.15	1.09	23.26	18.02	5.24	6.48
PIN 2	1.21	0.87	29.09	17.3	11.79	2.33
PIN 3	0.99	1.17	14.34	11.57	2.77	4.67
PIN 4	1.17	0.97	23.59	16.26	7.33	2.76
PIN 5	1.03	1.16	20.82	17.14	3.68	5.91
M-1	0.51	1.74	17	11.3	5.7	0.93
M-2	0.96	1.52	14.32	11.17	3.15	8.15
M-3	1.03	1.55	15.78	12.57	3.21	6.05
D-1	0.95	1.19	78.48	56.9	21.58	3.2
D-2	1.05	1.04	69.51	52.09	17.42	5.28
D-3	1.09	0.99	9.32	6.56	2.76	4.69

Notes: Total REE in ppm. LREE = Light REE (La-Sm). HREE = Heavy REE (Eu-Lu).
Eu/Eu* calculated after Tostevin et al. (2016) normalized to chondrite.
Ce/Ce* calculated after Lawrence et al. (2006) normalized to chondrite.
LREE/HREE(N) calculated as (La + Pr + Nd) / (Er + Tm + Yb + Lu), normalized to chondrite.
Magnesite and dolomite analyses from PIN 3.

(Simandl and Hancock 1991; Lugli et al. 2000; Azim Zadeh et al. 2015). The pinolitic textures at Quartz Creek locally show magnesite crystals with forms indicating growth in opposite directions (termed 'bipolar' textures in some literature) across relict fractures (Fig. 2), and the presence of broken crystals suggests that fracture development and crystal growth were closely linked in time. These and other textures shown in Figure 2 are remarkably similar to those described by Pohl and Siegl (1986; their photos 4, 5 and 8; p. 228, 229 and 231, respectively) from the Austrian and Spanish magnesite deposits. The evidence for multiple fracturing and associated growth episodes (Fig. 2A, 2G) is consistent with crystals formed from the migration of metasomatizing fluids along fractures and bedding surfaces.

There may be two or more generations of dolomite at Quartz Creek. Anhedral, irregularly-shaped dolomite microinclusions within magnesite (Fig. 3B) are consistent with dolomite as a precursor to magnesite formation. The microinclusions are interpreted as relict grains that result from incomplete dolomite replacement. Idiomorphic dolomite grains (Fig. 3A) probably formed later but it is not clear if they are earlier than, later than or contemporaneous with the enclosing magnesite. The relative time of formation or recrystallization of polygrain masses of anhedral dolomite (Fig. 3C) is also unclear and our dolomite analyses do not resolve different populations of dolomite.

Textural observations at some magnesite deposits in British Columbia have suggested a sedimentary and/or early diagenetic origin for magnesite followed by diagenetic or metasomatic replacement to form textures such as pinolite and sparry dolomite (Simandl and Hancock 1991, 1999; Marshall et al. 2004; Paradis and Simandl 2018). The textures from the Quartz Creek area may be similarly related to late hydrothermal replacement of dolomite, as suggested for the Mount Brussilof deposit (Marshall et al. 2004). Although the Quartz

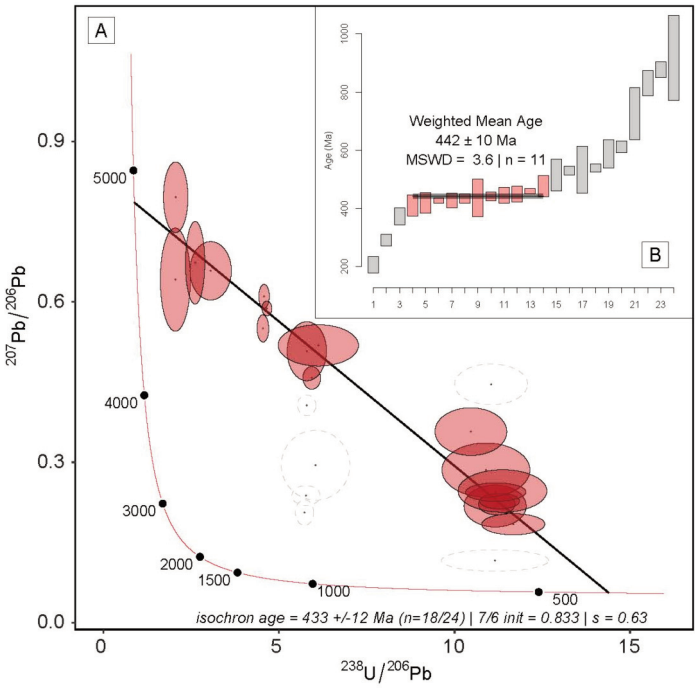

Figure 7. A) Tera-Wasserburg concordia diagram of *in situ* titanite analyses from specimen PIN 4. Red ellipses indicate data included in the calculated isochron age of ca. 433 Ma; unfilled grey dashed ellipses indicate data that were not included. B) a plot of ^{207}Pb-corrected ^{206}Pb/^{238}U ages, in which 11 of 24 determinations define a plateau from which a weighted mean age of ca. 442 Ma is calculated as shown.

Creek rocks and other deposits in British Columbia tend to be associated with dolomitized carbonate host rocks, the possibility of an early diagenetic origin for magnesite from calcite/aragonite limestones is supported by the experiments of Hobbs and Xu (2020). They argue that Veitsch-type magnesite is associated with evaporative environments and their experiments show that it might have formed from calcite through temperature (≤ 40°C) and pH cycling characteristic of evaporative/lagoon/playa environments.

The replacement of dolomite by magnesite proceeds through the following reaction:

$CaMg(CO_3)_2 + 2H+ \rightarrow MgCO_3 + Ca^{2+} + H_2CO_3$ (Aharon 1988; Lugli et al. 2000)

This reaction releases Ca^{2+}, which if accumulated in substantial amounts could reverse the reaction in favour of dolomite. Therefore, calcium must be flushed out by fluids in order for large quantities of magnesite to form (Lugli et al. 2000). This may help to explain textures indicative of dolomite recrystallization (Fig. 3A). Extensive recrystallization of dolomite is a common characteristic of magnesite deposits considered to have formed via metasomatic replacement processes (Aharon 1988; Lugli et al. 2000; Kilias et al. 2006).

The pinolite rocks at Quartz Creek appear to have formed by processes similar to those that generated sparry magnesite deposits in southeastern British Columbia and elsewhere. Other minerals identified in the Quartz Creek specimens, such as quartz and muscovite, along with accessory rutile, pyrite,

Table 4. Geochronology and U–Pb isotopic data for Quartz Creek pinolite titanite. See text for discussion.

Analysis	Approx. U ppm	U/Th	$^{238}U/^{206}Pb$	2SE† %	$^{207}Pb/^{206}Pb$	2SE %	$^{207}Pb/^{235}U$	2SE %	$^{206}Pb/^{238}U$	2SE %	rho
T1-1 C1	58	0.80	11.2	11.2	0.116	14.1	1.44	18	0.0897	11.2	0.62
T1-2 C1	7	0.34	11.2	6.5	0.218	14.7	2.69	16.1	0.0896	6.5	0.40
T1-3 C1	26	0.71	11.2	3.8	0.222	7.4	2.73	8.3	0.0893	3.8	0.46
T1-4 C1	48	0.57	11.7	6.3	0.184	8.8	2.17	10.8	0.0856	6.3	0.58
T2-1 C2	16	0.31	4.54	3.0	0.550	3.8	16.7	4.9	0.2201	3.0	0.62
T3-1 C2	1	0.17	2.05	17.1	0.642	12.3	43.2	21.1	0.4885	17.1	0.81
T4-1 C2	113	1.20	11.3	4.1	0.227	5.2	2.77	6.6	0.0886	4.1	0.62
T4-2 C2	18	0.44	5.94	3.5	0.458	3.8	10.6	5.2	0.1685	3.5	0.68
T5-1 C3	56	0.75	4.58	2.7	0.610	3.0	18.4	4.0	0.2186	2.7	0.67
T5-2 C3	53	0.77	4.66	2.5	0.588	1.9	17.4	3.2	0.2147	2.5	0.80
T6-1 C3	2	1.30	2.06	13.9	0.796	6.8	53.3	15.5	0.4860	13.9	0.90
T7-1 C4	4	0.25	5.80	7.9	0.508	8.9	12.1	11.9	0.1726	7.9	0.66
T8-1 C5	10	0.26	5.79	3.7	0.407	3.9	9.68	5.4	0.1727	3.7	0.68
T9-1 C5	7	0.23	10.9	9.4	0.285	14.5	3.61	17.3	0.0918	9.4	0.54
T10-1 C6	17	0.14	5.73	3.7	0.206	9.5	4.96	10.2	0.1746	3.7	0.36
T10-2 C6	13	0.19	5.77	5.7	0.238	6.4	5.68	8.6	0.1733	5.7	0.67
T10-3 C6	11	0.20	6.04	13.2	0.294	18.1	6.71	22.5	0.1655	13.2	0.59
T11-1 C7	18	0.42	6.12	15.3	0.519	6.1	11.7	16.5	0.1634	15.3	0.93
T11-2 C7	9	0.35	10.5	8.0	0.357	10.2	4.70	13.0	0.0955	8.0	0.62
T11-3 C7	141	0.66	11.2	6.3	0.244	5.8	3.01	8.5	0.0895	6.3	0.73
T11-4 C7	938	2.30	11.4	9.1	0.246	13.2	2.99	16.0	0.0880	9.1	0.57
T12-1 C8	5	0.15	3.06	15.8	0.658	6.8	29.7	17.2	0.3274	15.8	0.92
T13-1 C9	3	0.32	2.61	8.6	0.673	9.4	35.5	12.7	0.3830	8.6	0.68
T14-1 C9	11	0.56	11.0	7.7	0.446	7.0	5.56	10.4	0.0906	7.7	0.74

Table 4. *(continued)* Geochronology and U–Pb isotopic data for Quartz Creek pinolite titanite. See text for discussion.

Analysis	$^{207}Pb/^{206}Pb$ Date (Ma)	2SE ABS	$^{207}Pb/^{235}U$ Date (Ma)	2SE ABS	$^{206}Pb/^{238}U$ Date (Ma)	2SE ABS	$^{206}Pb/^{238}U^{*}$ Date (Ma)	2SE ABS
T1-1 C1	1900	530	904	230	554	64	515	61
T1-2 C1	2970	490	1330	370	553	38	446	38
T1-3 C1	2990	240	1340	210	551	22	442	21
T1-4 C1	2690	290	1170	210	530	35	449	31
T2-1 C2	4380	110	2920	610	1280	43	539	40
T3-1 C2	4600	360	3850	2300	2560	520	916	330
T4-1 C2	3030	170	1350	170	547	23	435	20
T4-2 C2	4110	110	2490	450	1000	38	530	30
T5-1 C3	4530	86	3010	560	1270	37	428	34
T5-2 C3	4480	56	2960	450	1250	35	460	23
T6-1 C3	4910	200	4060	2300	2550	420	206	210
T7-1 C4	4260	270	2610	900	1030	87	476	73
T8-1 C5	3930	120	2400	420	1030	41	612	32
T9-1 C5	3390	470	1550	490	566	55	410	50
T10-1 C6	2870	310	1810	410	1040	41	877	44
T10-2 C6	3100	200	1930	400	1030	64	831	55
T10-3 C6	3440	590	2070	930	987	140	725	120
T11-1 C7	4290	180	2580	1100	976	160	436	80
T11-2 C7	3740	320	1770	480	588	49	373	41
T11-3 C7	3150	190	1410	230	552	36	428	29
T11-4 C7	3160	430	1400	400	544	51	419	45
T12-1 C8	4640	200	3480	1800	1830	320	533	140
T13-1 C9	4670	270	3650	1700	2090	210	587	190
T14-1 C9	4070	210	1910	460	559	45	291	32

*^{207}Pb-corrected following the method of Stacey and Kramers 1975
†2SE = 2 standard error
Standards MMc and Fish gave weighted mean average ages of 528 ± 5 Ma (n=8; MSWD=0.65) and 27.9 ± 1 Ma (n=8; MSWD=0.99), respectively; for other details, see analytical methods.

apatite and zircon, are common relict minerals in many magnesite deposits interpreted to have formed from Mg-rich hydrothermal fluids (Kilias et al. 2006; Azim Zadeh et al. 2015). A fluid inclusion study of the Mount Brussilof deposit indicated temperatures between ~ 200 and 300°C at pressures < 2.6 Kbar (Marshall et al. 2004). Thus, sparry magnesite is apparently of hydrothermal origin but the dark matrix in the Quartz Creek pinolite probably represents relict wall rock as it contains carbonaceous material (graphite?) and zircon grains interpreted to be of detrital origin. The classification of zircon as detrital is based on large variations in the size and shape of zircon grains, and also on the proportions and types of inclusions (Fig. 3). Pyrite may also be detrital but could have formed from reducing hydrothermal fluids (Prochaska 2016). In summary, the sparry magnesite textures appear to reflect metasomatic transformation of dolomite by Mg-rich hydrothermal fluids, and the black matrix represents relict material from the original sedimentary rocks, including some accessory mineral populations.

Whole Rock and Mineral Compositions

Negative correlations of CaO and Sr with MgO and positive correlations between Fe_2O_3 and MgO in whole-rock analyses (Fig. 4) largely reflect the composition and varying proportions of magnesite, dolomite, and chlorite within the samples although there may be some influence from the closed-sum nature of these data. Given the small number of samples, it is difficult to draw further conclusions.

Because dolomite abundances control whole-rock Ca concentrations, and Sr^{2+} substitutes for Ca^{2+} in dolomite, the low and high Sr content in PIN 4 and PIN 5 likely reflects contrasting proportions of dolomite in each sample. FeO varies from 1.4 to 2.5 wt. % in mineral analyses of magnesite and chlorite (Table 2), where Fe^{2+} substitutes for Mg^{2+}. The modal abundances of magnesite are typically higher than those of chlorite, so it is likely that magnesite controls whole-rock Fe_2O_3 concentration in sparry magnesite rocks (Möller 1989). Whole rock Fe_2O_3 varies from 0.77 to 1.96 wt. % (Table 1; average 1.19) and these concentrations largely overlap those for other magnesite-bearing rocks from southeastern British Columbia discussed by Simandl (2002).

Whole-rock SiO_2 contents are controlled by the abundance of chlorite and quartz and the high SiO_2 concentrations in PIN 2 (Table 1) reflect the presence of a quartz vein. Magnesite and dolomite mineral analyses contain negligible Al_2O_3 (Table 2) so whole-rock Al_2O_3 concentrations (Table 1) may reflect the abundances of chlorite and minor clay minerals. The low contents of CaO (up to 0.86 wt. %; Table 2) in Quartz Creek magnesite likely reflect microinclusions of dolomite identified via petrographic studies. Azim Zadeh et al. (2015) attributed elevated CaO (up to 1.32 wt. %) in EMPA analyses of magnesite from the Hohentauern/Sunk sparry magnesite deposit to microinclusions of dolomite and/or redolomitization.

Comparisons with Other Pinolite and Magnesite Deposits

Magnesite and dolomite compositions from Quartz Creek and other sediment-hosted, metasomatic magnesite deposits hosting pinolite-textured rocks (Eugui and Rubian, Spain; Hohentauern/Sunk, Austria) are compared in Table 5 (data from Lugli et al. 2000; Kilias et al. 2006; Azim Zadeh et al. 2015). Mean contents of MgO in magnesite and MgO and CaO in dolomite at Quartz Creek tend to be slightly higher than for the same minerals in these magnesite deposits, but the FeO contents are similar (Table 5). Schroll (2002) determined that magnesite associated with ultramafic rocks contains up to 5 wt. % FeO, compared to only 1–2% FeO for magnesite derived from a sedimentary protolith (Table 5). The low FeO contents of magnesite from Quartz Creek and other deposits confirm that they are likely of sedimentary origin, consistent with the nature of their host rocks.

Trace Element Composition

Trace element (Cr, Ni, Co, Fe, Mn, Ba, Sr) concentrations in magnesite can distinguish types of magnesite deposits (Möller 1989; Azim Zadeh 2009) and have been used to discriminate the sources of Mg^{2+}. Figure 8 compares the concentrations of most of these elements in Quartz Creek magnesite to the mode and median values for magnesite reported by Azim Zadeh (2009; see Fig. 8 caption for details). Magnesite that is associated with ultramafic host rocks is typically enriched in Cr, Ni, and Co, but lower concentrations of these elements suggest formation by sedimentary processes or metasomatism (Azim Zadeh 2009; Kuşcu et al. 2017). Magnesite from Quartz Creek shows very low concentrations of Cr, Ni, and Co and some values are below detection limits. Compared to magnesite from most environments, Ba and Sr are low in Quartz Creek magnesite (Fig. 8). Low Sr and Ba concentrations in magnesite are consistent with its formation in a metasomatic environment because dissolution of primary/diagenetic dolomite releases significant amounts of Ca as well as Sr and Ba into fluids, and these elements are unlikely to replace Mg^{2+} in magnesite (Möller 1989; Azim Zadeh 2009).

Rare Earth Elements

The REE are useful indicators of fluid composition and the physio-chemical environment of mineral formation and can be used to identify the origins of carbonate rocks and minerals (Kiesl et al. 1990; Bau and Möller 1992). Rare earth element enrichment in carbonate minerals can occur by interaction with pore waters, from which REE are typically incorporated into the carbonate crystal lattice by substituting for Ca^{2+} and Mg^{2+}. They can also occupy lattice positions which are free due to structural defects and in some cases form separate REE carbonate minerals (Qing and Mountjoy 1994; Bau and Alexander 2006). Whole-rock (carbonate) REE signatures can be overprinted by interaction with fluids and can be difficult to interpret due to the presence of other minerals such as Fe-oxides, clay minerals, quartz and sulphides (Frimmel 2009; Zhang et al. 2014). The whole-rock REE patterns displayed by the Quartz Creek pinolite rocks differ significantly from the North America Shale Composite pattern and have convex-upward shapes with a modest peak at Sm and Eu (Fig. 6A). Previous studies on the formation of dolomite attributed high Sm_N/Yb_N to

Table 5. Mean MgO, CaO and FeO composition of dolomite and magnesite from Quartz Creek and other sparry magnesite deposits.

Deposit		Magnesite			Dolomite		
		MgO	CaO	FeO	MgO	CaO	FeO
Quartz Creek, Canada	Mean	49.38	0.56	1.80	24.88	33.33	0.53
	SD	1.04	0.40	0.62	0.68	0.60	0.05
	n	3	3	3	3	3	3
Rubian, Spain	Mean	47.8	0.41	1.16	22.7	26.6	0.42
	SD	1.4	0.25	0.63	1.8	1.6	0.11
	n	36	36	36	11	11	11
Eugui, Spain	Mean	45.8	0.41	1.82	21.3	30.2	1.04
	SD	1.4	0.26	1.91	1.6	0.5	1.1
	n	78	78	78	77	77	77
Hohentauern/Sunk, Austria	Mean	47.0	0.42	2.0	21.7	29.0	1.48
	SD	0.9	0.42	0.5	1.6	2.9	0.74
	n	17	17	17	6	6	6

Notes: Concentrations in oxide wt.%. SD = standard deviation and n = number of analyses.
Data from Table 2 and Lugli et al. 2000; Kilias et al. 2006; Azim Zadeh et al. 2015.

reducing Fe oxides in pore waters which preferentially take up REE in the middle part of the sequence (Sm to Gd) and release them into carbonates under reducing conditions (Haley et al. 2004; Huang et al. 2009; Navarro-Ciurana et al. 2017; Callen and Herrmann 2019). This suggests that the sedimentary dolomite precursor may have formed under reducing conditions and that later-formed magnesite and chlorite inherited its geochemical signature. The lack of characteristic seawater REE patterns and the similarity between REE profiles of each sample (Fig. 6A) and its constituent minerals (Fig. 6B) suggests that the original rocks reacted with fluids that did not have seawater geochemical signatures.

Evaporite magnesite typically shows very low REE contents. This reflects early removal of the REE from seawater as Ca-rich minerals precipitate prior to magnesite saturation (Möller 1989). Magnesite analyses from Quartz Creek samples have higher REE contents than seawater and thus are unlikely to represent evaporitic magnesite. Seawater-derived carbonate rocks typically exhibit depletion of light REE depletion relative to heavy REE, which is the exact opposite of the pattern show by whole-rock and mineral data from the Quartz Creek samples. The Quartz Creek whole-rock REE trends (Fig. 6A) are more consistent with precipitation from hydrothermal fluids that did not have seawater geochemical signatures (Callen and Herrmann 2019). Magnesite that precipitates directly from hydrothermal fluids tends to be depleted in light REE-because the heavy REE are more easily accepted into the magnesite crystal lattice (Möller 1989; Bau and Möller 1992; Lugli et al. 2000). In contrast, Quartz Creek magnesite displays an overall relative enrichment in the light REE (Fig. 6B).

Europium and/or Ce anomalies are common in carbonates and can be indicative of high-temperature hydrothermal fluids or reducing or oxidizing conditions in aqueous systems (Bau and Möller 1992). Normal seawater-derived carbonate rocks typically display negative Ce anomalies. These features are not present in the whole-rock REE profiles from the Quartz Creek samples, or in REE profiles for individual minerals at Quartz Creek (Fig. 6). The oxidation state of europium (Eu^{3+}/Eu^{2+}) is primarily controlled by temperature, and positive Eu anomalies can be indicative of high-temperature hydrothermal fluids (Frimmel 2009; Meyer et al. 2012; Tostevin et al. 2016). Calculated Eu anomalies (Eu/Eu*) for Quartz Creek magnesite are only weakly positive, but the negative Eu anomalies associated with sedimentary environments are not observed.

Age and Tectonic Implications

Powell et al. (2006) suggested that the magnesite deposits of southeastern British Columbia formed through the influence of Mg-rich brines mobilized by heat and faulting during Cambrian rifting and subsidence. The only stratigraphic constraint on when the pinolite textures at Quartz Creek formed is that they must either be of the same age or younger than their Neoproterozoic host rocks. The stratigraphic ages of sedimentary rocks hosting sparry magnesite deposits in southern British Columbia range from as young as Middle Cambrian (Mount Brussilof; Fritz and Simandl 1993; Marshall et al. 2004) to as old as Mesoproterozoic (Brisco and Driftwood Creek; Simandl and Hancock 1992).

Our Late Ordovician to Early Silurian titanite U–Pb age (433 ± 12 Ma) from Quartz Creek is based on isotopic analyses of many titanite grains, with no obvious textural differences, that are closely associated with pinolitic magnesite crystals and magnesite in micro-veins. We suggest that it provides a reliable estimate for the timing of formation of the pinolite textures, and it indicates that these are much younger than the Neoproterozoic depositional age of the Horsethief Creek Group host rocks. The Tera-Wasserburg concordia plot is interpreted to define a regression line caused by variable amounts of alteration of individual grains, which intersects the concordia curve at ~ 433 Ma. This is consistent with the 442 Ma age implied by the weighted average of $^{238}U/^{206}Pb$ ages (Fig. 7).

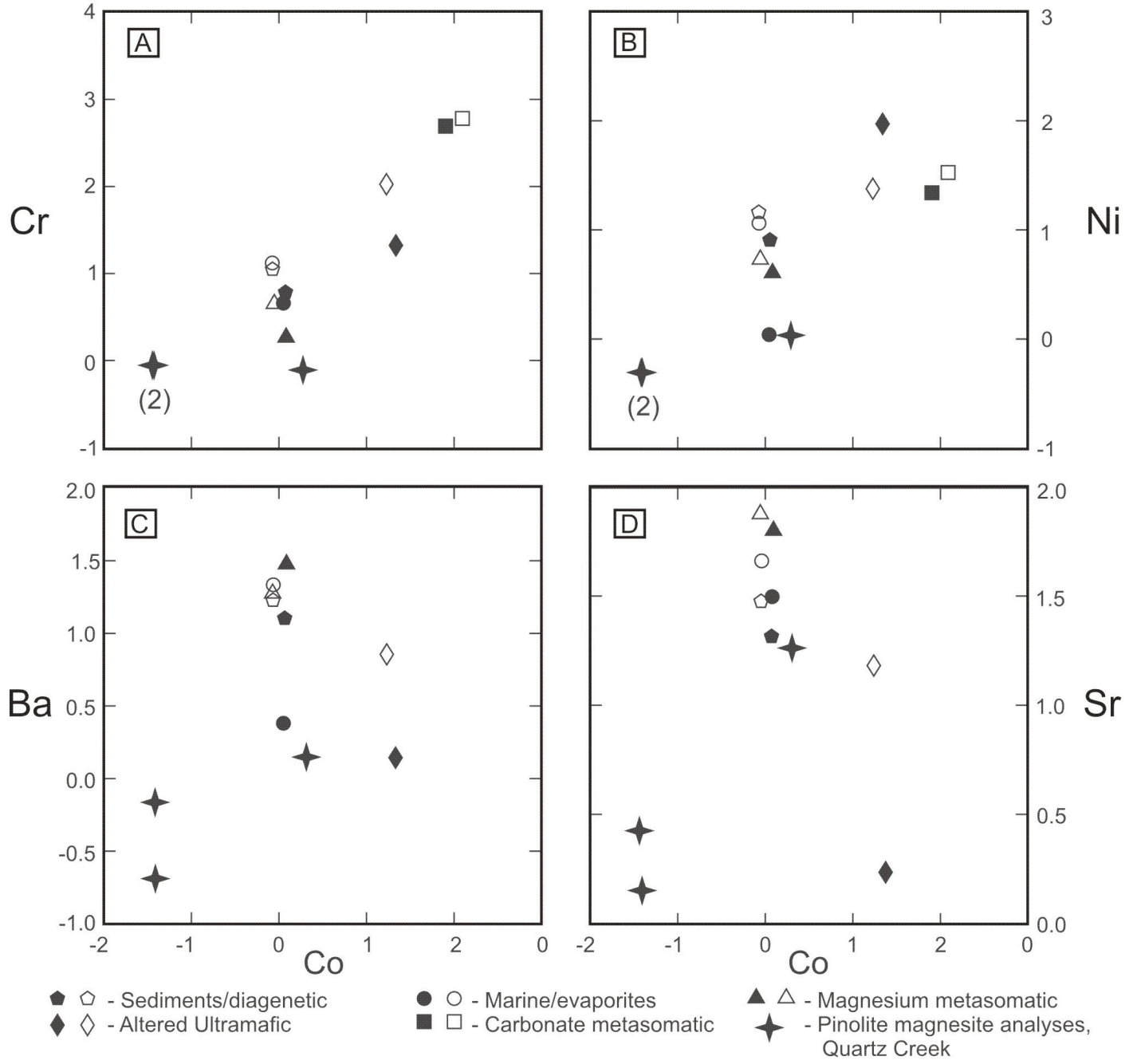

Figure 8. Log_{10} Co versus Log_{10} Ni, Cr, Ba and Sr plots comparing magnesite from the Quartz Creek pinolite rocks with the reported concentrations of these elements in magnesite from various environments. The Quartz Creek magnesite most closely resembles magnesite interpreted to be formed through metasomatic processes. It is also similar to evaporitic/marine magnesite but is distinctly different from magnesite in altered ultramafic and CO_2 metasomatic environments. The comparative data were extracted from element concentration-frequency graphs in Azim Zadeh (2009) that summarized data from Möller (1989). They reflect the most likely concentrations of elements in each environment while de-emphasizing outliers. Note that all Cr analyses and two Ni analyses from Quartz Creek were below the detection limit so comparisons for these elements may be unreliable.

The Late Ordovician to Early Silurian age suggested for the Quartz Creek pinolite locality is consistent with aspects of the regional geology. Cambrian to Late Ordovician mafic volcanic rocks and lithologically similar diatremes occur in a narrow, SE trending, 160 km-long belt that extends through Golden, BC (Pell 1986; Larson and Price 2006). Emplacement of these igneous rocks appears to have been controlled by basement faults defining the margin between the Paleozoic miogeocline to the west and the Laurentian craton to the east (Larson and Price 2006). The faulting, igneous activity and heat associated with these Cambrian to Ordovician tectonic events may have provided conduits, sources, and thermal energy for migrating hydrothermal fluids that formed the pinolite textures at Quartz Creek and perhaps other locations in southeastern British Columbia.

CONCLUSIONS

Distinctive and unusual pinolitic textures developed in carbonate rocks of the Neoproterozoic Horsethief Creek Group near Golden, British Columbia, are interpreted to have formed by metasomatic processes that led to the replacement of primary dolomite by magnesite, in response to the effects of Mg-rich hydrothermal fluids. Textural observations such as broken crystals, and multiple fracturing and growth episodes, support a model where metasomatic fluids moved along fractures and bedding surfaces. Petrographic observations of dolomite microinclusions within magnesite and evidence for recrystallization of dolomite are also consistent with metasomatic replacement. A Late Ordovician to Early Silurian U–Pb age for titanite grains that are intimately associated with magnesite indicates that the development of pinolitic textures occurred long after deposition of the Neoproterozoic host rocks of the Horsethief Creek Group. This age is also younger than the Middle Cambrian sedimentary rocks that host the Mount Brussilof magnesite deposit (Fritz and Simandl 1993; Marshall et al. 2004) and the Mesoproterozoic sedimentary rocks that host the Brisco and Driftwood Creek deposits (Simandl and Hancock 1992). The U–Pb titanite age from Quartz Creek is broadly coeval with fault-related diatremes and volcaniclastic rocks that may also have supplied heat and/or fluids for metasomatic processes.

Geochemical investigations of the Quartz Creek pinolite occurrence are hampered by the small number of analyzed samples, but preliminary data suggest that whole-rock and mineral compositions resemble those of other magnesite deposits that contain pinolitic textures, which have similarly been interpreted to result from metasomatic processes. In particular, REE profiles for samples and minerals from Quartz Creek lack the distinctive Ce and Eu anomalies that are associated with seawater, and REE concentrations are higher than those documented from magnesite of primary evaporitic origin. The similarity of REE profiles for individual minerals such as dolomite and magnesite, and the enrichment of light REE relative to heavy REE, are also consistent with an influence from hydrothermal fluids. It is suggested that systematic geochemical studies of other magnesite deposits, and efforts to obtain their formation ages through dating accessory minerals associated with pinolite, might prove useful avenues for future research on this and related topics.

ACKNOWLEDGEMENTS

Ian Burak and Canadian Pinolite Corporation provided samples and contributed to analytical expenses. D. Wilson took the sculpture photograph. The Department of Earth, Environmental and Geographic Sciences at UBC Okanagan also helped with analytical expenses. Larson acknowledges support from a NSERC Discovery Grant. Polished thin sections were prepared by S. Wood. The Fipke Laboratory for Trace Element Research (FiLTER) and technicians S. Shrestha and M. Button made possible mineral trace element and isotopic analyses. L. Ersay provided advice. R. Corney drafted two diagrams. Comments by an anonymous journal reviewer and J. Conliffe led to substantial improvements to the manuscript. Editor A. Kerr and copy editor S. Amor suggested wording improvements and modifications. Brian Pratt is thanked for his input as the section editor for the series.

REFERENCES

Aharon, P., 1988, A stable-isotope study of magnesites from the Rum Jungle uranium field, Australia: implications for the origin of strata-bound massive magnesites: Chemical Geology, v. 69, p. 127–145, https://doi.org/10.1016/0009-2541(88)90164-7.

Azim Zadeh, A.M., 2009, The genetic model of the Hohentauern/Sunk sparry magnesite deposit (Eastern Alps/Austria): Unpublished PhD thesis, University of Leoben, Leoben, Austria, 182 p.

Azim Zadeh, A.M., Ebner, F., and Jiang, S.-Y., 2015, Mineralogical, geochemical, fluid inclusion and isotope study of Hohentauern/Sunk sparry magnesite deposit (Eastern Alps/Austria): implications for a metasomatic genetic model: Mineralogy and Petrology, v. 109, p. 555–575, https://doi.org/10.1007/s00710-015-0386-2.

Bau, M., and Alexander, B., 2006, Preservation of primary REE patterns without Ce anomaly during dolomitization of Mid-Paleoproterozoic limestone and the potential re-establishment of marine anoxia immediately after the "Great Oxidation Event": South African Journal of Geology, v. 109, p. 81–86, https://doi.org/10.2113/gssajg.109.1-2.81.

Bau, M., and Möller, P., 1992, Rare earth element fractionation in metamorphogenic hydrothermal calcite, magnesite and siderite: Mineralogy and Petrology, v. 45, p. 231–246, https://doi.org/10.1007/BF01163114.

Callen, J.M., and Herrmann, A.D., 2019, In situ geochemistry of middle Ordovician dolomites of the upper Mississippi valley: The Depositional Record, v. 5, p. 4–22, https://doi.org/10.1002/dep2.51.

Frimmel, H.E., 2009, Trace element distribution in Neoproterozoic carbonates as palaeoenvironmental indicator: Chemical Geology, v. 258, p. 338–353, https://doi.org/10.1016/j.chemgeo.2008.10.033.

Fritz, W.H., and Simandl, G.J., 1993, New middle Cambrian fossil and geological data from the Brussilof magnesite mine area, southeastern British Columbia: Geological Survey of Canada, Paper 93-1A, p. 183–190, https://doi.org/10.4095/134205.

Gromet, L.P., Haskin, L.A., Korotev, R.L., and Dymek, R.F., 1984, The "North American shale composite": Its compilation, major and trace element characteristics: Geochimica et Cosmochimica Acta, v. 48, p. 2469–2482, https://doi.org/10.1016/0016-7037(84)90298-9.

Haley, B.A., Klinkhammer, G.P., and McManus, J., 2004, Rare earth elements in pore waters of marine sediments: Geochimica et Cosmochimica Acta, v. 68, p. 1265–1279, https://doi.org/10.1016/j.gca.2003.09.012.

Hancock, K.D., and Simandl, G.J., 1992, Geology of the Marysville Magnesite Deposit, Southeastern British Columbia: British Columbia Ministry of Energy, Mines and Petroleum Resources, Exploration in British Columbia, Part B, p. 71–80.

Hobbs, F.W.C., and Xu, H., 2020, Magnesite formation through temperature and pH cycling as a proxy for lagoon and playa paleoenvironments: Geochimica et Cosmochimica Acta, v. 269, p. 101–116, https://doi.org/10.1016/j.gca.2019.10.014.

Huang, J., Chu, X.L., Chang, H.J., and Feng, L.J., 2009, Trace element and rare earth element of cap carbonate in Ediacaran Doushantuo Formation in Yangtze Gorges: Chinese Science Bulletin, v. 54, p. 3295–3302, https://doi.org/10.1007/s11434-009-0305-1.

Kiesl, W., Koeberl, C., and Körner, W., 1990, Geochemistry of magnesites and dolomites at the Oberdorf/Laming (Austria) deposit and implications for their origin: Geologische Rundschau, v. 79, p. 327–335, https://doi.org/10.1007/BF01830629.

Kilias, S.P., Pozo, M., Bustillo, M., Stamatakis, M.G., and Calvo, J.P., 2006, Origin of the Rubian carbonate-hosted magnesite deposit, Galicia, NW Spain: mineralogical, REE, fluid inclusion and isotope evidence: Mineralium Deposita, v. 41, p. 713–733, https://doi.org/10.1007/s00126-006-0075-5.

Krupenin, M.T., 2005, Geological-geochemical types and REE systematization in deposits of the South Urals magnesite province: Doklady Earth Sciences, v. 405, p. 1253–1256.

Krupenin, M.T., and Ellmies, R., 2001, Genetic features of sparry magnesites in Proterozoic carbonate rocks of the Southern Urals: Ethnographic Praxis in Industry Conference Proceedings, v. 6, p. 997–999.

Kubli, T.E., 1990, Geology of the Dogtooth Range, Northern Purcell Mountains, British Columbia: Unpublished PhD thesis, University of Calgary, Calgary, Canada, 324 p. https://doi.org/10.11575/PRISM/19577.

Kuşcu, M., Cengiz, O., and Kahya, A., 2017, Trace element contents and C-O isotope geochemistry of the different originated magnesite deposits in Lake District (Southwestern Anatolia), Turkey: Arabian Journal of Geosciences, v. 10, 339, https://doi.org/10.1007/s12517-017-3102-1.

Larson, K.P., and Price, R.A., 2006, The southern termination of the Western Main Ranges of the Canadian Rockies, near Fort Steele, British Columbia: stratigraphy, structure, and tectonic implications: Bulletin of Canadian Petroleum Geology, v. 54, p. 37–61, https://doi.org/10.2113/54.1.37.

Lawrence, M.G., Greig, A., Collerson, K.D., and Kamber, B.S., 2006, Rare earth ele-

ment and Yttrium variability in southeast Queensland Waterways: Aquatic Geochemistry, v. 12, p. 39–72, https://doi.org/10.1007/s10498-005-4471-8.

Lugli, S., Torres-Ruiz, J., Garuti, G., and Olmedo, F., 2000, Petrography and geochemistry of the Eugui magnesite deposit (Western Pyrenees, Spain): Evidence for the development of a peculiar zebra banding by dolomite replacement: Economic Geology, v. 95, p. 1775–1791, https://doi.org/10.2113/95.8.1775.

Marshall, D., Simandl, G., and Voormeij, D., 2004, Fluid inclusion evidence for the genesis of the Mount Brussilof magnesite deposit, *in* Simandl, G.J., McMillan, W.J., and Robinson, N.D., *eds.*, Industrial Minerals with Emphasis on Western North America: British Columbia Ministry of Energy and Mines, Geological Survey Paper 2004–2, p. 65–75.

McDonough, W.F., and Sun, S.-s., 1995, The composition of the Earth: Chemical Geology, v. 120, p. 223–253, https://doi.org/10.1016/0009-2541(94)00140-4.

Meyer, E.E., Quicksall, A.N., Landis, J.D., Link, P.K., and Bostick, B.C., 2012, Trace and rare earth elemental investigation of a Sturtian cap-carbonate, Pocatello, Idaho: Evidence for ocean redox conditions before and during carbonate deposition: Precambrian Research, v. 192–195, p. 89–106, https://doi.org/10.1016/j.precamres.2011.09.015.

Möller, P., 1989, Minor and trace elements in magnesite monograph series on mineral deposits: Gebrüder Borntrager, Berlin-Stutgart, v. 28, p. 173–195.

Navarro-Ciurana, D., Cardellach, E., Galindo, C., Fuenlabrada, J.M., Griera, A., Gómez-Gras, D., Vindel, E., and Corbella, M., 2017, REE and Sm–Nd clues of high temperature fluid rock interaction in the Riópar dolomitization (SE Spain): Procedia Earth and Planetary Science, v. 17, p. 448–451, https://doi.org/10.1016/j.proeps.2016.12.113.

Nesbitt, B. E., and Prochaska, W., 1998, Solute chemistry of inclusion fluids from sparry dolomites and magnesites in Middle Cambrian carbonate rocks of the southern Canadian Rocky Mountains: Canadian Journal of Earth Sciences, v. 35, p. 546–555, https://doi.org/10.1139/e98-006.

Paradis, S., and Simandl, G.J., 2018, Are there genetic links between carbonate-hosted barite-zinc-lead sulphide deposits and magnesite mineralization in southeast British Columbia?, *in* Rogers, N., *ed.,* Targeted Geoscience Initiative: 2017 Report of Activities, Volume 1, Geological Survey of Canada Open File 8358, p. 217–227, https://doi.org/10.4095/306478.

Pearce, N.J.G., Perkins, W.T., Westgate, J.A., Gorton, M.P., Jackson, S.E., Neal, C.R., and Chenery, S.P., 1997, A compilation of new and published major and trace element data for NIST SRM 610 and NIST SRM 612 glass reference materials: Geostandards Newsletter, v. 21, p. 115–144, https://doi.org/10.1111/j.1751-908X.1997.tb00538.x.

Pell, J., 1986, Diatreme breccias in British Columbia: Geological Fieldwork 1985, British Columbia Ministry of Energy, Mines and Petroleum Resources, Paper 1986-1, p. 243–253.

Pohl, W., 1989, Comparative geology of magnesite deposits and occurrences: Monograph Series on Mineral Deposits, v. 28, p. 1–13.

Pohl, W., 1990, Genesis of magnesite deposits - models and trends: Geologische Rundschau, v. 79, p. 291–299, https://doi.org/10.1007/BF01830626.

Pohl, W., 2011, Economic Geology: Principles and Practice: Wiley-Blackwell, 678 p., https://doi.org/10.1002/9781444394870.

Pohl, W., and Siegl, W., 1986, Sediment hosted magnesite deposits, *in* Wolf, K.H., *ed.,* Handbook of Stratabound and Stratiform ore deposits: Elsevier, v. 14, p. 223–260.

Poulton, T.P., 1973, Upper Proterozoic 'Limestone Unit', Northern Dogtooth Mountains, British Columbia: Canadian Journal of Earth Sciences, v. 10, p. 292–305, https://doi.org/10.1139/e73-026.

Poulton, T.P., and Simony, P.S., 1980, Stratigraphy, sedimentology, and regional correlation of the Horsethief Creek Group (Hadrynian, Late Precambrian) in the northern Purcell and Selkirk Mountains, British Columbia: Canadian Journal of Earth Sciences, v. 17, p. 1708–1724, https://doi.org/10.1139/e80-179.

Powell, R., Green, E.C.R., Marillo Sialer, E., and Woodhead, J., 2020, Robust isochron calculation: Geochronology, v. 2, p. 325–342, https://doi.org/10.5194/gchron-2-325-2020.

Powell, W.G., Johnston, P.A., Collom, C.J., and Johnston, K.J., 2006, Middle Cambrian brine seeps on the Kicking Horse Rim and their relationship to talc and magnesite mineralization and associated dolomitization, British Columbia, Canada: Economic Geology, v. 101, p. 431–451, https://doi.org/10.2113/ gsecongeo.101.2.431.

Prochaska, W., 2016, Genetic concepts on the formation of the Austrian magnesite and siderite mineralizations in the Eastern Alps of Austria: Geologia Croatica, v. 69, p. 31–38, https://doi.org/10.4154/GC.2016.03.

Qing, H., and Mountjoy, E.W., 1994, Formation of coarsely crystalline, hydrothermal dolomite reservoirs in the Presqu'ile Barrier, Western Canada Sedimentary Basin: AAPG Bulletin, v. 78, p. 55–77, https://doi.org/10.1306/BDFF9014-1718-11D7-8645000102C1865D.

Redlich, K.A., 1909, Die Typen der Magnesitlagerstätten: Zeitschr. f. prakt. Geologie, v. 17, p. 300–310.

Schroll, E., 2002, Genesis of magnesite deposits in the view of isotope geochemistry: Boletim Paranaense de Geociências, v. 50, p. 59–68, https://doi.org/10.5380/geo.v50i0.4158.

Simandl, G.J., 2002, The chemical characteristics and development potential of magnesite deposits in BC, *in* Scott, P.W., and Bristow, C.M., *eds.*, Industrial Minerals and Extractive Industry Geology: Geological Society of London, p. 169–178.

Simandl, G.J., and Hancock, K.D., 1991, Geology of the Mount Brussilof magnesite deposit, southeastern British Columbia, *in* Geological Fieldwork 1990, British Columbia Ministry of Energy, Mines and Petroleum Resources, Paper 1991-1, p. 269–278.

Simandl, G.J., and Hancock, K.D., 1992, Geology of the Dolomite-hosted Magnesite Deposits of Brisco and Driftwood Creek areas, British Columbia, *in* Geological Fieldwork 1991, British Columbia Ministry of Mines and Petroleum Resources, Paper 1992-1, p. 461–478.

Simandl, G.J., and Hancock, K., 1999, Sparry magnesite, *in* Selected mineral deposit profiles, volume 3 - industrial minerals and gemstones: British Columbia Ministry of Energy and Mines, British Columbia Geological Survey Open File 1999-10, p. 39–41.

Simandl, G.J., Hancock, K.D., Fournier, M.A., Koyanagi, V.M., Vilkos, V., Lett, R.E., and Colbourne, C., 1992, Geology and major element geochemistry of the Mount Brussilof magnesite area, Southeastern British Columbia (082J/ 12, 13): British Columbia Ministry of Energy, Mines and Petroleum Resources, Mineral Resources Division, Geological Survey Branch, Open File 1992-14, p. 1–14 plus map.

Stacey, J.S., and Kramers, J.D., 1975, Approximation of terrestrial lead isotope evolution by a two-stage model: Earth and Planetary Science Letters, v. 26, p. 207–221, https://doi.org/10.1016/0012-821X(75)90088-6.

Tostevin, R., Shields, G.A., Tarbuck, G.M., He, T., Clarkson, M.O., and Wood, R.A., 2016, Effective use of cerium anomalies as a redox proxy in carbonate-dominated marine settings: Chemical Geology, v. 438, p. 146–162, https://doi.org/10.1016/j.chemgeo.2016.06.027.

Wheeler, J.O., and Fox, P.E., 1962, Geology, Rogers Pass, Golden, West Half, British Columbia – Alberta: Geological Survey of Canada Map 43-1962, 1 Sheet, https://doi.org/10.4095/108810.

Zhang, W., Guan, P., Jian, X., Feng, F., and Zou, C., 2014, *In situ* geochemistry of Lower Paleozoic dolomites in the northwestern Tarim basin: Implications for the nature, origin, and evolution of diagenetic fluids: Geochemistry, Geophysics, Geosystems, v. 15, p. 2744–2764, https://doi.org/10.1002/2013GC005194.

Received February 2021
Accepted as revised September 2021

For access to the Littlejohn-Regular et al. (2021) Supplementary Material: *Appendix A: Detailed Analytical Methods*, please visit the GAC's open source GC Data Repository for the Heritage Stone Series: at: https://gac.ca/gc-data-repository/.

SERIES

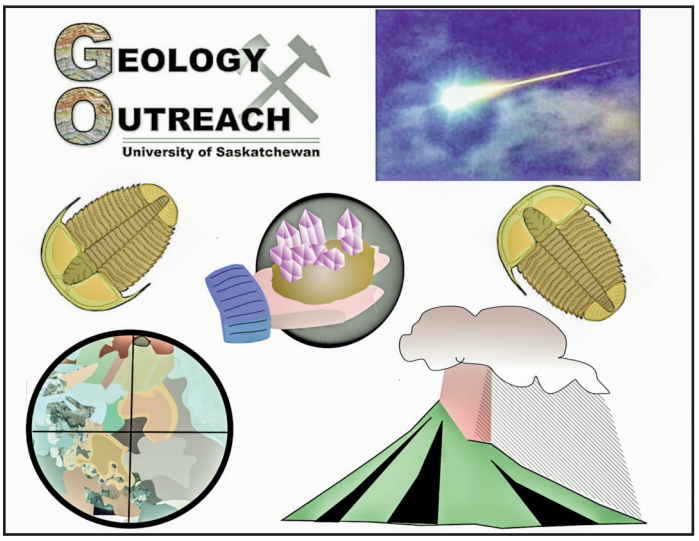

Earth Science Education 6. Lessons Learned: Organizing a Geoscience Outreach Program at the University of Saskatchewan

Courtney Onstad

Department of Earth Sciences, Simon Fraser University
8888 University Drive, Burnaby, British Columbia
V5A 1S6, Canada
E-mail: courtney_onstad@sfu.ca

SUMMARY

Geology Outreach at the University of Saskatchewan was initiated during the 2018/19 academic year as a free and informal education opportunity for K–12 educators and their students in Saskatchewan. The program was 100% volunteer-run by undergraduate and graduate students in the Department of Geological Sciences at the University of Saskatchewan. We estimate reaching more than 1000 students in Saskatoon and surrounding areas following two years of outreach offerings. Hands-on activities offered included 'Rocks and Minerals', 'Fossils', 'Meteorite Impacts' and 'Volcanoes' and also involved a tour of the Museum of Natural Sciences when completed on campus. The overall intent of these activities was to foster excitement about the Earth Sciences. Typically, Educators who booked our program taught grades 4–7, where the Earth Sciences are strongly represented in Saskatchewan's science curriculum. Most outreach offerings occurred on the University of Saskatchewan campus, but some were offered remotely at elementary schools and various Girl Guides of Canada events. During the 2019/20 academic year, we booked every outreach event planned for that year within two days and had a waiting list of more than 30 teachers across the province. The demand for geoscience outreach in Saskatchewan is high, and we hope to continue providing engaging, relevant, and fun educational outreach opportunities. University departments across Canada should allocate funds for community and school outreach initiatives and hire science communicators to oversee programs such as this.

RÉSUMÉ

Le programme « Geology Outreach » de l'Université de la Saskatchewan a débuté au cours de l'année universitaire 2018/19 en tant qu'opportunité d'éducation gratuite et informelle pour les éducateurs de la maternelle à la 12e année et leurs étudiants en Saskatchewan. Le programme était géré à 100% par des étudiants bénévoles de premier cycle et des cycles supérieurs du Département des sciences géologiques de l'Université de la Saskatchewan. Nous estimons atteindre plus de 1 000 étudiants à Saskatoon et dans les régions voisines après deux années d'offres de sensibilisation. Les sujets des activités pratiques proposées comprenaient « Roches et minéraux », « Fossiles », « Impacts de météorites » et « Volcans », et impliquaient également une visite du Musée des sciences naturelles quand les activités étaient proposées sur le campus. L'objectif général de ces activités était de susciter de l'enthousiasme pour les sciences de la Terre. En règle générale, les éducateurs qui ont fait la demande de notre programme enseignaient aux élèves de la 4e à la 7e année, où les sciences de la Terre sont fortement représentées dans le programme des sciences de la Saskatchewan. La plupart des activités de sensibilisation ont eu lieu sur le campus de l'Université de la Saskatchewan, mais certaines ont été offertes à distance dans les écoles élémentaires et lors de divers événements des Guides du Canada. Au cours de l'année scolaire 2019/20, toutes les offres de sensibilisation pour cette année ont été réservées en deux jours et nous avions une liste d'attente de plus de 30 enseignants à travers la province. La demande de sensibilisation géoscientifique en Saskatchewan est élevée, et nous espérons continuer à offrir des opportunités de sensibilisation

Geoscience Canada, v. 48, https://doi.org/10.12789/geocanj.2021.48.178 pages 133–139

éducative engageantes, pertinentes et amusantes. Les départements universitaires à travers le Canada devraient allouer des fonds aux initiatives de sensibilisation communautaire et scolaire et embaucher des communicateurs scientifiques pour superviser des programmes comme celui-ci.

Traduit par la Traductrice

INTRODUCTION

In Saskatchewan's science curriculum, the Earth Sciences are well represented in grades 1 through 10 (Government of Saskatchewan 2021). Unfortunately, Earth Science topics are often skipped over or taught primarily from worksheets and textbooks. Classrooms may not have access to resources and materials to demonstrate Earth Science processes or concepts effectively, and many teachers do not have a background in Earth Sciences. Thus, creating additional geoscience-related educational resources for educators is a practical approach to supplement classroom learning.

During a summer job with the University of Saskatchewan (U of S), through the College of Arts and Science's "Science Ambassador Program", I was assigned to the small northern community of Île-à-la-Crosse, Saskatchewan. While working in this community, I had the opportunity to give presentations and design hands-on experiments for K–12 students focusing on the Earth Sciences. These lessons included volcanology, rocks and minerals, fossils, erosional features, plate tectonics and earthquakes. There were also outdoor field activities where we explored local boulders featuring volcanic and plutonic rocks from the Precambrian shield. The students' amazement that ~ 1.8 billion years ago they would have been standing amongst volcanoes stuck with me and initiated my desire to start a formal outreach program at the University of Saskatchewan.

At the time, I was a graduate student in the Department of Geological Sciences at the University of Saskatchewan. I was well aware of the educational resources available within the department. Common to all university Earth Science departments, U of S has an excellent collection of rocks, minerals, and fossils from across the world. The U of S Museum of Natural Sciences provided a perfect opportunity for guided tours of the various displays, exhibits, and informative signage. Diverse rock and mineral samples, a space for activities and/or tours, expertise on the material, and students' willingness to help were necessary factors to initiate the outreach program. This paper reviews the initial planning, the outreach offerings, and the feedback received. It then takes a closer look at the lessons learned, benefits to those involved, and makes suggestions for future outreach initiatives.

INITIAL PLANNING

Points to Consider

Before initiating the outreach program, extensive planning was necessary to ensure that students and teachers had an enjoyable, organized, and meaningful experience. Some of the details addressed in planning include:

1. Funding to acquire supplies for hands-on experiments.
2. Personnel to present, answer questions, set up materials and clean up after a session (typically 2–4 people).
3. Determine the most effective approaches for communicating with students.
4. Develop content that would align hands-on activities with the 'Earth and Space Science' component of Saskatchewan's K–9 science curriculum
5. Ensure appropriate media platforms for communication with educators and a space to organize materials after booking an event.

Funding

The financial support received by the Canadian Geological Foundation (2021), TakingITGlobal (2021), and the U of S Department of Geological Sciences enabled this outreach program's success. The funding was used to have eight microscope transport cases made (Fig. 1) and to purchase supplies for hands-on activities. In-kind funding from the Department of Geological Sciences allowed for use of the departmental truck and coverage of operating expenses for outreach trips to schools and communities that could not travel to the U of S.

Modes for Communicating

Various methods have been proposed for communicating in outreach settings including the three prominent models for science communication (deficit, dialogue, and participation models; Metcalfe 2019). Among many issues (e.g. it assumes supremacy of western knowledge) the deficit model utilizes a one-way, top-down transmission of information from the presenter (expert) to the audience (layperson). This assumes that by audiences gaining more knowledge, they will inevitably have a positive attitude towards the topic (Reincke et al. 2020). The dialogue model is a form of two-way communication involving a transfer of information between presenter and layperson and vice-versa. It builds on mutual respect, encourages listening and learning, with the audience as a helpful resource and the expert as the facilitator (Reincke et al. 2020). Lastly, the par-

Figure 1. Transport cases for petrographic microscopes used for remote outreach activities.

ticipation model uses multidirectional communication through engagement rather than the transmission of information. Audiences take on an active role and are considered co-creators alongside the expert (Metcalfe 2019).

Considering this outreach offering was solely organized and run by volunteers with no formal science communication training, there was no knowledge on the various approaches for communication. Thus, no specific communication goals were established early on; key for effective science communication. Nevertheless, through trial and error during the first year, it was noted that the dialogue model in combination with the deficit model was best-suited to our situation.

Volunteers

An information session (with free pizza) was hosted to gauge initial interest in the outreach program and recruit volunteers. This event gave students a sense of the activities to be taught, how participating would advance their science communication skills, and the significant experiential opportunities they would be providing for youth and teachers attending. As a result, there were 18 and 19 graduate and undergraduate student volunteers during the first and second years, respectively. Students had a range of roles during the events, including presenting, answering students' questions, running tours through the museum, and setting up and removing materials.

Designing and Organizing Hands-On Activities

Activities were designed using existing lessons and activity ideas. Developing relationships with others working in the geoscience education space was influential in developing new outreach activities. Online educational resources from organizations such as Mining Matters, the Saskatchewan Mining Association, and *Impact Earth* from Western University were also used. There were opportunities for student volunteers to express ideas and create lessons as well.

Promotion and Booking

A landing page for the outreach program was added to the department website with information regarding what would be expected during an outreach event. The website linked to a SurveyMonkey® form where interested teachers could indicate what activity topics they wanted, the preferred dates, provide some details about their class, and establish contact information.

A Facebook page and a Twitter account were also created to spread awareness and update the community about our outreach program. Initially, targeted Facebook advertisements were used to spread the word about our program through the Saskatchewan education community. This approach proved very effective and resulted in all outreach sessions for the entire school year becoming booked in two days (more than 20 sessions). More than 30 teachers remained interested in participation after all slots were filled and they were added to a waiting list. This demand demonstrates how sought-after geoscience outreach activities are in Saskatchewan.

OUTREACH PROGRAMMING

Hands-on Activities

Rock and Mineral Lesson: This lesson involved a 10 to 20-minute presentation (approximately) with accompanying hands-on activities. The first component focused on minerals, with each slide discussing a specific mineral property (e.g. colour, lustre, hardness) used for identification. Minerals were pre-organized in groups to specifically bring students' attention to the property being discussed. For example, after presenting the slide on specific gravity, we passed out galena (heavy) and talc (light) samples together to show the notable difference.

Following this activity, we looked at minerals under a microscope. Before starting, to ensure that the students handled the microscopes carefully, presenters told students that each microscope was worth $1,000,000; this exaggeration was justified in emphasizing that students should use extra caution! This was the student's first time seeing rocks under a microscope (Fig. 2), so no advanced observations were made. Instead, a volunteer switched between cross-polarized and plane-polarized light and sometimes inserted the gypsum plate, to get students' attention!

Figure 2. Homeschool student observing minerals under a petrographic microscope.

https://doi.org/10.12789/geocanj.2021.48.178

Next, we discussed rocks and introduced the three rock types, how they formed, and how to identify them. Similar to the mineral activity, groups of rocks were distributed to students. Each group of rocks would have a sedimentary, metamorphic, intrusive, and extrusive rock. Students worked together to identify the rocks, while volunteers worked with groups to discuss their observations.

A 'mineral matching' activity from Mining Matters was excellent for getting students thinking about the importance of minerals in their everyday lives. First, students were organized into groups, each with ten mineral cards (describing the properties of a specific mineral), ten corresponding mineral samples, and ten objects that these minerals are used to make. Then, students worked together to match each mineral to the item that the mineral is used to produce.

Fossil Lesson: This lesson started with a 10-minute presentation about fossils and dinosaurs. The hands-on component involved analyzing fossils from the department's collection and included a station where students could look at fossils in 3D. Students used a camera to scan fossil cards using an iPad app, "WyoFossil", created at the University of Wyoming Geological Museum (2021). A 3D image was produced of what that fossil or animal would have looked like in real life. While this activity was in progress, two volunteers would be preparing the 'fossil dig' activity. Small plastic bowls (~ 12 cm diameter) were half-filled with sand. One volunteer would make the cast mix, which used Plaster of Paris and water. A sand-filled plastic bowl and plastic fossil molds (purchased online) were provided, and students pressed their mold into the sand, creating a compression. With volunteers' assistance, students poured the Plaster of Paris mixture into their bowls to set.

While the fossil casts dried, the lesson was broken up with a museum tour (discussed below). While students were on the tour, volunteers flipped the fossil casts onto newspaper with the sand now covering the top of the casts. When students returned, they were given a toothbrush and dental pick to carefully remove excess sand until they could extract their fossil (Fig. 3). Students were thrilled and even got to take their fossils home to show their parents!

Meteorite Impact Lesson: Students were given a quick (~ 5 min) presentation on meteorites and meteorite impacts. Dr. Mel Stauffer kindly loaned meteorite specimens from his collection to use for the outreach program, including iron meteorites (the Toluca, Campo del Cielo, and Canyon Diablo meteorites) and a stone meteorite. These samples were carefully passed around under supervision by volunteers for 5–10 minutes. While samples were passed around, one volunteer set up the hands-on experiment, which demonstrates how a meteorite impact occurs. The volunteer used a clear plastic container and poured a layer of flour (~ 3 cm thick), and sifted a thin layer of cocoa powder (~ 2 cm thick) on top. Next, a student volunteer was asked to throw a small rubber ball at the cocoa powder in the container creating an impact crater (Fig. 4a). Students used their observational skills to draw the crater's shape and discussed what factors could change it. Finally, a new volunteer threw the ball with a change in the angle, height, or speed (Fig. 4b).

Figure 3. Students carefully using toothbrushes to uncover their fossil casts.

Volcanoes Lesson: This lesson included a ~ 10-minute presentation on the types of volcanoes and volcanic eruptions, combined with a hands-on component analyzing volcanic and intrusive rock samples. Students then went outside to an area where a volunteer had a small pile of ammonium dichromate on tinfoil. Students were asked to keep a 2-metre distance from the 'volcano' for safety reasons. The ammonium dichromate was lit with a match, and students watched as the exothermic reaction simulated a volcanic eruption and a cinder cone formation. The final component of this lesson involved 3 hours of preparation, with a volunteer making a bowl of gelatin. Once the gelatin was set (in a volcano shape), it was transferred on a pegboard, elevated by two bricks. A magma solution was created from red food colouring and water and was added to a syringe. A volunteer then injected 'magma' into the gelatin volcano by inserting the syringe upwards through a hole in the pegboard.

Museum Tour: The museum tour was often referred to as the highlight of a student's trip to the University. This success is attributed to volunteers' tremendous science communication skills, especially Drake Meili (aka Drake the Geologist), Simran Kharal, and Iliajah Pidskalny. Drake typically started the tour by asking students a question about something they'd learned that day. Whoever answered correctly became Drake's 'Assistant Geologist' for the day and involved wearing his prospector hat (Fig. 5) for the rest of the tour. During the tour, students saw the pristine mineral specimens and rock samples in display cases, the animals in the museum (Fig. 6), and the fossils in the Tyndall stone walls.

At the end of each of the above lessons, students were given a 'Certified Junior Geologist', 'Certified Junior Paleontologist', 'Certified Junior Meteorite Expert', or 'Certified Junior Volcanologist' button (Fig. 7) to take home with them!

A Typical Outreach Day

On the day of an outreach event, this was the typical sequence of events before, during, and after students arrived. The setup was relatively straightforward if the event was taking place on

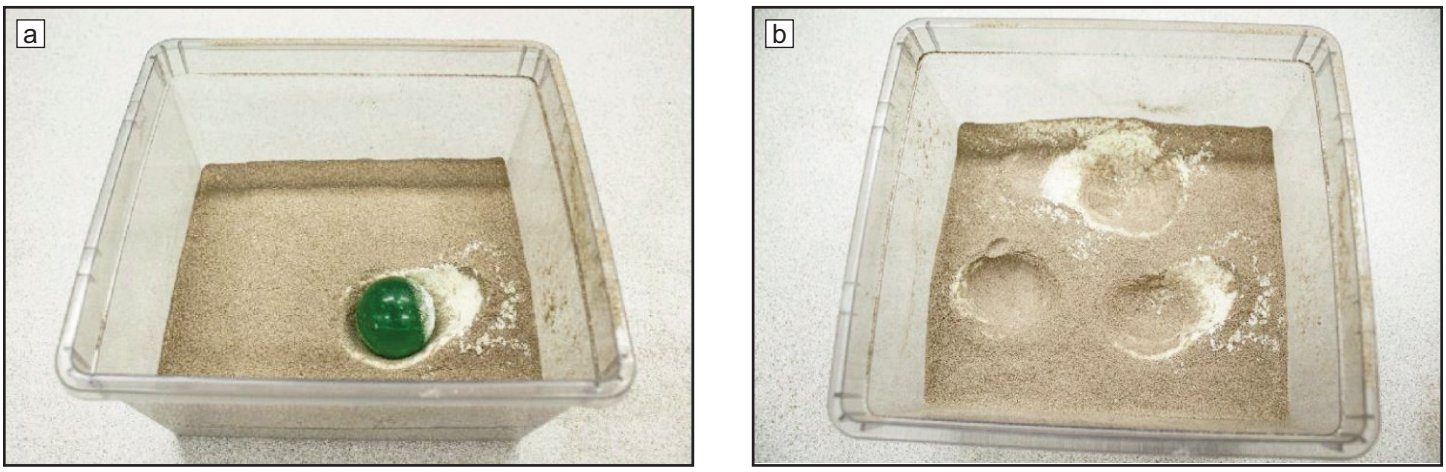

Figure 4. Meteorite impact structure(s) resulting from a rubber ball toss (a) and tosses thrown from varying angles and velocities (b).

Figure 5. Geology Outreach University of Saskatchewan volunteer Drake Meili (Drake the Geologist) in his outreach attire.

Figure 6. Drake Meili leading the museum tour for Grade 5 students in the Museum of Natural Sciences at the University of Saskatchewan.

campus as the classroom already had rock, mineral, and fossil samples organized from a previous session. Thirty minutes before the event, volunteers arrived to set up the equipment and materials needed and ensured that all technology worked. Once the class arrived, we completed one or two of the lessons described above, typically over two hours. When the class left, volunteers assisted with clean-up and ensured that all samples were organized to be ready for the next event. Typical post-outreach tasks involved compiling survey results following the event, returning supplies to storage, and making social media posts to promote the event.

When we were asked to travel to a school during an off-campus trip, more organization before the event was required. Volunteers typically arrived one to two hours ahead of time to gather all materials needed for the hands-on activities, loaded microscopes into transport cases, organized worksheets, and loaded everything into the U of S departmental truck. Typically, two or three volunteers led these off-campus events. Upon arriving at the school, volunteers checked in at the front office and were directed to a classroom. Because the supplies were previously organized at the University, minimal setup was needed. After completing the activities, volunteers packed up, brought the supplies back to the University campus, and returned them to storage.

Feedback from Surveys

To determine the effectiveness, enjoyment, and areas for improvement of our outreach activities, we provided post-outreach surveys for a sample of students and teachers. These surveys were done in late March 2020 before the COVID-19 pandemic and included 63 Grade 4 students who completed the

Figure 7. Badges distributed to students who completed our 'Rocks and Minerals', 'Fossils', 'Volcanoes', and 'Meteorite Impact' lessons.

'Rocks and Minerals' activity. Based on their answers, the percentages of students who enjoyed particular components most were as follows: 50% of students enjoyed the museum tour, 30% liked looking at samples under the microscope, 10% enjoyed looking at rock and mineral hand samples, whereas 5% enjoyed the mineral matching activity and 5% couldn't decide and enjoyed everything. When asked what they learned, here are some typical responses:

"It's important to know Earth's history."
"I learned that we need minerals to survive."
"Without rocks, we wouldn't be here, and neither would the university or the tires on our cars."
"I learned that minerals make our world a better world."

When asked if they would recommend the program to colleagues, teachers also noted:

"*Of course, hope to come again!*" and
"*Yes, it was a great way to get students out and learning, and it was a lot of fun.*"

REVIEW AND RECOMMENDATIONS

Lessons Learned

After two years of running *Geology Outreach* at the U of S, lessons learned from the successes and setbacks are summarized below:

1. It worked best with less lecturing and more hands-on activities – Geology is tactile. We should use this to our advantage and promote hands-on learning with discussion, rather than solely lecturing about geological concepts. We found the most success by lecturing in short segments (1-minute maximum) and breaking this up by allowing students to see or touch something.
2. The 'dialogue model' (Reincke et al. 2020) proved to be the most appropriate for presenting in our unique situation (100% volunteer-run; explained in "Modes for Communicating"). This model allows presenters to use a 'conversation style' approach to communicating where volunteers and students can ask one another questions, explain reasonings for proposed answers, and engage in a way that lecturing does not permit.
3. Activities should be no longer than 30 minutes – The idea behind this stems from the cognitive overload theory. That is, students, especially in today's technology-focused society, tend to lose attention after shorter periods, when overloaded with new information (356 Labs 2021). We found that 30 minutes should be the maximum amount of time spent on one activity. Over two hours, we tried to include at least four activities to avoid losing the students' attention.
4. Give them something to bring home – Often, we associate memories with objects. The intent of handing out our 'Junior Certified' pins was that students would attach their pin to their backpack or some other belonging and remember the experience they had with us!
5. Network – Find out what others in Earth science outreach are doing. For example, there are nonprofit organizations in Canada involved in similar ventures (e.g. Mining Matters - https://miningmatters.ca/, MineralsEd - https://mineralsed.ca/, National EdGeo Program - https://www.edgeo.org/). There are also international efforts (e.g. Earth Learning Ideas - https://www.earthlearningidea.com/, SERC Carleton - https://serc.carleton.edu/index.html). All of these organizations and projects have put time and expertise into creating K–12 geoscience lessons. Sharing resources, experience, and expertise is essential to advancing geoscience communication initiatives.
6. Get student volunteers – Many university students are interested in volunteering but may not have ample time to commit to off-campus activities. Having an outreach program at a university becomes convenient for students and gives them a fun break from their academic studies. Not only is it rewarding for volunteers, but it also improves their science communication skills.

7. Create a website and social media page(s) – Nowadays, assume people don't know about you unless you're on the web. We were able to reach many teachers with our Facebook page and a simple $30 Facebook advertisement. Social media is also a great way of keeping followers updated on your offerings, important dates, etc.
8. Provide fewer facts and have more fun – Our intent with outreach was not necessarily for students to remember *all* of the properties of a mineral. If they did, it was a bonus. The main goals were to make sure students had fun and gained interest in the science of the Earth. Making an activity seem fun is especially important as many of the events were aimed at elementary students.
9. Organization is vital – With the sheer number of things to remember during an outreach session, having an organized schedule and checklist was imperative. Supply lists ensured that every material necessary for each lesson was accounted for and located together in one place. A schedule including detailed steps for setup, the activities, and take-down was crucial to ensuring a smooth event. Organized plans also ensured that the program could be run by different people, which supports program flexibility.

Benefits

K–12 students, their teachers as well as undergraduate and graduate volunteers all benefited from this program. K–12 students benefited from seeing mineral, rock, and fossil specimens that they would not usually have access to in their classrooms. They also benefited by learning about geological processes from volunteers who actively learn about such topics in their degree programs. These volunteers may also act as young role models in geoscience to K–12 students. The teachers benefited from this program since this is a free resource that they can use to supplement any classroom teaching they have done on the subject. Lastly, the U of S volunteers greatly benefited from this program as they can keep introductory geology information fresh and learn science communication, organizational, and leadership skills during the program.

Future Opportunities in University Outreach

Moving forward, university departments should set aside designated funding for community outreach initiatives and consider hiring science communicators to run programs like this. Organizing this program typically involved ~ 4–8 hours of volunteer work each week for the outreach coordinator. However, bringing a program to its full potential would easily require a full-time position. By hiring full-time employees with relevant training, departments could expect a research-guided approach to outreach initiatives, potentially resulting in 1) greater public interest of and trust in the geoscience industry; 2) increased enrollment in their geoscience program; and 3) meaningful engagement within local communities. In addition, science communication training would equip undergraduate and graduate students with the skills necessary for engaging with various audiences, including peers within their disciplines. This training has tremendous applications for geoscientists' future endeavors whether in industry, academia, or the public sector. Most importantly, having outreach programs accessible to communities and educators, who may not have the resources or geological background to discuss these subjects thoroughly, is an invaluable resource.

ACKNOWLEDGEMENTS

Many people and organizations made this outreach program so successful. First and foremost, the dedication of U of S undergraduate and graduate student volunteers was tremendous. On top of a busy university schedule of lectures, labs, and research, there were always volunteers to count on for showing up and bringing their best attitudes forward. The Canadian Geological Foundation, TakingITGlobal, Mining Matters, the Museum of Natural Sciences at U of S, and the Department of Geological Sciences at U of S are all thanked for their generous financial and in-kind support. Dave Lovelace from the University of Wisconsin-Madison Geology Museum is thanked for providing fossil casts and directions on making an improved fossil hands-on activity. Erica Bird, Laura Clinton, Terry Johanson, Tim Prokopiuk, and Kevin Ansdell are also thanked for their guidance and support during this program.

REFERENCES

Canadian Geological Foundation, 2021, About [website]. Retrieved from http://www.canadiangeologicalfoundation.org/?page_id=2. [Last accessed: 7/9/2021].

Government of Saskatchewan, 2021, Saskatchewan Curriculum [website]: Government of Saskatchewan Ministry of Education. Retrieved from https://www.edonline.sk.ca/webapps/moe-curriculum-BB5f208b6da4613/. [Last accessed: 8/9/2021].

Metcalfe, J., 2019, Comparing science communication theory with practice: An assessment and critique using Australian data: Public Understanding of Science, v. 28, p. 382–400, https://doi.org/10.1177/0963662518821022.

Reincke, C.M., Bredenoord, A.L., and van Mil, M.H.W., 2020, From deficit to dialogue in science communication: EMBO (European Molecular Biology Organization) Reports, v. 21, e51278, https://doi.org/10.15252/embr.202051278.

TakingITGlobal, 2021, #RisingYouth: community service grants [website]: TakingITGlobal. Retrieved from: https://www.risingyouth.ca/. [Last accessed: 7/9/2021].

356 Labs, 2021, The cognitive load theory and your presentations [blog]: 356 Labs Agency, Sofia, Bulgaria. Retrieved from: https://356labs.com/blog/cognitive-load-theory-presentations/. [Last accessed: 11/22/2021].

University of Wyoming Geological Museum, 2021, WyoFossil Augmented Reality App [website]: University of Wyoming, Laramie, WY. Retrieved from: http://www.uwyo.edu/geomuseum/wyofossil/. [Last accessed: 7/9/2021].

Received August 2021
Accepted as revised November 2021

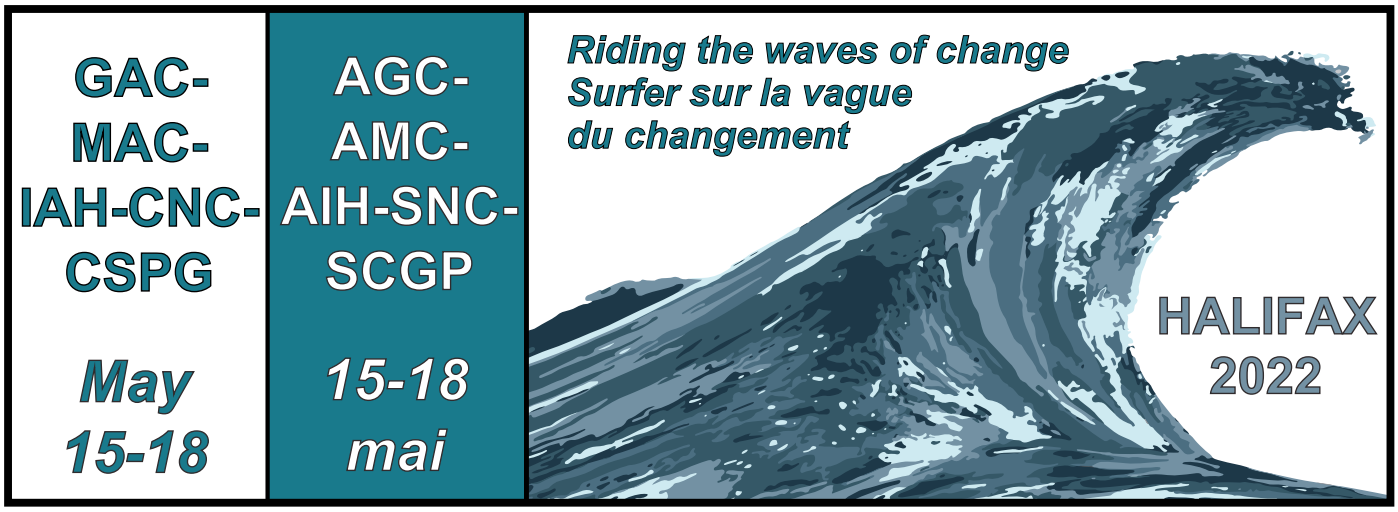

Abstract submission for the Halifax 2022 GAC-MAC-IAH-CNC-CSPG Joint Meeting is now open (December 1, 2021). The conference will be held in Halifax, Nova Scotia from May 15-18, 2022. Halifax 2022 is a joint meeting of the Geological Association of Canada (GAC), the Mineralogical Association of Canada (MAC), the International Association of Hydrogeologists – Canadian National Committee (IAH-CNC), and the Canadian Society of Petroleum Geologists (CSPG). The hosting society is the Atlantic Geoscience Society (AGS). Several other groups will also be providing content and coordinating with Halifax 2022. The overall theme for Halifax 2022 is "Riding the waves of change – Surfer sur la vague du changement", and certainly COVID-19 has made that theme even more appropriate than we anticipated! The conference will consist mainly of oral and poster contributions, arranged in thematic special sessions and symposia as well as in general topical sessions. https://halifax2022.atlanticgeosciencesociety.ca/technical-program/

The schedule will be organized to promote discussion among meeting participants. At this time, we are planning for a mostly in-person conference with the possibility of streaming or recorded access to oral sessions, and both in-person and virtual options for poster presentations. In addition to the 61 symposia, special sessions, and general sessions, there are 11 field trips and 8 short-courses.

Abstracts can be submitted through the conference website. Registration opens on January 1, 2022.
https://halifax2022.atlanticgeosciencesociety.ca/abstract-submissions-and-registration/

Make sure to follow us on Facebook (G A C M A C Halifax), Twitter (@GACMAC2022), and Instagram (gacmac2022).

See you all in Halifax!

A TRIBUTE

Gerard Viner Middleton FRSC: 1931–2021

It is with sadness that we report the recent passing of Gerard V. Middleton, one of the leading pioneers of sedimentology. Gerry, as he was known to his many friends and colleagues, was born in South Africa of English parents, and was educated in England, obtaining his Ph.D. in geology from Imperial College in 1954. For his thesis research, he mapped an area of Devonian rocks in Devon, and one of his earliest papers (1959) is a taxonomic documentation of the tetracorals contained in those rocks. Immediately upon graduation, he emigrated to Canada where he worked first for California Standard Oil Company in Calgary for one year, after which he joined McMaster University, Hamilton, Ontario, in 1955, starting as a Lecturer in Geology. He remained there for his entire professional career. Interestingly, this appointment came on his second application; his first as a paleontologist had been unsuccessful! Perhaps because much of his Ph.D. research involved carbonate rocks, he initially undertook research on the facies and diagenesis of limestones in both Alberta and Ontario, spending summers working for Shell Oil where he met many of the leading carbonate researchers of the day. However, he found the local limestones "boring", and switched his attention to sandstones. His first work on them was petrographic and geochemical in focus and involved some of the earliest work in sedimentary geology to use advanced statistical techniques, an interest that continued to the end of his career.

Because he appreciated that a deeper understanding of the origin of sandstones would require knowledge of the physical processes responsible for transporting and depositing sediment, Gerry educated himself in fluid mechanics through reading the civil engineering literature. In 1964, he organized a research symposium at the AAPG meeting in Toronto, the papers from which were published as SEPM Special Publication 12 "*Primary Sedimentary Structures and Their Hydrodynamic Interpretation*", which he edited. This presented the now classic flow-regime concept to geologists and popularized the series of bedforms that develop as current speed increases. This volume can be credited with introducing fluid mechanics into sedimentology, something that has become central to an enormous body of subsequent research.

One of the particularly hot topics of the time (late 1950s and 1960s) was the "greywacke/flysch problem", namely the origin of the ubiquitous graded beds that occurred in what were widely thought to be deep-water deposits. Early work by Keunen and others had raised the possibility that they were emplaced by turbidity currents, a process that was then poorly understood. Using his extensive network of connections, Gerry arranged to undertake a series of experiments on density currents at Caltech that formed the basis of the classic series of papers published in 1966–1967, that, together with a 1965 paper on antidune structures and a follow-up paper on "flysch sedimentation" in 1970, represents the foundation of nearly all modern work on turbidity currents! In 1973 and again in 1976, together with Monty Hampton, he expanded on this earlier work and published a more comprehensive process-based classification of sediment gravity flows that remains the basis for most interpretations of the origin of deep-water deposits. Var-

Geoscience Canada, v. 48, https://doi.org/10.12789/geocanj.2021.48.179 pages 141–143

ious additional studies with students, commonly but not exclusively based in the Gaspésie region of Quebec, added soundly-based outcrop interpretations to the repertoire of examples that have been extensively used by workers over the years. Gerry published his final synthesis paper on deposition from turbidity currents in 1993. In addition to this primary focus of his research, Gerry also contributed to important papers on such diverse topics as the origin of upper-flow-regime parallel lamination, the interpretation of grain-size distributions in sand, and tidal sedimentation in the Bay of Fundy. Later in life, he turned his attention to topics in the history of geology, and to the origin of the various building stones used in construction in and around Hamilton in the 19th century.

Education in various forms was central to Gerry's character and contribution to the sedimentological community. As he himself said, he was always "… *trying to put in order (in my mind) an area of scientific knowledge* …": he had a passion for synthesizing information and passing that knowledge to others, something that may have arisen because most of his own knowledge in clastic sedimentology was self-taught. Most notable was the general textbook "*Origin of Sedimentary Rocks*", coauthored with Harvey Blatt and Raymond Murray, which appeared in 1972, with a second edition in 1980. This was the first comprehensive textbook to take a rigorous process-based approach to sedimentary geology, rather than the descriptive, petrographic approach that prevailed in previous textbooks. Gerry was also the lead author, with John Southard, of the highly influential SEPM Short Course Notes "*Mechanics of Sediment Movement*" (1977, 1984) that introduced many clastic sedimentologists to the intricacies of fluid mechanics. This was preceded by the first-ever SEPM Short Course that he organized with Arnold Bouma "*Turbidites and Deep Water Sedimentation*" (1973), followed by short courses on the application of fluid and solid mechanics in the whole of geology, the notes from which became the textbook "*Mechanics in the Earth and Environmental Sciences*" (1994), cowritten with Peter Wilcock. Middleton also returned to his love of statistical methods near the end of his career, organizing short courses on "*Nonlinear Dynamics, Chaos and Fractals with Applications to Geological Sciences*" (GAC 1991), and "*Nonlinear Dynamics and Fractals: New Numerical Techniques for Sedimentary Data*" (SEPM 1995), given with Roy Plotnick and David Rubin, and writing the book "*Data Analysis in the Earth Sciences Using MATLAB*" (2000). Indeed, he was fearless in his choice of research topics, taking risks on novel subjects and tackling a wider range of topics than most other workers then or now, making him an ideal person to edit the comprehensive *Encyclopedia of Sediments and Sedimentary Rocks* (2003). In addition to all of this, Gerry was also the behind-the-scenes instigator of the widely popular text "*Facies Models*" edited by his long-time colleague and foil, Roger Walker, commissioning the initial series of articles for the Geological Association of Canada's journal *Geoscience Canada*, which he founded, serving as the inaugural editor. Furthermore, he had a knack for passing his love of education and scholarship to his graduate students, of whom 6 of 13 Ph.D. students went on to university academic careers themselves, expanding Gerry's legacy enormously.

Gerry's involvement in geological and sedimentological societies was a life-long passion. He drew inspiration from the colleagues that he interacted with at meetings, and he instilled this passion in his students as well. He was Vice-President and President of the Geological Association of Canada (1986–1988); a Council Member of the International Association of Sedimentologists for many years and Vice-President from 1978–1982, and he held positions on many SEPM committees. He once boasted that he was the only person to ever run for office in SEPM three times, and to be defeated each time. All of these societies and others have recognized his immense contributions: he was inducted into the Royal Society of Canada in 1970; he is one of only five people to be named an Honorary Member of both the International Association of Sedimentologists (IAS) and SEPM, as well as of the Canadian Society of Petroleum Geologists (CSPG); he has received the highest award given by both the Geological Association of Canada (GAC—the 1980 Logan Medal) and SEPM, which awarded him both the Pettijohn Medal (1994) and Twenhofel Medal (2003). The Geological Society of London also awarded him the Major John A'Deane Coke Medal in 1995. In many ways, given all of the books and sets of notes that he coauthored, the most relevant honour was the Grover E. Murray Memorial Distinguished Educator Award that he received from the American Association of Petroleum Geologists (AAPG; 1998). The Canadian Sedimentology Research Group (CSPG) also named its sole award in Gerry's name.

Gerry, the person, was gregarious and thoroughly enjoyed his interactions with colleagues. As he himself said, "*I was always interested in acting, from early highschool days, and elecution (sic), debating, etc. I take after my father too, in liking to talk!*". He had a "presence" that caused people to pay attention to what he was saying, no matter what other conversations might have been going on. His critical ability and insight were second to none. Harold Reading, another notable pioneer in the field, once said that Gerry's greatest qualities were "… *your wisdom and your ability to see to the heart of a question, to analyse it and come up with an answer. You express your thoughts truthfully and sometimes with bluntness. … You once said to me I am only rude to my friends and to those whom I respect.*" Gerry was, despite his great accomplishments, a humble man, saying that "… *contacts with my contemporaries (e.g., John Ramsay, who was a fellow student at Imperial) had convinced me that my abilities in geological research were modest*". He thought of himself as a scholar rather than a researcher. He also had a dry, self-deprecating humour, as is indicated by some of the comments quoted above, and he liked good food and wine. An anecdote that we remember from our early days as graduate students, involved Middleton telling his students, in all seriousness, while driving between outcrops after a particularly terrible meal at a nameless restaurant, about his "Rolaids Scale" for restaurants, Rolaids® being a popular antacid tablet. He argued that all measurement scales required a standardized benchmark and for this he chose Howard Johnson's® restaurants, at that time a widespread restaurant chain (now with only one remaining location) that served adequate, if unremarkable, food. Gerry considered it to represent zero on his Rolaids Scale. He was proud that it was an inverse scale, like the then popular phi

size scale, with meals that were better than the benchmark receiving a negative Rolaids score, and worse meals a progressively higher positive numbers of Rolaids.

In summary, Gerard V. Middleton was an innovative researcher, sometimes well ahead of the field, with a deep interest in understanding how sediments were created. He was a profound and deeply critical thinker, a trait that he, together with Roger Walker, instilled in their students by means of their facies-models course and home seminar series, a trait that became feared when, in later years, these former students reviewed manuscripts for publication. He was passionate about passing on knowledge to others, and about his involvement with scientific societies. He was justly decorated for his many services to sedimentary geology, and his many publications continue to be widely cited because of they helped to establish the foundations for our present-day understanding, especially of gravity-flow processes. Beneath all of this external evidence, he was a deeply human individual, who loved his wife of 62 years, Muriel. He is survived by Muriel and their three children, Laurence, Teresa and Margaret, their spouses and Gerry's grandchildren.

Robert W. Dalrymple, Queen's University
Janok Bhattacharya, McMaster University
We thank Teresa and Laurence for their assistance in preparing this tribute.

For those who would like to give a donation in honour of Gerry's legacy, contributions can be made to the Middleton/Walker Prize in Sedimentary Geology or the Walker/Middleton Fieldwork Scholarship, both at McMaster University, at:

https://secureca.imodules.com/s/1439/17/giving/form.aspx?sid=1439&gid=1&pgid=770&cid=1859&dids=2607&bledit=1

Information about these scholarship awards can be found at:

https://www.science.mcmaster.ca/ees/undergraduate/undergrad-scholarships-awards.html#application-required

Or you can contact: giving@mcmaster.ca

https://doi.org/10.12789/geocanj.2021.48.179

GEOLOGICAL ASSOCIATION OF CANADA
(2021-2022)

CORPORATE MEMBERS

PLATINUM

MEMORIAL UNIVERSITY

GOLD

NORTHWEST TERRITORIES GEOLOGICAL SURVEY

SILVER

ROYAL TYRRELL MUSEUM

YUKON GEOLOGICAL SURVEY

BRITISH COLUMBIA GEOLOGICAL SURVEY

NICKEL

UNIVERSITY OF WATERLOO

GEOSCIENCE CANADA AND THE GEOLOGICAL ASSOCIATION OF CANADA ARE GRATEFUL TO THE CANADIAN GEOLOGICAL FOUNDATION FOR THEIR FINANCIAL SUPPORT OF THIS JOURNAL

Canadian Geological Foundation — Fondation Géologique du Canada

OFFICERS

President
Deanne van Rooyen
Past President

Vice-President
Alwynne Beaudoin
Treasurer
Michael Michaud
Acting Secretary
Tim Fedak

COUNCILLORS

Paul Alexandre
Alwynne Beaudoin
Stefanie Bruekner
Tim Fedak
Alana Hinchey
Rebecca Hunter
Phil McCausland
Michael Michaud
Diane Skipton
Colin Sproat
Deanne van Rooyen

STANDING COMMITTEES

Communications: Rebecca Hunter
Finance: Michael Michaud
GAC Lecture Tours: Stefanie Bruekner
Publications: Alana Hinchey
Science Program: Phil McCausland

REVIEW

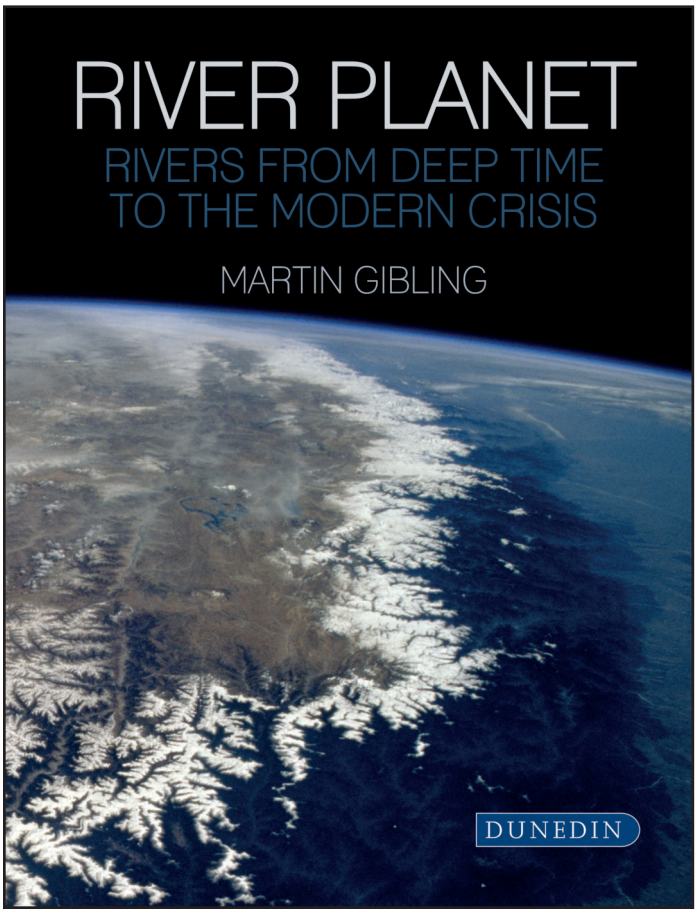

River Planet: Rivers from Deep Time to the Modern Crisis

Martin Gibling

Published by: Dunedin Academic Press Limited
Published: 2021; 240 p.
Colour illustrations throughout
Purchase price: $61 (CND; Hardback)
In North America, contact Independent Publishers Group
E-mail: orders@jpgbook.com

Reviewed by Ellen Wohl
Colorado State University
Department of Geosciences
Fort Collins, Colorado, 80523-1482, USA
E-mail: ellen.wohl@colostate.edu

River Planet examines the world's rivers from the perspective of a geologist. Written in an engaging and accessible style, the text is designed for the non-specialist reader interested in natural and environmental history. Gibling takes on the huge task of exploring rivers large and small throughout the planet's history, including the last few thousand years of human alteration of Earth's surface.

The book is divided into five basic sections. The first section starts with a chapter that reviews the history of geological thinking and explains how geologists interpret sedimentary rocks and paleoenvironments (Figs. A, B). As with each of the succeeding chapters, the vignettes and personal details of historical figures make the story more appealing to the general reader. The next chapter describes the geological histories of the oldest terrestrial rivers and of Martian rivers. The third

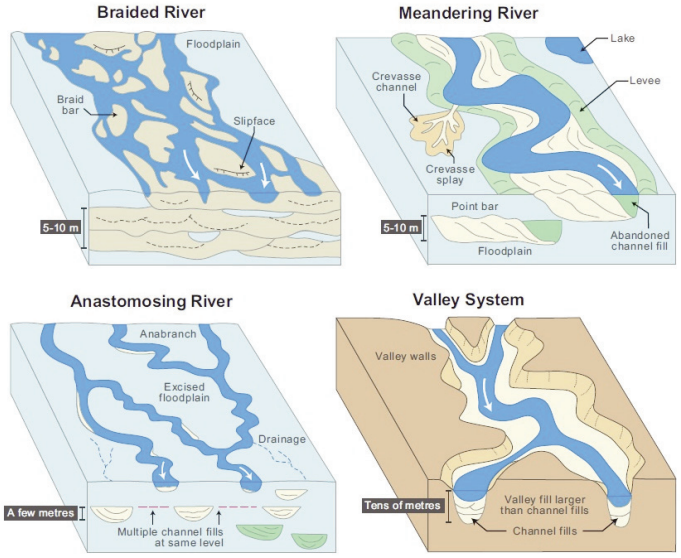

Figure A. Figure 1.5 from *River Planet*. Common river channel forms with the models' front face showing the differences in channel outcrop.

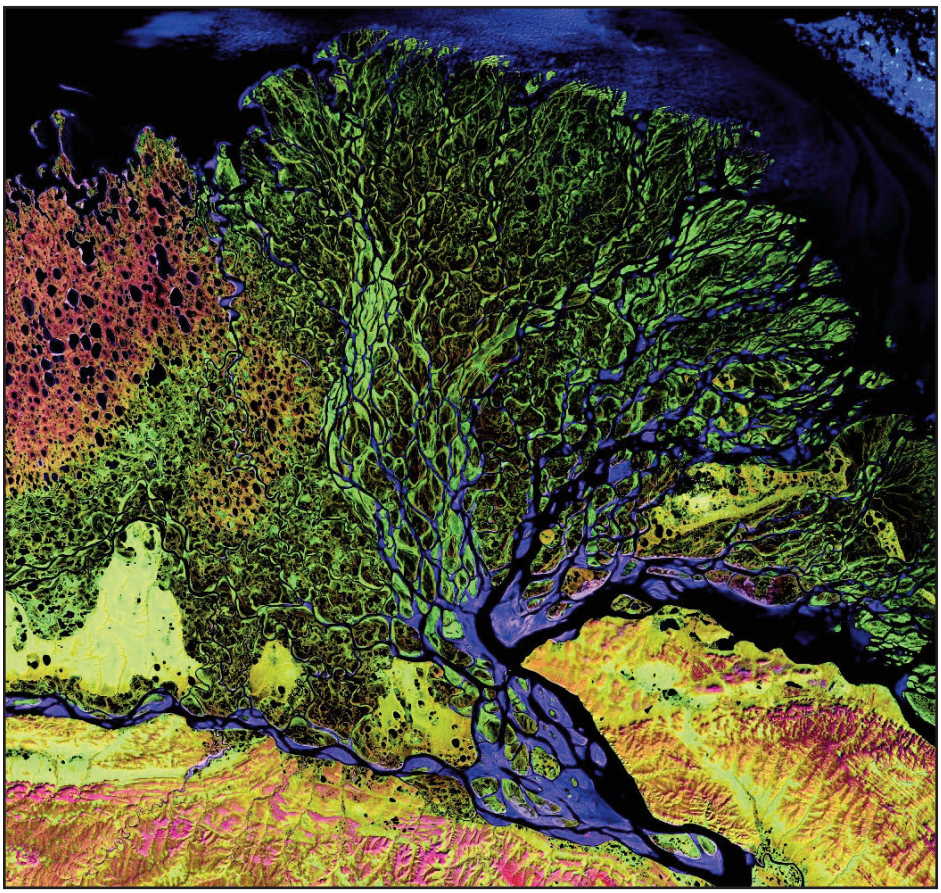

Figure B. Figure 1.6 from *River Planet*. False-colour image of Lena River Delta, Russia. Courtesy of United States Geological Survey.

chapter explores the geological history of interactions between rivers and vegetation.

In the second section of the book, seven chapters explore major rivers of specific geographic regions in the context of tectonic and human history. Chapters on Africa, the southern Pacific region (Australia, New Zealand, and Antarctica), Asia, Europe, South America, and North America are followed by a chapter on the ancient Canadian Bell River. Each of the chapters in this section of the book illustrates key points about rivers in the region, rather than providing a systematic or complete list of all rivers and all river characteristics.

The third section focuses on the Quaternary Ice Age, with chapters on continental ice sheets and river adjustments during and after glaciation; megafloods during glacial retreat; and ancient rivers drowned by rising sea level during the Quaternary.

The fourth section examines human interactions with rivers, starting with prehistoric changes in land cover that influenced river process and form, and then concluding with two chapters focused on specific examples. These latter examples are the Saraswati River in India, in which flow largely ceased as a result of Holocene climate change, and China's Yellow River, which has been significantly altered through centuries of artificial levee and dam construction.

The final section of the book examines engineered rivers, with chapters on the effects of dams, mining, and pollution; large dams; the Saskatchewan River and the effects of multiple dams; agriculture; urban rivers in London buried in pipes; and river restoration.

River Planet is unique in providing an integrated view of rivers in the context of geologic and human history. Gibling describes rivers as endangered species. This insight grows from a geologist's understanding of deep time, geological history, and biological evolution. Gibling also writes with a humanist scholar's appreciation of the individual personalities of famous historical scientists and engineers. The heartfelt writing makes the text a pleasure to read and the abundant, visually appealing colour photographs and diagrams effectively illustrate concepts described in the text. Gibling also brings himself into the book, opening and closing the text with descriptions of his own experiences with rivers and deftly weaving personal narrative into technical material throughout the book. In a sense, *River Planet* is a personal retrospective on a successful life and a career that included rivers across the planet and from contemporary environments to those interpreted from the rock record. The later sections of the book seem less coherent in terms of a clear structure and progression of information between chapters, but I think the book succeeds as a collection of brief explorations of the diverse rivers of the world. As such, it engages both the professional scientist and the reader interested in natural history and provides a distinctive, geological perspective on the world's rivers.

GEOSCIENCE CANADA

JOURNAL OF THE GEOLOGICAL ASSOCIATION OF CANADA
JOURNAL DE L'ASSOCIATION GÉOLOGIQUE DU CANADA

2021 VOLUME 48 GSCNA7 48 97-146
PRINT EDITION ISSN 0315-0941
ONLINE EDITION ISSN 1911-4850